uOttawa

Experimental and Numerical Investigation of Liquid Storage Tanks Under Seismic Excitation

A THESIS

Submitted to the Faculty of Graduate and Postdoctoral Studies in Partial Fulfillment of the Requirements for the

Degree of Master of Applied Science in Civil Engineering

By

Iman Bahreini Toussi

Supervisors:

Dr. Abdolmajid Mohammadian (University of Ottawa)

Dr. Reza Kianoush (Ryerson University)

Department of Civil Engineering

Faculty of Engineering

University Of Ottawa

Ottawa, Ontario,

Canada

The M.A.Sc. in Civil Engineering is a joint program with Carleton University administered by the Ottawa-Carleton Institute for Civil Engineering

Abstract

Liquid storage tanks are a crucial type of structures. They are used to store various types of liquids and liquefied gases in different situations. In seismic regions, functionality of these structures after severe earthquakes is an important factor in their design. In earthquake-prone regions, the sloshing phenomena has an important role in the design procedure.

Current design codes and guidelines (e.g. ACI 350.3 and ASCE 7) are based on analytical studies that in some cases can be inaccurate in prediction of forces and pressures. Since a long time ago scientists have studied the sloshing phenomena in liquid storage tanks with different methods including analytical, numerical and experimental studies. In the current study, rectangular ground-supported tanks are studied and the effect of seismic loading on them is investigated both experimentally and numerically. For the experimental tests, the tanks were placed on a shaking table and using high-speed HD cameras, tests were filmed and later analyzed frame by frame to capture the critical moments. To investigate the bi-lateral effect of base excitation on the tanks, they were oriented on the table with four different angles. In the numerical study, a computational fluid dynamics tool - OpenFOAM - was used to simulate the tank motion and finally the results were compared with the experiment in order to develop a reliable model.

Acknowledgments

I would like to give a special gratitude to those who without their support and guidance, I would not have been able to do this thesis.

I first and foremost want to thank my dear supervisor, Dr. Majid Mohammadian who helped me step-by-step during my academic career with his knowledge and guidance. Thanks for the infinite support and time.

I also want to give gratitude to my co-supervisor, Dr. Reza Kianoush of Ryerson University for his helpful advice and comments during my project.

I also want to say a thank you to Dr. Moslem Majeed for his help during my experimental study.

During my career as a master's student in the University of Ottawa, I was blessed with the positive atmosphere in our department. I want to offer my gratitude to all my professors, the staff of the Civil Engineering department, my friends, my fellow students and whoever helped me during my two-year study here. Thank you all.

Last but not least, my sincerest gratitude goes to my family, especially my beloved parents, without whose support and encouragements I would have never been able to start and finish this degree.

Table of contents

List of Tables

List of Figures

List of Symbols

A: Displacement amplitude (m)

B: Tank width (m)

f: Excitation frequency (Hz)

g: Acceleration due to the gravity (9.81 m/s^2)

h_c: Height of the convective part (m)

h_i: Height of the impulsive part (m)

H_L: Total height of the liquid (m)

L: Length of the tank (m)

m_c: Mass of the convective part (kg)

m_i: Mass of the impulsive part of the liquid (kg)

PGA: Peak Ground Acceleration (g)

t: Time (s)

T: Excitation period (s)

T_c: Sloshing period of the system (s)

u: Displacement (m)

u(t): Displacement at time t (m)

W_c: Weight of the convective part (N)

W_i: Weight of the impulsive part of the liquid (N)

W_L: Total weight of the liquid (N)

λ: Coefficient

μ: Dynamic viscosity of the liquid ($N.s/m^2$)

ρ: Density of the liquid (kg/m^3)

ω: Excitation frequency (rad/s)

ω_c: Sloshing frequency (rad/s)

Chapter 1

Introduction

1.1. Background

On average 200 earthquakes with magnitude of greater than 6 Richter occur all around the world each year (Figure 1- 1). There are more than 4000 earthquakes in Canada every year, at times very strong. Some of the world's largest earthquakes have happened in Canada such as the 2012 offshore Haida Gwaii earthquake (5.9 Richter), the 1988 Sagwanay earthquake (5.9 Richter) and two earthquakes in 1985 Nahanni region, northwest territories (6.9 & 6.6 Richter, respectively). The largest recorded earthquake in Canada is 1949 Queen Charlotte Islands, off the coast of BC with a magnitude of 8.1 Richter (look e.g. Natural resources Canada, Earthquakes Canada).

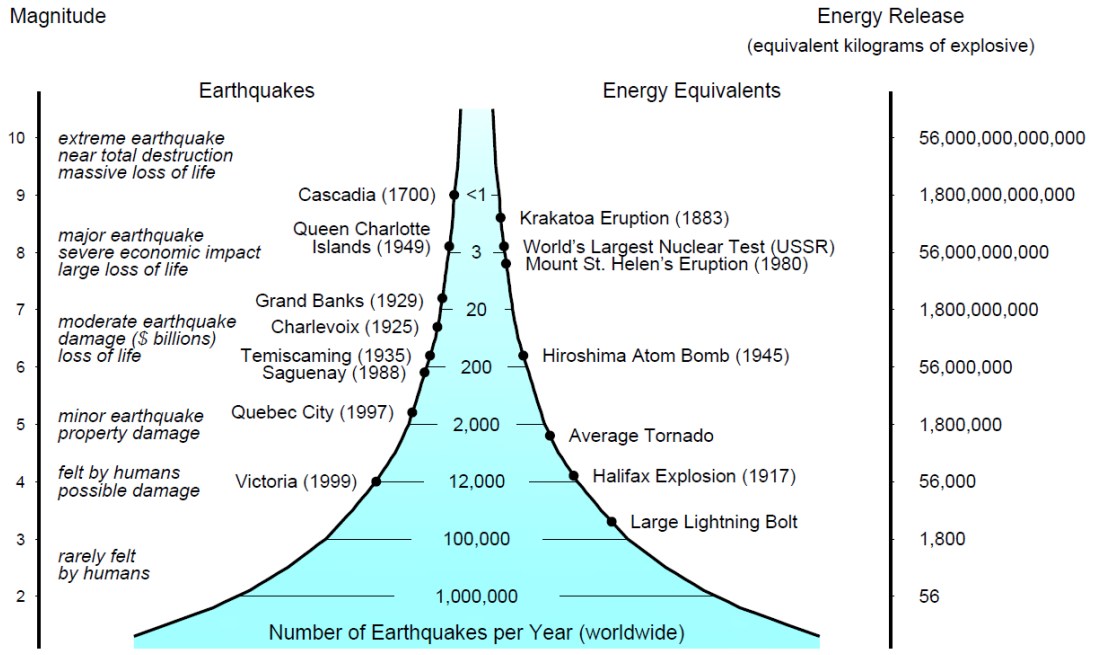

Figure 1- 1 Global frequency of earthquakes
(http://www.earthquakescanada.nrcan.gc.ca/info-gen/magfreq-en.php)

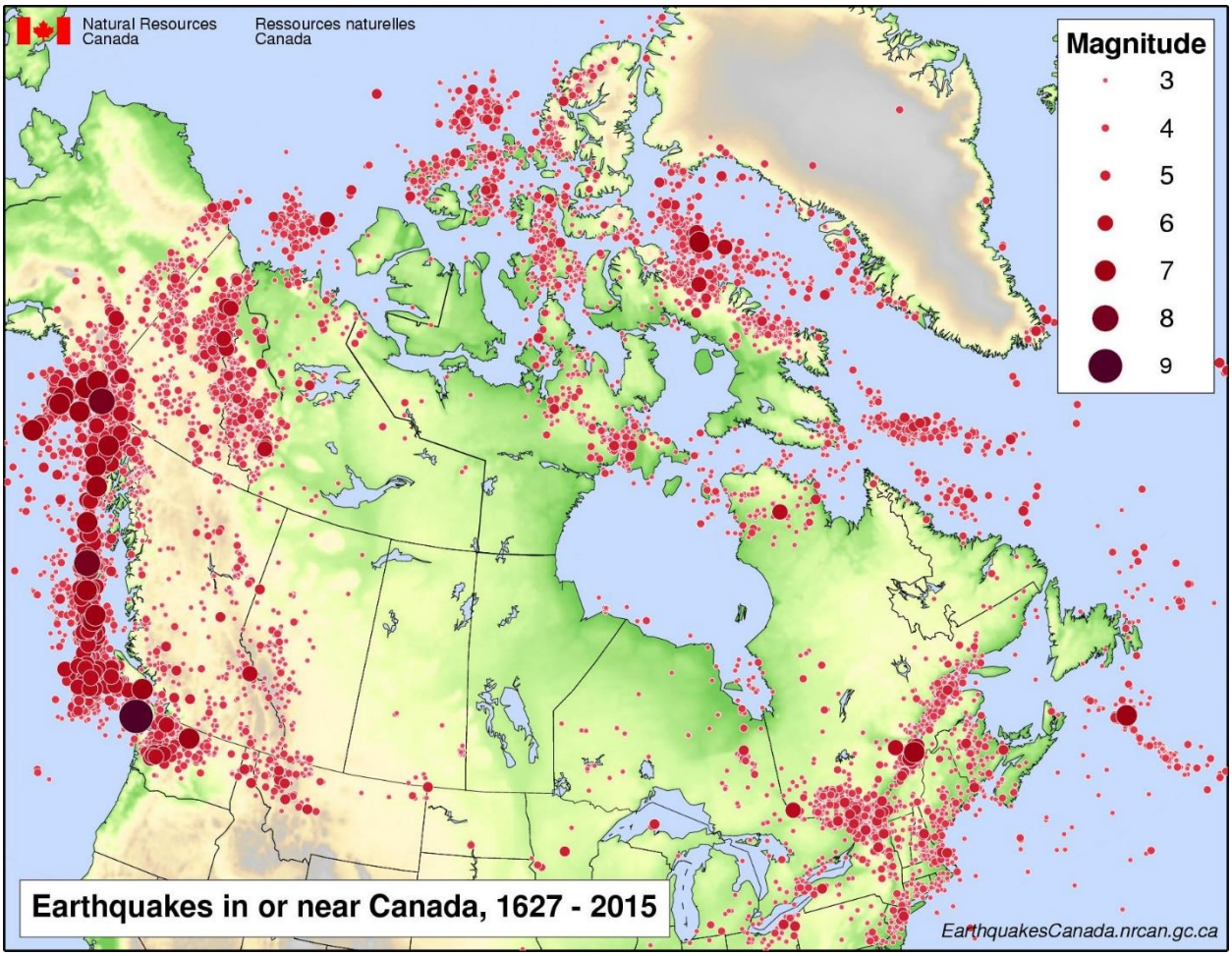

Figure 1- 2 Earthquake map of Canada
(http://www.earthquakescanada.nrcan.gc.ca/historic-historique/caneqmap-en.php)

Liquid storage tanks are widely used to store different types of materials in industry (e.g. oil, petroleum, toxic & flammable), food production (e.g. dairy factories), municipalities (e.g. drinking and firefighting water), transportation (e.g. cargo ships, trucks), construction (e.g. water, concrete), and buildings (water) etc. These structures vary in shape and size; they can have circular, rectangular, or square cross sections.

In numerous past earthquake events, severe damages and economic losses have occurred due to poor seismic performance of tanks containing hazardous materials (e.g. uncontrollable fires in petroleum tanks during the 1964 Niigata and 2011 Tokohu earthquakes in Japan, huge damage to

water reservoir during 1960 Chilean earthquake, structural failure of tanks due to 1992 Landers and 2010 Calexico earthquakes in California (Figures 1-3 through 1-5).

Another important point is that serviceability of water reservoirs during and after an earthquake is important because of their crucial role in extinguishing fires caused by the earthquake (Housner; 1963) as well as supplying the drinking water to people suffering from the event. It is also crucial for the hospitals where injured people are being treated to have access to fresh water during earthquake events.

Figure 1- 3 Damages to liquid tanks during 1992 Landers earthquake in California (http://www.johnmartin.com/earthquakes/eqshow/lan_0004.htm, http://www.murbachgeotech.com/water.html)

Figure 1- 4 Damages to liquid tanks during 2010 Calexico earthquake in California
(http://www.fema.gov/media-library/assets/images/56703)

Figure 1- 5 Fire due caused by earthquakes in oil refineries in Japan
a) 1964 Niigata earthquake
(http://docsteach.org/documents/69098/detail?mode=browse&menu=closed&era%5B%5D=postwar-united-states&page=2)
b) 2011 Tohoku earthquake
(http://geologylearn.blogspot.ca/2015/11/how-do-earthquakes-causes-damage.html)

1.2. Objectives, scope and novelty of the current study

There are various types of liquid tanks. The difference can be in their shape, support type, or material. From elevated circular cylindrical tanks to ground-supported or buried rectangular ones. Rectangular tanks can have different length to width ratios depending on the implementation conditions and feasibility.

Shape

Liquid storage tanks are available in different shapes such as cubic, rectangular, cylindrical, conical, polygon, etc. (Figure 1-6). The selected shape for a tank depends on many parameters such as budget, material of the tank and the type of liquid to be stored.

Support type

Reservoirs can be buried under the ground (e.g. septic tanks), ground-supported (e.g. petroleum tanks) or elevated (water tanks). Elevated tanks can be supported on concrete shafts, steel columns or a combination of both.

Material

Reinforced concrete and steel are most commonly used materials for liquid storage tanks. However, different types of liquid tanks made from polyethylene and fiber-reinforced plastic are becoming popular due to their lower cost and chemical resistance.

a) http://orencocomposites.com/products/rectangular-tanks/

b) http://www.southerntank.net/rectangular-tanks/

c) http://www.nasa.gov/content/liquid-hydrogen-the-fuel-of-choice-for-space-exploration

d) http://www.liquidtanks.com/

e) http://baydeltaoffice.water.ca.gov/sdb/af/photos/LiqO2Tank.html

f) https://blogjob.com/trmeson/types-of-liquid-transportation-tanks/

g) 

h) 

http://www.chinatanksandvessel.com/liquid-oxygen-liquid-nitrogen-liquid-argon-storage-tanks.html

Figure 1- 6 Different ypes of liquid (or liquefied gas) storage tanks:

a, b) Rectangular, c) spherical, d, g) Circular cylindrical, e, f, h) horizontal cylindrical

In the past decades, development of computers and ease of access to them leaded to popularity of Computational Fluid Dynamics (CFD) methods among researchers. Using different types of commercial or free applications, scientists tried to obtain solutions for sloshing phenomena in liquid containing structures.

Despite numerous studies in this field, there are limited number of codes for seismic design of liquid storage tanks in North America. The only available codes are ACI 350.3 and ASCE 7 (?) which are both US based, thus more research in Canada is essential for development of Canadian codes.

The focus of the current study is on seismic loading of rectangular, ground-supported liquid storage tanks that are used for numerous applications in industry (Figures 1-7 and 1-8).

Figure 1- 7 Old water tank in Hanover, Germany
(https://upload.wikimedia.org/wikipedia/commons/0/01/Water_tank_Hanover_Germany.jpg)

Figure 1- 8 Used oil tank (http://www.westeel.com/rectangular-recycoil-tanks-and-rectangular-fuel-vault-tanks)

A series of experimental and numerical studies were conducted in this study to find the effect of different types of base excitations on liquid surface in its container. The results were then compared in order to calibrate the numerical model. Once calibrated, the model can be applied to larger tank sizes in order to predict the hydrodynamic forces on the walls and roof.

There are different methods of studies in this field. Analytical, numerical, experimental or a combination of these methods can be applied to a study. The adopted method is dependent to availability of equipment and instruments.

There is a new approach used in this study which is changing the tank orientation on shaking table. This causes a bi-lateral base excitation on the tank and makes the liquid behavior different from single directional excitation. In addition differences between applying an actual earthquake (i.e. North-South component of 1940 El-Centro earthquake) and its downscaled and harmonic base excitations are investigated.

1.3. Structure of the thesis

This thesis consists of five chapters. The first chapter (i.e. the current chapter) gives a brief introduction of the problem and the justification to work on this topic.

Next chapter is a review of the previous studies in sloshing phenomena in liquid storage tanks. Different methods used by scientists are presented along with their pros and cons.

Experimental study is fully described in the third chapter. Liquid tanks, shaking table, types of loading, observations, and data analysis method are all explained.

Chapter 4 will cover the numerical study as well as a comparison between numerical and experimental observations and results. In this chapter OpenFOAM which is the adopted numerical tool in this research will also be presented.

The final part of the thesis - Chapter 5 - will conclude the research project. In this chapter the results will be summarized and also topics for future studies will be recommended.

Chapter 2

Literature review

2.1. Introduction

Analytical, numerical and experimental investigations of liquid storage tanks have been carried out by several researchers during the past decades. Different scientists have studied various aspects of the sloshing problem, from fluid viscosity to linearity or nonlinearity effect to tank flexibility (Wu and Chen, 2012). Fluid-Structure interaction problems require knowledge in several topics including fluid mechanics and structural engineering and the ability to find the relationship between them. Due to difficulties in finding direct analytical solutions (Xiong and Xing, 2008) numerical and experimental methods have become more popular among scientists, although there have been efforts (e.g. Housner, 1963 and Isaacson, 2010) in analytical studies.

In this chapter, first a brief review is presented on the codes available for designing and building liquid storage tanks and then, analytical solutions for sloshing problem will be studied. The chapter will continue to different numerical methods and numerical studies for sloshing problem. Experimental studies will be discussed and finally a conclusion will wrap up the chapter.

2.2. Review of available codes

In a study by Jaiswal et al. (2007), development of different codes for construction of liquid storage tanks has been reviewed. There are two main differences between analysis of liquid containing tanks and buildings: 1- There is a hydrodynamic force from the liquid to the walls and base in a tank, and 2- Liquid storage tanks are less observed than buildings. Because of the above-mentioned

differences, under seismic loading, a tank will have a higher design load than a building with similar dynamic characteristics. Another reason for higher lateral load is the higher importance factor considered by codes for tanks. In their study, Jaiswal et al. (2007) reviewed and highlighted the differences of ten codes including ACI 350.3 (American Concrete institute), AWWA D100, D110, D115 (American Water Works Association), API 650 (American Petroleum Institute), etc. Table 2.1 summarizes the reviewed codes.

Table 2- 1 Review of design codes (Jaiswal et al., 2007)

Code	Release Year	Ground Supported		Elevated		Seismic Force level
		RC or PSC	steel	On Shaft-Type Tower	On Frame-Type Tower	
ACI 350.3	2001	✓	×	✓	×	ASD
API 650	2005	×	✓	×	×	ASD
ASCE 7	2005	✓	✓	✓	✓	SD
AWWA D-100	2005	×	✓	✓	✓	ASD
AWWA D-110	1995	✓	×	×	×	ASD
AWWA D-115	1995	✓	×	×	×	ASD
Eurocode 8	1998	✓	✓	✓	✓	SD
IBC	2006	✓	✓	✓	✓	SD
NZSEE		✓	✓	✓	✓	SD

Among the above-mentioned codes, 2006 IBC, Eurocode 8 and NZSEE are national codes, while others are institutional codes from United States. A few of the codes use Strength Design (SD) level. In this method, factored loads are used and the structure approaches the ultimate level. Other codes use Allowable Stress Desig (ASD) level in which the loads are not factored, but the allowable stress is limited to elastic state of the material.

2.3. Analytical methods

As it is obvious from the name, analytical methods try to provide formulations based of which the problem could be solved. The most famous analytical solution for liquid storage tanks was presented by Housner (1963). His formulations are still used in many codes including ACI 350.3.

While a completely full or completely empty tank can be treated as a one-mass structure, a partially filled liquid tank with free surface has a different dynamics. Housner (1963) introduced an analytical solution for ground supported liquid storage tanks. In his method, the liquid with free surface is divided into two parts: convective and impulsive. The former is the sloshing part of the liquid that acts like an oscillating mass connected to the tank walls by a spring and the later is the part of the liquid that moves back and forth along with the tank and applies a reactive force on the walls like a rigidly connected mass (Figures 2-1 and 2-2). His formulations gives good results for vibration amplitude less than 20% of the tank dimension; hence, while nonlinearity effects for higher amplitudes make the method less accurate. In the case of elevated reservoirs, an equivalent mass of the structure was added to the impulsive mass of the liquid in order to find the equivalent impulsive mass.

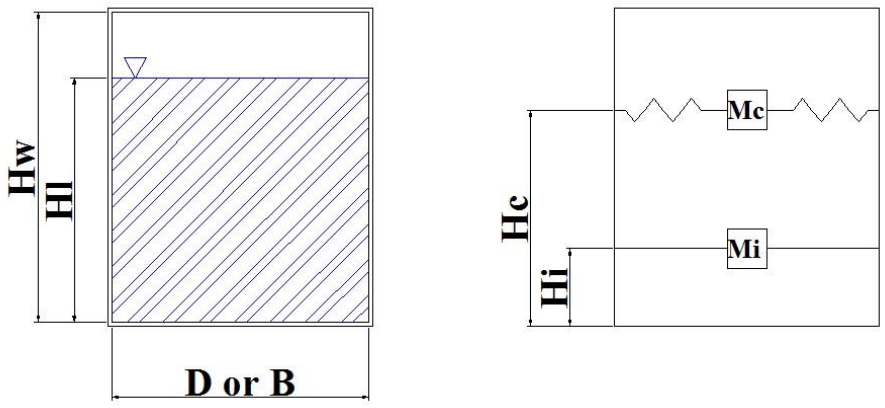

Figure 2- 1 Schematic shape for Housner's model for ground supported tanks

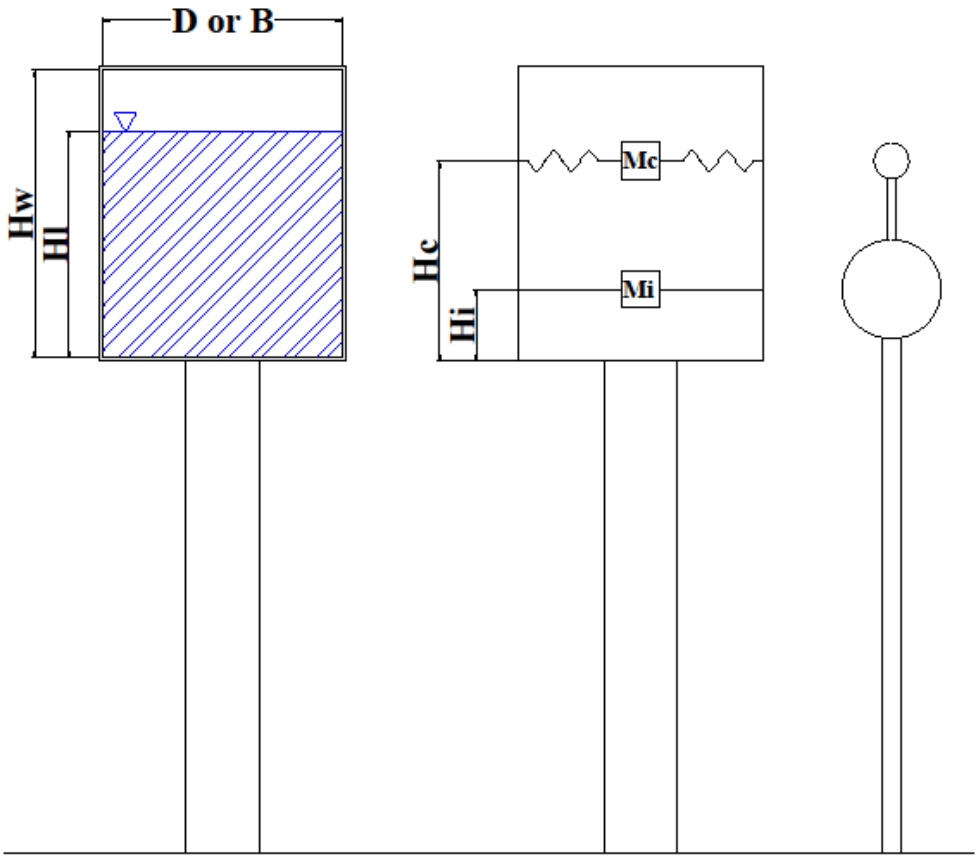

Figure 2- 2 Schematic shape for Housner's model for elevated tanks

Isaacson (2010) estimated hydrodynamic forces on the roof of a rectangular tank under harmonic and seismic base excitations. He assumed the tank to have no roof and predicted the liquid elevation. Then he added the roof to the tank and found the applied uplift forces. His formulation was based on consideration of impact and buoyancy force components. The impact force was estimated using the analogy with the case of flow past a flat plate. The maximum force was found to be dependent on either maximum impact or maximum buoyancy force; hence possible to calculate. He finally recommended a procedure for design of rectangular tanks (Figure 2-3).

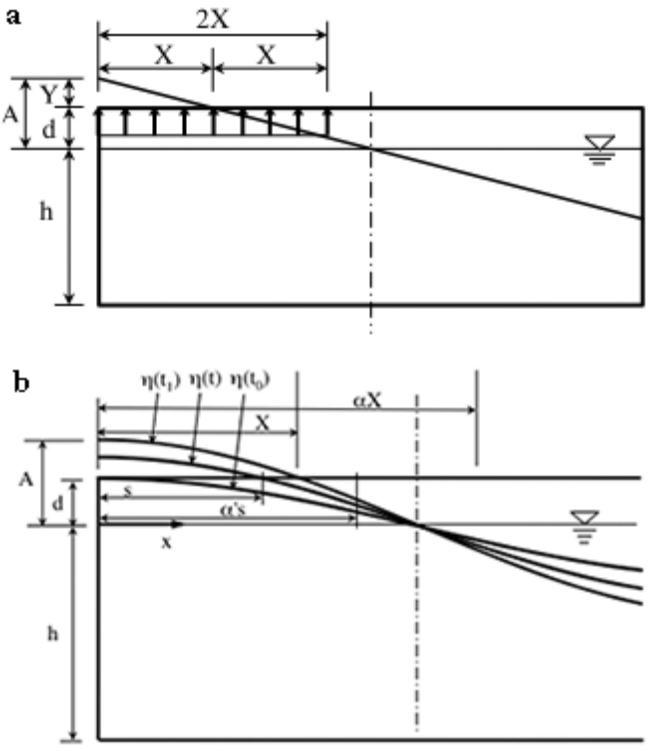

Figure 2- 3 Definition sketch for the loading on the roof:
a) San Francisco Public Utilities Commission (SFPUC 2003) formulation: b) proposed formulation by Isaacson (2010)

2.4. Numerical methods

Numerical methods are used for solving problems involving complicated geometries, loadings and material properties for which obtaining an analytical solution is hard or in some cases impossible. Hence, one may need to rely on acceptable numerical methods such as Finite Element Method (FEM), Finite Volume Method (FVM), Finite Difference Method (FDM), etc. In these methods, equations are formulated for each single element (or control volume) and the solution of the whole body is obtained by combining the solutions of all elements.

Numerical methods are based on matrices, thus digital computers are necessary for solving such complicated problems. There are two general methods for solving numerical problems by a computer. One is to use commercial programs such as Abaqus, ANSYS and SAP2000 that are designed to solve different types of problems. The other way is to develop specific programs that

are able to solve limited number of problems. In addition, open source softwares such as OpenFOAM that are specifically designed to solve CFD problems have become popular recently (See e.g. Logan, 1986).

2.4.1. Finite Element Method (FEM)

Finite Element Method (FEM) is a numerical approach for solving a large variety of engineering problems including structural analysis, heat transfer, fluid flow, mass transport and electromagnetic potential. Although it is not clear when the first finite element studies took place, this method was developed to use in structural engineering in 1940s. In this part, finite element studies on liquid storage tanks will be briefly reviewed.

Some features such as wall flexibility, effect of combined horizontal and vertical accelerations and effect of base fixity are not considered in previous studies as well as the Housner's method that is adopted by the major codes for construction of liquid storage tanks in North America (ACI 350.3 and ASCE 7-05).

Moslemi and Kianoush (2012) developed a finite element model for analysis of a "tall" and a "shallow" circular cylindrical liquid storage tank (figure 2-4). In their study, Kianoush and Moslemi investigated parameters such as aspect ratio of the tank, vertical components of earthquake, sloshing of the free surface, wall flexibility, and higher modes of impulsive and convective masses as well as accuracy of their code. As mentioned above, the code neglected the effect of combination of the horizontal and vertical accelerations. Instead, it approximated the vertical acceleration by two third of the horizontal response spectrum which can be debatable. Base fixity that is another neglected factor in the literature can affect the system period, hence the hydrodynamic forces. Authors assumed the fluid to be incompressible, irrotational and inviscid

with no mean flow, therefore an ideal fluid. They modeled two different types of tanks: shallow and tall, such that the aspect ratio for the tall tank is 3 times higher than the shallow one and the dimensions are adjusted in a way that the volume of the fluid is equal in both. Their results showed that in the shallow tank (with aspect ratio of about 0.115), regardless of wall flexibility, the vertical ground acceleration affects the convective hoop force, bending moment and base shear more than same impulsive components, but the effect is generally negligible. In the tall tank (with aspect ratio of about 0.324), combined vertical and horizontal ground accelerations show a significant increase in all impulsive and convective components. The reason for this increase can be the stronger P-Δ effect in tall tanks. In both shallow and tall tanks, wall flexibility increases the impulsive pressure significantly, while it has minor effect on convective pressure.

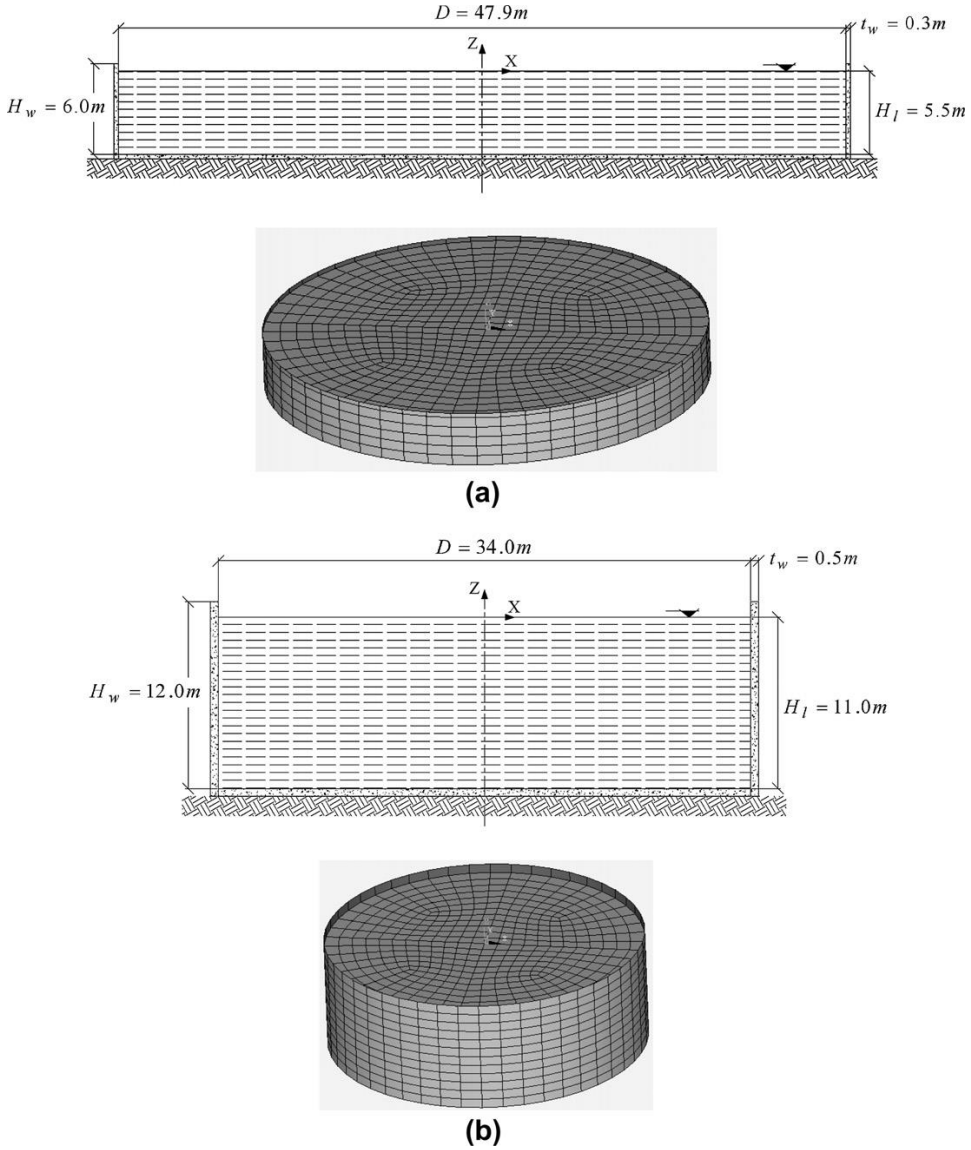

Figure 2- 4 Tank models analyzed by Moslemi and Kianoush (2012): (a) ''Shallow'' tank. (b) ''Tall'' tank.

In another study, Moslemi et al. (2011) evaluated seismic response of a water reservoir elevated on a reinforced concrete shaft by using finite element method. The method was proved to be accurate for circular cylindrical ground-supported tanks in a previous study (Ghaemmaghami et. al., 2010). They obtained the response time history by using modal superposition technique. In their finite element method, they accounted for damping of the liquid and considered impulsive and convective parts separately as an advantage in comparison with previous analytical methods. In addition to that, their method has the possibility to be used with complicated tank shapes such

as conical tanks; hence using the equivalent cylindrical tank is not needed (Figures 2-5 and 2-6). They studied base shear and overturning moment and considered the effect of wall flexibility and sloshing of the liquid in their finite element analysis. Modal finite element analysis showed a good agreement with Housner's model (Housner, 1963) in terms of the convective and impulsive natural frequencies. Impulsive and convective modes had different time of peak values; hence the effect of sloshing could be either positive or negative. The computed finite element time history agreed well with the results from the study and the model was verified.

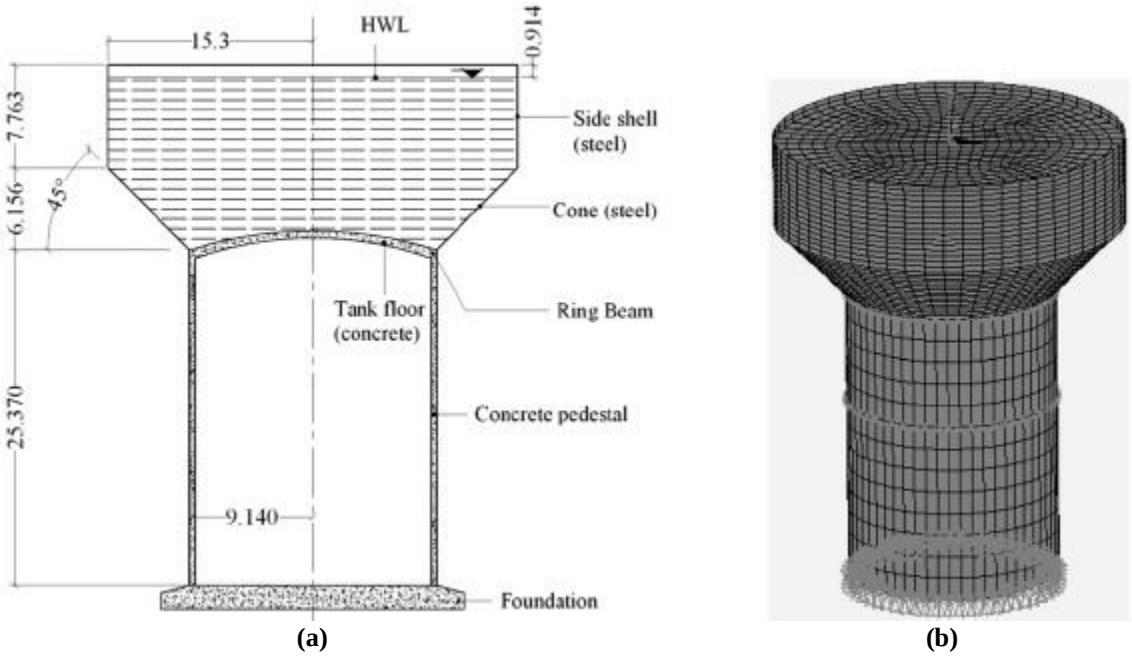

Figure 2- 5 a) Elevated tank geometry, b) FE idealization for the elevated tank model

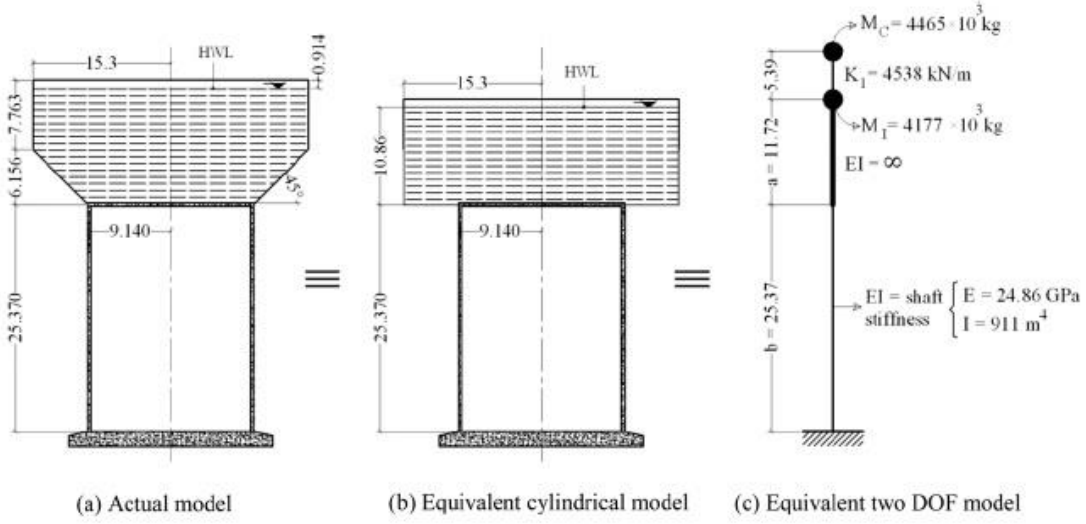

Figure 2- 6 Elevated tank model and its equivalent dynamic system

Mitra and Sinhamahapatra (2007) studied the sloshing characteristics (e.g. displacement, frequencies, mode shapes) and the hydrodynamic pressure on the walls for rectangular liquid storage tanks. In addition, they discussed the effect of height and aspect ratio as well as the use of an internal block on the above-mentioned characteristics. The problem was defined by 4-noded quadrilateral elements and Galerkin principle and the results were compared with existing solutions. Due to assumption of small amplitude waves, their analysis was limited to linear problems. In comparison with the displacement, they found advantages for the pressure formulations (e.g. only one unknown for each node). In addition to that, they were able to find the pressure with a low computational cost. They finally developed a computer code to estimate the sloshing characteristics as well as the pressure on the walls. The estimation of sloshing height and the wall displacement was found useful for design of liquid storage tanks.

Vertical excitation creates waves that were first inspected experimentally by Faraday (Faraday, 1831); hence they were called Faraday waves. These resonant waves, occur when the ratio between the excitation frequency and natural frequency of the tank is two. This state is called parametric resonance.

Sriram et al. (2006) investigated sloshing of a 2D rectangular model based on finite element method excited in both vertical and horizontal directions to explore the sway and heave modes of a ship motion. Both regular and random motions were studied. In regular horizontal excitation, the critical sloshing motion occurred at the frequency equal to the first mode frequency of the tank, while in regular vertical excitation it happened at the excitation frequency equal to twice the first mode frequency of the tank.

Kolukula and Chellapandi (2013) used finite element method based on mixed Eulerian-Lagrangian scheme. The reason was the different behaviors of free surface and interior nodes, which behave like Lagrangian and Eulerian particles respectively. Four-nodded isoparametric elements were adopted for the analysis. In their approach, it was necessary to calculate accurate velocities to obtain accurate results. They used the least square method to find the velocity field from the velocity potential and fourth-order Runge-Kutta method to advance the results in time. During the simulation, the Lagrangian behavior of free surface nodes caused them to get close to each other and make a numerical instability in the case of steep waves. To solve the instability, Kolukula and Chellapandi (2013) adopted a cubic spline interpolation to consistently re-grid the free surface. In their study, they assumed the tank material to be rigid and the liquid height was considered to be half the length (aspect ratio, $h_l/L=0.5$). The simulation was carried out with both resonance and non-resonance horizontal excitation frequencies. Two phenomena were observed: resonance and beating. The former occurred when the excitation frequency was same as the fundamental slosh frequency. The later happened when the excitation frequency was close to the fundamental frequency, but not equal.

Jaiswal et al. (2008) studied the dynamic characteristics of non-uniform circular and rectangular liquid containing tanks in two parts; experimental (Figure 2-7) and numerical. In the numerical

part, they modeled different tanks with proper finite elements using ANSYS software and found the sloshing characteristics (e.g. resonant frequency) of the liquid storage tanks with and without obstruction. In the experimental work, the same characteristics were investigated through tests on prototype models of tanks on a small shaking table that was harmonically excited.

Figure 2- 7 Experiment setup by Jaiswal et. al. (2008)

The results for regular shape tanks (circular, square and rectangular) showed a very good agreement between numerical model, experiment and analytical solution based on Housner's model (Housner, 1963). For tanks with irregular shapes, their results showed that codes' method for prediction of the sloshing period is reasonable for many types of tanks; however, in some cases, the numerical and experimental studies didn't agree well. Their final conclusion indicated need for further studies to be done.

Xiong and Xing (2008) conducted a finite element model based on air - water - elastic tank interaction. A computer program named FSIAP was used in the research. Four different types of interaction were investigated: pure liquid - rigid tank, pure liquid - elastic tank, air - water - rigid tank and air water - elastic tank. Natural frequencies and mode shapes of each interaction type were studied. The system was subjected to harmonic ground excitation as well as the El-Centro earthquake. The study showed that presence of air caused an increase in the natural frequency of

the system. In addition, accounting for air reduced the response amplitudes of displacement and pressure. The effect of elasticity depended on the tank's structural frequency. In a high-frequency tank, the elasticity did not have a great impact on the sloshing characteristics but in large tanks with lower frequencies, effect of elasticity was more crucial. At the end, authors claimed that entering pressurized air to sealed tanks can help in reducing the sloshing effects.

2.4.2. Finite Volume Method (FVM)

Finite volume method is another numerical method used in many computational fluid dynamic packages including OpenFOAM.

Gui and Jiang (2014) investigated 2D and 3D sloshing tank problems, free surface motions and hydrodynamic behavior of the liquid under resonant excitation using OpenFOAM. They used the two-phase viscous fluid flow model and investigated the differences between the 2D and 3D tanks. For their 2D model, they subjected a rectangular tank with length B=0.57 m, height H=0.30 m and liquid height h_l=0.15 m to a harmonic sinusoidal horizontal motion $x(t)=x_0 \sin(\omega t)$ where the amplitude x_0=0.005 m and the angular frequency ω is equal to the structure's natural frequency ω_1. Their results showed a good agreement with numerical and experimental results of Liu and Lin (2014), who proved that the potential flow theory that has been widely used in the past is not accurate in resonance frequency range due to rotational and nonlinear effects. Gui and Jiang (2014) used the same dimensions for their 3D tank with a width W=0.31 m. Again, they found an agreement between their numerical results and those by Liu and Lin (2014). Their numerical results in both 2D and 3D models showed that there were two peak values for the impulsive load on the wall tank. One was when the free surface reaches the tank roof while the other, which was relatively larger, occurred when the free surface went back down. Their 3D model showed that

there were large impact loads near the sharp corners; hence the 2D model may underestimate that parameter, specifically near the roof corners. In addition, OpenFOAM had good results in 3D nonlinear range in their test.

Li et al. (2012) used the Finite Volume Method to simulate the global motion of sloshing flow. They adopted the Impulse-Response Function (IRF) to solve the time domain analysis of the ship motion. The IRF method is based on linear frequency domain theory and in case of linear motion of the ship can easily be coupled with sloshing analysis. OpenFOAM was adopted for numerical simulation of potential flow theory and viscous flow theory. The validation of the results through experimental data showed a good agreement. Their results showed that the liquid sloshing in the tank had a great impact on rolling motion of the ship.

2.4.3. Finite Difference Method (FDM)

Like finite element and finite volume, finite difference method is a numerical approach to solve differential equations. This method uses difference equations.

Chen et al. (2009) developed a numerical approach for prediction and analysis of the sloshing part of the liquid in different types of tanks. They measured the sloshing pressures and loads acting on the tank walls and simulated the free surface. They used Reynolds-averaged Navier-Stokes (RANS) equations to describe the liquid motion. LSM which is a numerical method for estimating the free surface was used in their study. They performed computations for a rectangular tank and two chamfered corner tanks with different filling levels excited by different frequencies. Although a reasonable agreement between the proposed numerical method and the measured data for both impulsive and convective pressures either on the roof or on the walls was found, the accuracy of the method needs more study to be proofed.

Wu and Chen (2012) proposed a finite deference method to find the response of the liquid in a tank subjected to dimensionless base excitations. A wide range of frequencies were applied to the tank in three dimensions with action of six degrees of freedom. Different types (shapes) of waves were observed including single-directional, square-like, irregular and swirling. Results were compared with previous studies and showed an acceptable agreement. The study showed that square-like and irregular waves happened during a horizontal ground motion, regardless of excitation frequency and angle. An important conclusion of their study was that frequency of the first mode mostly affected diagonal, single-directional and square-like waves in resonant excitation. For rotating waves, in addition to the first mode, the second mode was also effective. In case of irregular waves, the odd natural modes had a great impact on the system.

2.4.4. Coupled methods

Coupled (combined) methods use at least two different combined approaches in order to either increase the accuracy or decrease the computation cost of the problem.

Cho and Cho (2007) investigated the seismic response of a circular cylindrical liquid storage tank. They proposed a method by combining finite element method and boundary element method. The study formulated the ‘coupled dynamic system’ in the time domain to find out the response of the reservoir under seismic loading by taking the effect of ‘fluid-structure interaction’ and the ‘sloshing of the free surface’ into account. In order to couple the finite elements of the structure and the boundary elements for the fluid, they used equilibrium and compatibility conditions. They also developed a numerical algorithm in three-dimensional coordinate system to analyze the dynamic response of a circular cylindrical steel reservoir. In their study, modal and seismic analysis results found by the coupled method showed a reasonable agreement with the literature.

Koshizuka and Oka (1996) introduced a Moving Particle Semi-Implicit (MPS) method for simulation of particles of incompressible fluids. In this method, each particle of the fluid is in interaction with the surrounding particles; hence movement of any particle depends on its neighbors.

Lee et al. (2007) used a coupled finite element method to analyze the sloshing in fluid-shell structure interaction where the structure was modeled by MITC4 shell elements and the analysis of the fluid was by using MPS method. Their study consisted of coupling between the fluid and structural solvers. They recommended a semi-implicit time integration scheme for the fluid and an explicit symplectic time integration scheme for the structure. They found their method helpful in solving sloshing problems.

2.4.5 Volume of Fluid (VOF)

Volume of Fluid method can be employed in conjugation with other numerical methods for simulation of the free surface of the flow. In this method - that was first proposed by Hirt and Nicols (1981) - the free surface of the liquid is divided into sections parallel to the coordinates. The original method is called Simple Linear Construction (SLIC) that was later improved to Piecewise Linear Interface Construction (PLIC).

As mentioned above, in the VOF method, the free surface is formed by geometric approach. But it should be indicated that computational cost for reconstruction of the surface is high. In their study, Ming and Duan (2010) recommended a method in which the free surface was assumed to be a physical discontinuity that can be taken by a high-order scheme. Navier-Stokes equations were employed for the sloshing motion. The gas-liquid interface was treated as a physical discontinuity with sudden changes in properties. For their method, the authors used the

experimental data published by South Korea's Daewoo Shipping and Marine Engineering Company in 2005 as a verification reference for their study. The above-mentioned data was recommended by 23rd ITTC Committee and was used by many researchers. Ming and Duan (2010) used a rectangular tank with length L=0.8 m, width W=0.35 m and height H=0.5 m and was filled up to %30 with liquid (h_l=0.3 H). Excitation frequencies were 0.8, 0.9, 1.0 and 1.2 of the natural frequency of the tank respectively with the motion amplitude of 0.02 m. They found a good agreement between the numerical and analytical results, which showed that the method is reliable. They also compared the 2D and 3D results in a sample simulation. 2D simulation was taken from the middle plane of the long direction. The comparison showed that the 3D effects on pressure are negligible; hence the 2D simulation was done for the rest of the study. GAMBIT - a commercial mesh generating software - was used to mesh the domain. Results were compared with the ones from Daewoo's experimental and Ansys' CFX11 and showed an agreement for lower frequencies while there was a small difference between experiment and the proposed method in higher frequencies.

Liu and Lin (2008) used VOF method in their study to investigate a two-phase fluid flow model for solving the Navier-Stokes equations in a liquid storage tank under arbitrary base excitation with 6 degrees of freedom and introduced a linear analytical model for the sloshing problem. The model, which was called NEWTANK (Numerical Wave Tank), was used for both viscous and inviscid liquid sloshing in rectangular tanks in 2D and 3D cases. The model was validated with previous theories and experimental data from other researchers. The results for both 2D and 3D validations showed an excellent agreement for small amplitude sloshing. For larger amplitudes there was a large gap between the numerical and analytical results due to the strong wave non-linearity; however, a good agreement occurred for the experimental results.

Rebouillat and Liksonov (2010) studied different numerical approaches for the sloshing problem available in the literature and published a summary in a table. In this section, that table is expanded (Table 2-2) to cover the review by Rebouillat and Liksonov (2010) and the author.

Table 2- 2 Summary of reviewed numerical studies by Rebouillat and Liksonov (2010) and the author of the thesis

Author(s)	Reviewed by		Tank			Baffle(s)	Fluid(s)	Method	Liquid Model	Boundary Conditions	Results		Application
	Author	Reboillat & Liksonov	Shape	Size	Material						Validation (compared with ...)	Agreement	
Chen et al. (2009)	✓	✓	Rectangular	0.8 * 0.5 * 0.4 m	Rigid	×	Water & Air	FDM	Invicid, incompressible, two phases, Navier/Stokes, Euler	Partially filled, sine translation with gravity	Experiment	Acceptable	LNG Carriers
Mitra & Sinhamahapatra (2007)	✓	✓	Rectangular	30 * 13 * 15 m	Rigid	Submerged blocks	N/I	FEM 2D	Invicid, Compressible, monophase, homogeneous	Partially filled, EQ excitation with gravity	Solutions by others	Good	Seismic response of LST
Liu & Lin (2008)	✓	✓	Rectangular	0.57 * 0.15 * 0.31 m	Rigid	×	Water & Air	FDM 2D & 3D	Both Viscous and invicid models, incompressible, two phases, Navier/Stokes	Partially filled, sine translation with gravity	Theory, experiment and other simulation results	Good agreement with experiment	Naval
Lee et al. (2007)	✓	✓	Rectangular	0.8 * 0.3 m (2D)	Rigid / Elastic	×	Water	FEM 2D & coupled particle	Invicid, incompressible, monophases	Partially filled, sine acceleration with gravity	Experiment	Good	N/I
Moslemi & Kianoush (2012)	✓	×	Circular cylindrical	shallow: D=47.9 H=6m / Tall: D=34 H=12m	Rigid / Flexible compared	×	Water	FEM 3D	Invicid, incompressible, irrotational, No mean flow	Partially filled, horizontal and vertical EQ excitation	Well-proved analytical methods	Excelent	Seismic response of LST
Moslemi et al. (2011)	✓	×	Conical, Elevated, RC shaft: H=25m, R=9.14m	R=15.3, H=13.9m , 45-degree lower chamfer	Flexible	×	Water	FEM 3D	No clear indication	Partially filled, unidirectional horizontal seismic excitation	Previous studies	Very good	Seismic response of LST
Jaiswal et al. (2008)	✓	×	Various shapes	-	N/I	×	Water	FEM	No clear indication	Partially filled, sine translation	Experiment	Further studies required	Water system, Petroleum, etc.
Gui & Jiang (2014)	✓	×	Rectangular	0.57 * 0.31 * 0.3 m	N/I	×	Water & Air	FVM 2D & 3D	Viscous, two phase, Based on OpenFOAM package	Partially filled, resonant excitation	Available theoretical, numerical and experimental results	Good	Oil and LNG carriers
Cho & Cho (2007)	✓	×	Circular cylindrical	Tall: R=7.32, H=22/ Broad: R=18.3, H=12.2	Flexible	×	Water	Coupled FE-BE method	Inviscid, incompressible, irrotational	Partially filled, EQ excitation with gravity	Published results	Good	municipal water supply and fire fighting systems
Ming & Duan (2010)	✓	×	Rectangular	0.8 * 0.35 * 0.5 m	N/I	×	Water & Air	VOF	Two phases, Navier/Stokes	Partially filled, harmonic excitation	Daewoo shipping and marine Engineering company, 2005	Good	LNG Carriers
Wu & Chen (2012)	✓	×	Square base		N/I	×	N/I	FDM 3D	No clear indication	Partially filled, 3D base excitation	Previous studies	Good	

Eswaran et al. (2009)	×	✓	Cubic	0.6 * 0.6 * 0.6 m	Elastic	Elastic, Different configurations	Water	FEM 3D	Invicid, incompressible, monophases, Newtonian	Partially filled, sine translation with gravity	Experiment	Good	Many cited
Mitra & Sinhamahapatra (2008)	×	✓	Rectangular	19.6 * 12.3 m (2D)	Elastic walls, Rigid bottom	×	Water	FEM 2D	Invicid, Compressible, homogeneous	Partially filled, EQ excitation with gravity	Simulation results by others	Good	Drinking water container
Aliabadi et al. (2003)	×	✓	Ellipsoid section, elongated	2.0 * 1.4 m, 4.0 m long	Rigid	×	Fuel	FEM 3D	No clear indication	Partially filled, linear acceleration	Another model	Depends	Road vehicles
Popov et al. (1992)	×	✓	Rectangular	Varies	Rigid	×	N/I	FEM 2D	Viscous, incompressible, monophase	Partially filled, arbitrary acceleration, gravity	Experiment	Good	Road vehicles
Godderidge et al. (2009)	×	✓	Rectangular	1.2 * 0.6 m (2D)	Rigid	×	Water & Air	FEM 2D	Viscous, compressible, multiphase	Partially filled, sine translation with gravity	Experiment	Good for inhomogenous model	LNG Carriers
Sriram et al. (2006)	×	✓	Rectangular	2 * 1 m (2D)	Rigid	×	Water	FEM 2D	Invicid, monophase	Partially filled, sine and random excitation in two directions with gravity	Experiment	Good	Naval

2.5. Experimental method

In this part, experimental studies on seismic excitation of liquid storage tanks will be presented.

Panigrahy et al. (2009) conducted a series of experiments to find out the pressure and changes of the free surface in a sloshing tank. A square tank placed on a shaking table that worked with a DC motor was used for the experiment. Pressure and displacement of the free surface were measured by using different excitation frequencies and fill levels in the tank. Main part of their study was to investigate the effect of baffles in the tank; hence, they carried out the experiment with and without them and compared the results. Panigrahy et al. (2009) observed that the sloshing of the liquid is a function of several factors e.g. liquid height, size of the tank, excitation amplitude and frequency and density of the liquid. They measured the pressure in tanks with different fill levels as well as the sloshing height of the free surface. A relationship between the wave amplitude and the liquid height was found in their study. They found out that the pressure on the tank wall is a function of the excitation period and shows a great variation near the free surface rather than the deeper parts. Due to self-damping property of liquids, for a specific excitation frequency, it was observed that

increasing the liquid height decreases the sloshing. As part of their study, they investigated the effect of baffles on the sloshing and a considerable reduction was observed. They also compared different types of baffles and found the ring baffles more effective.

Akyildiz and Ünal (2005) performed a series of experiments to study the sloshing of the liquid as well as the pressure distributions at different points in a rectangular tank. A 92×62 cm tank with 46 cm width was used in their tests in order that they could have a 3D motion. To investigate the effect of baffles, the tank was designed to have removable baffles in different directions on walls, roof and bottom. Piezoresistive pressure transducers were installed in different locations to measure the pressure distribution in the tank. Various sets of experiment with different excitation frequencies and different fill depths were carried out. The results showed that baffles remarkably reduce the motion of the liquid, but there was not enough data to find out the effect of fluid viscosity on pressure, hence more experimental work was necessary.

2.6. Summary

Different approaches for investigating seismic behavior of liquid storage tanks that were available in the literature were discussed in this chapter. Among analytical methods Housner (1963) and Isaacson (2010) are more well-known. Housner's simplified model is accurate enough and is adopted by most design codes.

Numerical methods became more popular with development of personal computers. These methods are divided to different categories including finite element method, finite difference method, finite volume method and volume of fluid. In addition coupled methods were also used by a number of scientists.

The next approach reviewed in this chapter was experimental method. Due to technical difficulties (e.g. shaking table size and weight limitations), real-size experimental tests were not done by researchers. Some used pressure transducers (e.g. Akyildiz and Ünal, 2005) and some just investigated the liquid surface. Effect of baffles and internal blocks on sloshing of the liquid were also inspected.

Most of the studies proved the accuracy of Housner's simplified model in prediction of the resonance frequency of the system, while some claimed the method does not predict the forces (and thus the pressures) well. In addition, effect of nonlinear waves in resonance frequency was another issue of study which is not considered by the codes.

Chapter 3

Experimental study

3.1. Introduction

Numerical models can be validated through experimental studies. Experiment can also be used as a method for development of formulations and is helpful to solve equations easier. Like any other study, solving the sloshing phenomena for liquid storage tanks relies on experimental study to validate the analytical or numerical solutions. In this thesis a series of experimental tests were performed to investigate the sloshing in a liquid containing structure.

3.2. Experiment setup

In this series of experiments, total of eighty tests were done. The tests included two sizes of rectangular tanks excited on a uni-axial shaking table. To consider the bi-directional effect of excitation, the tanks were placed in different orientations on the shaking table (i.e. 0, 30, 60, 90 degrees). The tanks were filled to a specified height with water. The tests were performed under relatively constant room temperature (23±2 °C). The tanks were made of transparent glass with polyester leads. In order to have a better visualization, the water was coloured with dye. For each angle, three dimensionless harmonic (sinusoidal) excitations and two earthquake excitations were applied. Earthquake excitations included (i) actual N-S component of 1940 El-Centro earthquake (California) with peak ground acceleration of 0.319g and (ii) scaled down of the same earthquake with peak ground acceleration of 0.2g. A shaking table in the structural laboratory of University of Ottawa was used in this project.

3.2.1. Liquid Storage Tank

Two different glass tanks were used in this research as liquid storage tanks. The tanks had plan dimensions of 755×305 mm and 495×245 mm respectively with a height of 300 mm for both cases. Polyester (plastic) plates were used as leads, glued to the tanks by silicon sealant. The tanks are assumed to have rigid walls and roof, which is considered acceptable due to their size. It should also be noted that previous research investigations have shown that wall flexibility has little effect on the sloshing behaviour of tanks as described in Chapter 2.

3.2.2. Shaking table

There are different types of shaking tables with different numbers of degrees of freedom. A typical single-degree-of-freedom shaking table that moves back and forth in one direction usually consists of the following components:

- Moving Plate
- Motivator (actuator)
- Control unit (usually a computer software)

Various types of actuators are available that are categorized based on effective length, force, static and dynamic stroke, etc.

In this study, the actuator that moved the shaking table was MTS 244.12 model. In this model of single-degree-of-freedom actuator, a hydraulic pump is required to pumps oil to the actuator. The actuator is connected to the control system. This combination of shaking table and actuator can move within a 250 mm domain. It can generate both harmonic and time-history base excitations.

Inside the actuator, an LVDT (Linear Variable Differential Transformer) sensor is installed that measures the movement of the rod. The control unit reads the sensor and based on the data from the sensor, the system decides whether to continue the current movement or change the speed or the direction.

Figure 3- 1 Shaking table actuator from different views

Table 3-1 summarizes the actuator specifications:

Table 3- 1 Actuator specifications

Model: MTS 244.12		
Force	kN	25
Rod Diameter	mm	44.5
Effective Piston Area	cm^2	13.5

3.2.3. Video recording

The sloshing action in the tank was captured by two high-speed HD video cameras. Frames frame the videos were all extracted and snapshots of critical moments were marked. Since the snapshots of the tank were not perfect rectangles, they were cropped in a perspective way using Adobe Photoshop software.

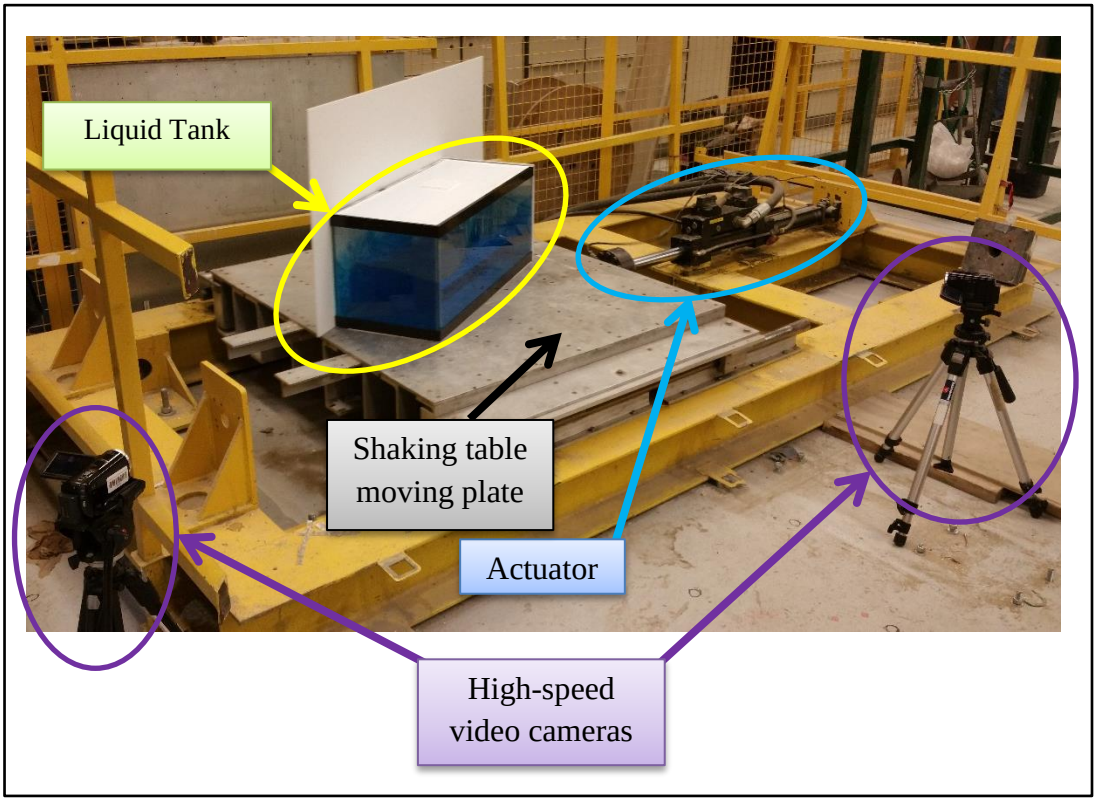

Figure 3- 2 Experiment setup

3.3. Description of the tests

The tanks were attached to the shaking table by double-sided tape. Due to its low thickness, the tape was assumed to be rigid, so that there was no relative displacement between the tank and the moving part of the table. Water was poured and colour was added to the tank and the system was shaken by different sinusoidal (harmonic) excitation and time-history (earthquake) motion.

3.3.1. Harmonic base excitation

A simple harmonic sinusoidal excitation is formulated as:

$$u(t) = A \sin \omega t \qquad (3\text{-}1)$$

Where

u is the displacement;

A is the displacement amplitude;

ω is the excitation frequency;

t is the time.

There is also the following relationship between excitation frequency and excitation period:

$$T = {}^{2\pi}/_{\omega} \qquad (3\text{-}2)$$

Where T is the excitation period.

In this study, there were three sinusoidal excitations with different frequencies per tank per liquid depth. In each case, one of the excitation frequencies was the resonant frequency of each tank for that specific depth. Since Housner's model [Housner (1963)] was proven to be reliable for estimating the resonant frequency of the first mode of liquid storage tanks in previous studies (e.g. Jaiswal et. al., 2008, Moslemi et. al., 2011, Barakati, 2015) the frequency calculated by this model was used as the resonant frequency of the tank. The two other excitation frequencies were chosen within $\pm 50\%$ of the resonant frequency.

The amplitude of the sinusoidal excitation was five percent of the maximum length of the tank; hence, the total displacement was ten percent (1/10) of the tank length. For tank 1, the amplitude was 35 mm while for tank 2 it was 25 mm.

3.3.2. Earthquake excitation

The north-south component of 1940 El-Centro ground motion was used. Both tanks having two different depths of water were excited by the same earthquake excitations. Some features of the selected ground motion are:

- Duration: 31.16 sec
- Peak ground acceleration: 0.319g = 3.13 m/s^2
- Maximum velocity: 361.4 mm/s
- Ground displacement range: (-213.4 : +28.6) mm

The reader is referred to Chopra (1995) for the definition of the above parameters.

In addition, a downscaled form of the earthquake with peak ground acceleration of 0.2g with the following specifications was used:

- Duration: 31.16 sec
- Peak ground acceleration: 0.2g = 1.962 m/s^2
- Maximum velocity: 226.7 mm/s
- Ground displacement range: (-133.9 : +18) mm

Acceleration-time history, velocity-time history and displacement-time history graphs of the actual and downscaled earthquakes used in this study are presented in Figures 3.3 and 3.4 respectively.

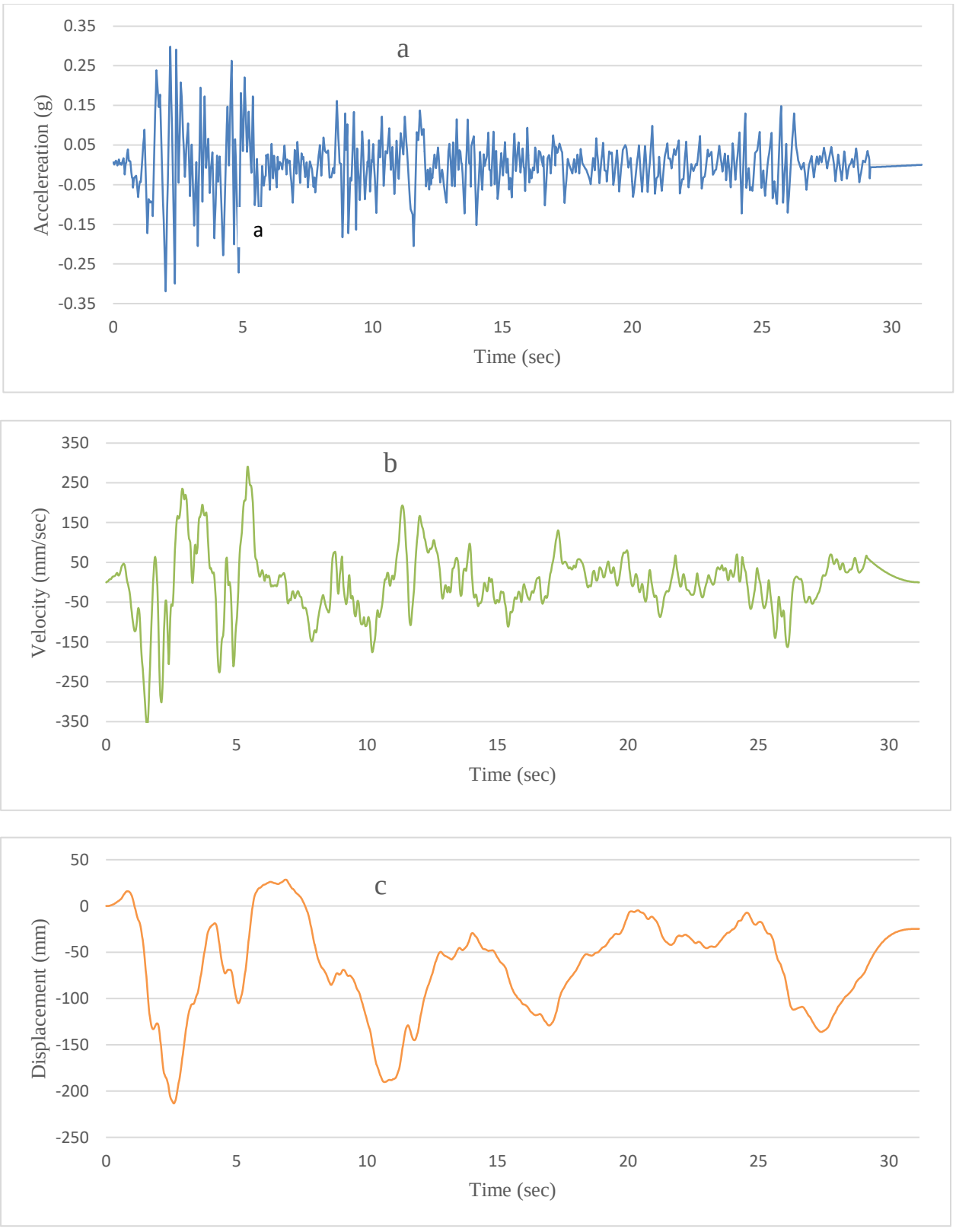

Figure 3- 3 a) Acceleration, b) Velocity and c) Displacement time history graphs for actual El-Centro earthquake

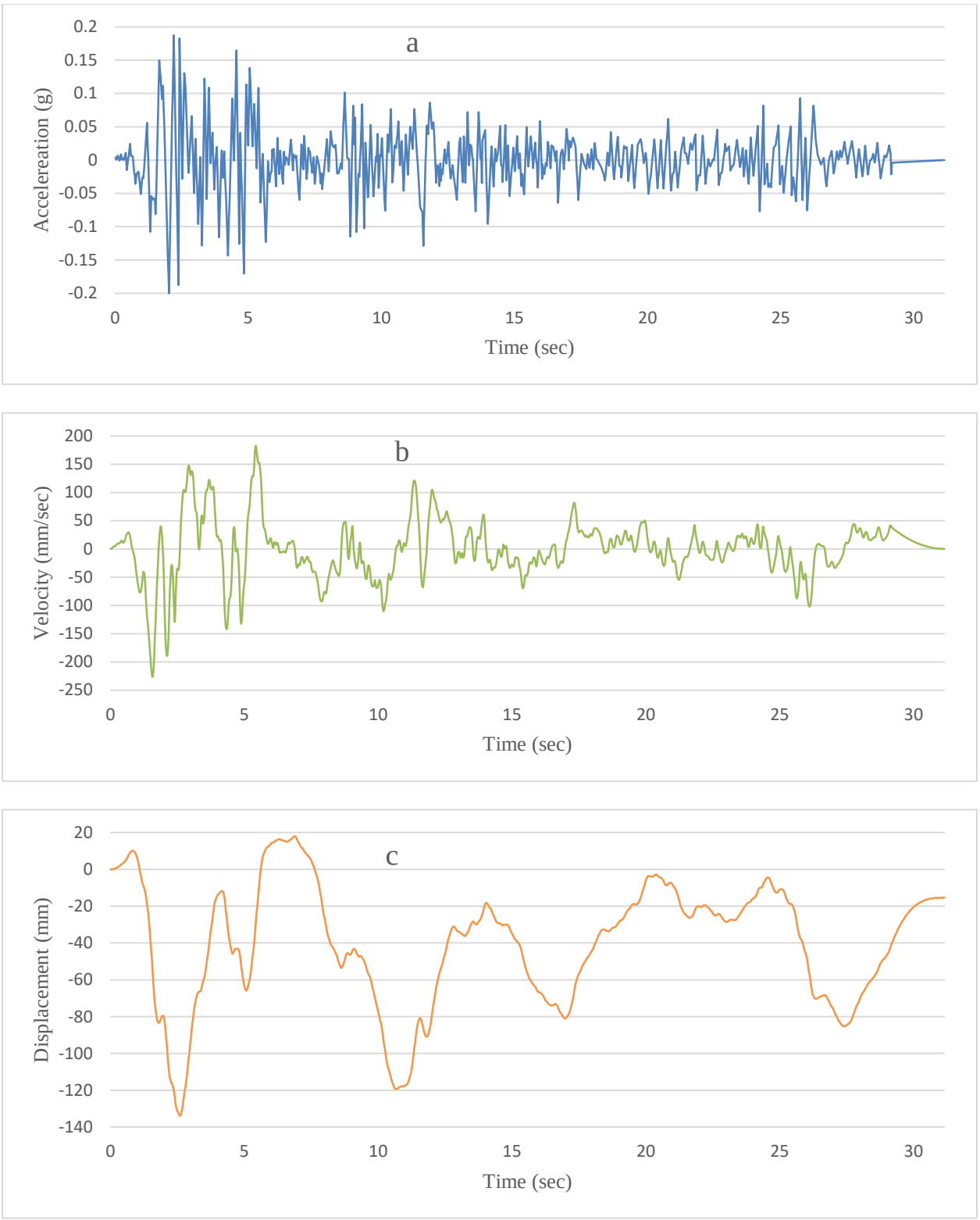

Figure 3- 4 a) Acceleration, b) Velocity and c) Displacement time history graphs for downscaled El-Centro earthquake

3.3.3. Detailed calculation and information

Based on ACI 350.3-6, the resonant sloshing frequency and period are calculated by the following formulation. These equations are similar to those defined by Housner (1963):

$$\frac{W_i}{W_L} = \frac{\tanh[0.866\left(\frac{L}{H_L}\right)]}{0.866(\frac{L}{H_L})} \qquad (3\text{-}3)$$

$$\frac{W_c}{W_L} = 0.264(\frac{L}{H_L}) \tanh[3.16\left(\frac{H_L}{L}\right)] \qquad (3\text{-}4)$$

Since in all cases in this study $\frac{L}{H_L} \geq 1.333$,

$$\frac{h_i}{H_L} = 0.375 \quad (3\text{-}5)$$

$$\frac{h_c}{H_L} = 1 - \frac{\cosh[3.16\left(\frac{H_L}{L}\right)]-1}{3.16(\frac{H_L}{L}) \sinh[3.16\left(\frac{H_L}{L}\right)]} \quad (3\text{-}6)$$

$$\lambda = \sqrt{3.16g \tanh[3.16\left(\frac{H_L}{L}\right)]} \quad (3\text{-}7)$$

$$\omega_c = \frac{\lambda}{\sqrt{L}} \qquad (3\text{-}8)$$

$$T_c = \frac{2\pi}{\omega_c} = (\frac{2\pi}{\lambda})\sqrt{L} \qquad (3\text{-}9)$$

Where

W_L is the total weight of the liquid,

W_i is the weight of the impulsive part,

W_c is the weight of the convective part,

L is the length of the tank,

H_L is the total height of the liquid,

h_i is the height of the impulsive part,

h_c is the height of the convective part,

ω_c is the sloshing frequency,

T_c is the sloshing period of the system.

In the following sections, frequencies of harmonic excitations, displacement amplitude, and other necessary characteristics for each set of tests are presented with detailed calculation.

3.3.3.1. Tank 1, Water depth 100 mm

Calculation procedure of impulsive and convective masses and heights as well as the resonance frequency for the partially filled tank (figure 3-5) is as follows:

$$L = 755\ mm$$

$$B = 305\ mm$$

$$H_l = 100\ mm$$

$$W_l = 0.755 * 0.305 * 0.100 * 1000 = 23.0275\ kg \qquad (3\text{-}10)$$

$$\frac{W_i}{W_L} = \frac{\tanh[0.866(\frac{755}{100})]}{0.866(\frac{755}{100})} = 0.1529 \Rightarrow W_i = 0.1529 * 23.0275 = 3.5209\ kg \qquad (3\text{-}11)$$

$$\frac{W_c}{W_L} = 0.264\left(\frac{755}{100}\right)\tanh\left[3.16\left(\frac{100}{755}\right)\right] = 0.7887 \Rightarrow W_c = 0.7887 * 23.0275 = 18.1618\ kg \qquad (3\text{-}12)$$

$$\frac{h_i}{H_L} = 0.375 \Rightarrow h_i = 0.375 * 100 = 37.5\ mm \qquad (3\text{-}13)$$

$$\frac{h_c}{H_L} = 1 - \frac{\cosh\left[3.16\left(\frac{100}{755}\right)\right]-1}{3.16\left(\frac{100}{755}\right)\sinh\left[3.16\left(\frac{100}{755}\right)\right]} = 0.5072 \Rightarrow h_c = 0.5072 * 100 = 50.72\ mm \qquad (3\text{-}14)$$

$$\lambda = \sqrt{3.16g\tanh[3.16\left(\frac{100}{755}\right)]} = 3.5024\sqrt{{}^{m}/_{s^2}} \qquad (3\text{-}15)$$

$$\omega_c = \frac{\lambda}{\sqrt{L}} = \frac{3.5024}{\sqrt{0.755}} = 4.0308\ rad/s \qquad (3\text{-}16)$$

$$T_c = \frac{2\pi}{\omega_c} = \left(\frac{2\pi}{\lambda}\right)\sqrt{0.755} = 1.5588\ s \qquad (3\text{-}17)$$

Displacement time history graphs of the base excitation for this tank with the mentioned depth are shown in figure 3-6.

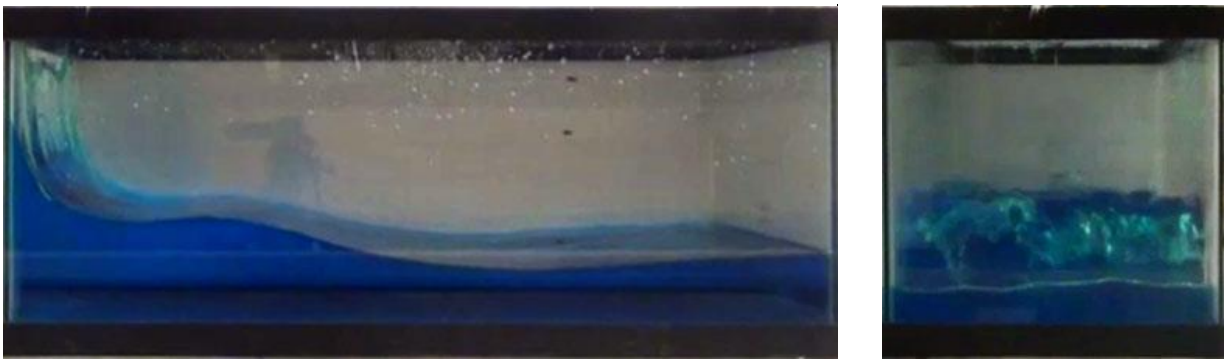

Figure 3- 5 Tank 1, depth 100 mm

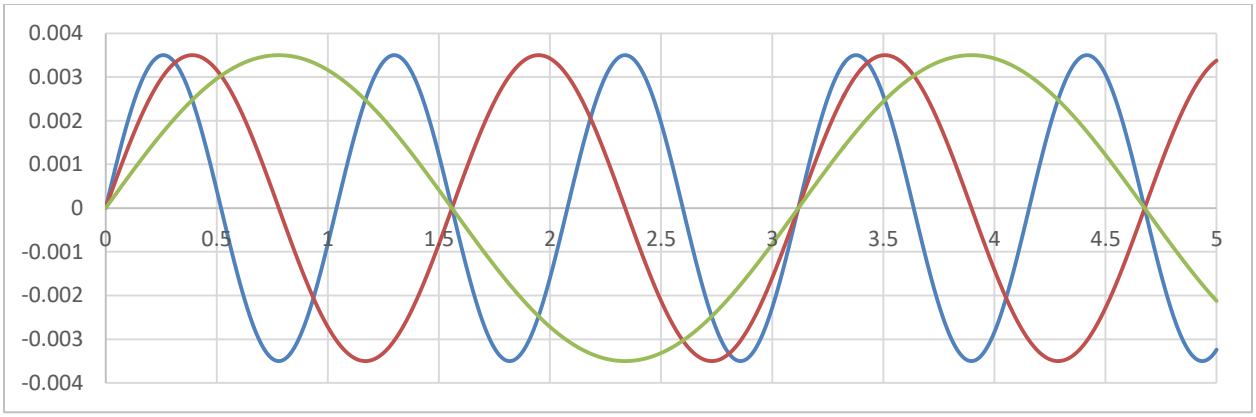

Figure 3- 6 Displacement time history for harmonic excitations of tank 1, water depth 100 mm

3.3.3.2. Tank 1, Water depth 200 mm

The same procedure is followed for the new water depth (i.e. 200 mm) for this tank (figure 3-7) with the displacement time history graphs shown in figure 3-8.

$$L = 755\ mm$$

$$B = 305mm$$

$$H_l = 200\ mm$$

$$W_l = 0.755 * 0.305 * 0.200 * 1000 = 46.055\ kg \quad (3\text{-}18)$$

$$\frac{W_i}{W_L} = \frac{\tanh[0.866(\frac{755}{200})]}{0.866(\frac{755}{200})} = 0.3050 \Rightarrow W_i = 0.3050 * 46.055 = 14.0468\ kg \quad (3\text{-}19)$$

$$\frac{W_c}{W_L} = 0.264\left(\frac{755}{200}\right)\tanh\left[3.16\left(\frac{200}{755}\right)\right] = 0.6819 \Rightarrow W_c = 0.6819 * 46.055 = 31.4049\ kg$$

(3-20)

$$\frac{h_i}{H_L} = 0.375 \Rightarrow h_i = 0.375 * 200 = 75.0\ mm \quad (3\text{-}21)$$

$$\frac{h_c}{H_L} = 1 - \frac{\cosh\left[3.16\left(\frac{200}{755}\right)\right]-1}{3.16\left(\frac{200}{755}\right)\sinh\left[3.16\left(\frac{200}{755}\right)\right]} = 0.5273 \Rightarrow h_c = 0.5273 * 200 = 105.45\ mm$$

(3-22)

$$\lambda = \sqrt{3.16g\tanh[3.16\left(\frac{200}{755}\right)]} = 4.6056\sqrt{m/s^2} \quad (3\text{-}23)$$

$$\omega_c = \frac{\lambda}{\sqrt{0.755}} = 5.3005\ rad/s \quad (3\text{-}24)$$

$$T_c = \frac{2\pi}{\omega_c} = \left(\frac{2\pi}{\lambda}\right)\sqrt{0.755} = 1.1854\ s \quad (3\text{-}25)$$

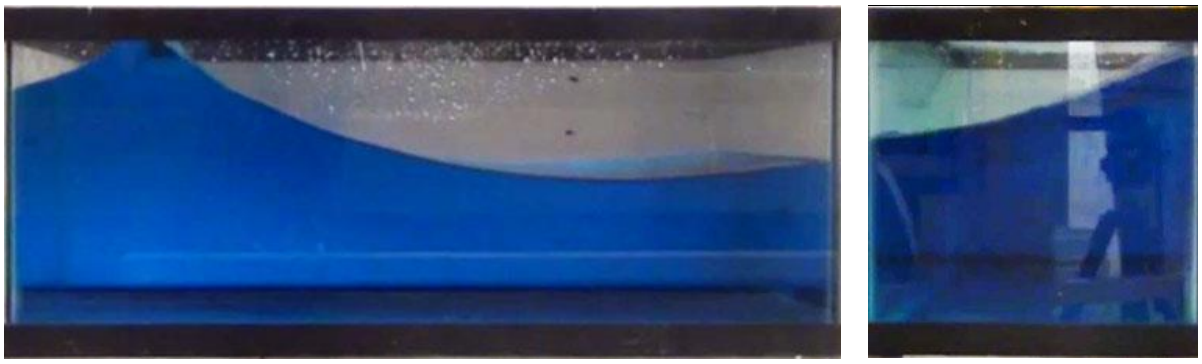

Figure 3- 7 Tank 1, depth 200 mm

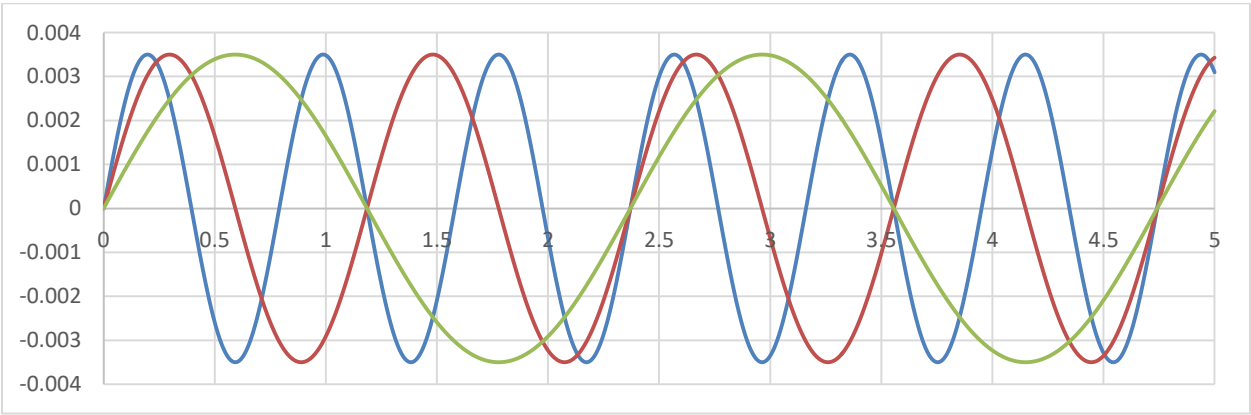

Figure 3- 8 Displacement time history for harmonic excitations of tank 1, water depth 200 mm

3.3.3.3. Tank 2, Water depth 100 mm

Impulsive and convective masses and heights, and resonance frequency for this tank (figure 3-9) are calculated by the following formulations. In addition, graphs showing the applied base excitations are presented (Figure 3-10).

$$L = 495\ mm$$

$$B = 245\ mm$$

$$H_l = 100\ mm$$

$$W_l = 0.495 * 0.245 * 0.100 * 1000 = 12.1275\ kg \qquad (3\text{-}26)$$

$$\frac{W_i}{W_L} = \frac{\tanh[0.866(\frac{495}{100})]}{0.866(\frac{495}{100})} = 0.233 \Rightarrow W_i = 0.233 * 12.1275 = 2.8257\ kg \quad (3\text{-}27)$$

$$\frac{W_c}{W_L} = 0.264\left(\frac{495}{100}\right)\tanh\left[3.16\left(\frac{100}{495}\right)\right] = 0.7368 \Rightarrow W_c = 0.7368 * 12.1275 = 8.9355\ kg$$

(3-28)

$$\frac{h_i}{H_L} = 0.375 \Rightarrow h_i = 0.375 * 100 = 37.5\ mm \qquad (3\text{-}29)$$

$$\frac{h_c}{H_L} = 1 - \frac{\cosh\left[3.16\left(\frac{100}{495}\right)\right]-1}{3.16\left(\frac{100}{495}\right)\sinh\left[3.16\left(\frac{100}{495}\right)\right]} = 0.5163 \Rightarrow h_c = 0.5163 * 100 = 51.63\ mm$$

(3-30)

$$\lambda = \sqrt{3.16g\tanh[3.16\left(\frac{100}{495}\right)]} = 4.1806\sqrt{{}^{m}/_{s^2}} \qquad (3\text{-}31)$$

$$\omega_c = \frac{\lambda}{\sqrt{0.495}} = 5.9421\ rad/s \qquad (3\text{-}32)$$

$$T_c = \frac{2\pi}{\omega_c} = \left(\frac{2\pi}{\lambda}\right)\sqrt{0.495} = 1.0574\ s \quad (3\text{-}33)$$

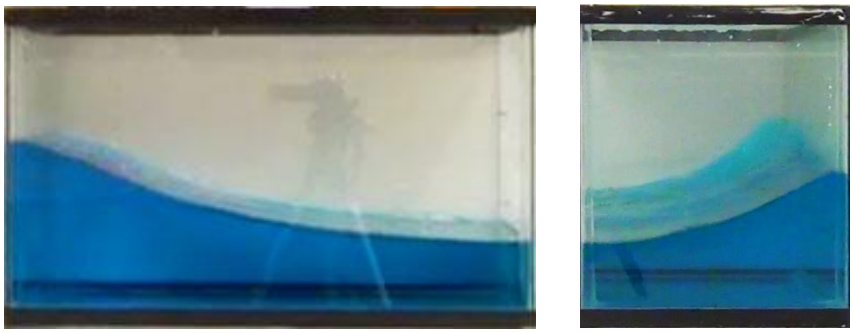

Figure 3- 9 Tank 2, depth 100 mm

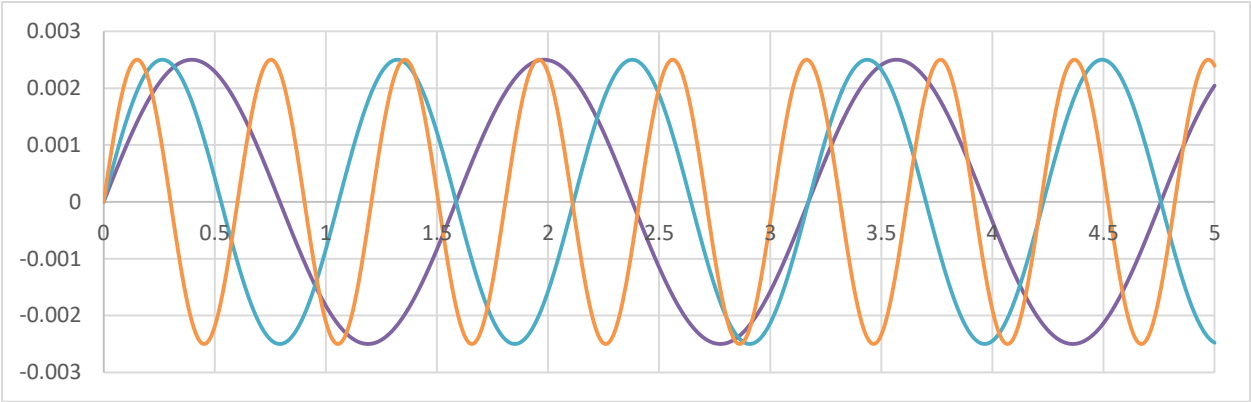

Figure 3- 10 Displacement time history for harmonic excitations of tank 2, depth 100 mm

3.3.3.4. Tank 2, Water depth 200 mm

Shown in Figure 3-11, calculations for this partially filled tank are presented as follows. In addition, displacement time history graphs for this part of the experiment are presented in Figure 3-12.

$$L = 495\ mm$$

$$B = 245\ mm$$

$$H_l = 100\ mm$$

$$W_l = 0.495 * 0.245 * 0.200 * 1000 = 24.255\ kg \quad (3\text{-}34)$$

$$\frac{W_i}{W_L} = \frac{\tanh[0.866(\frac{495}{200})]}{0.866(\frac{495}{200})} = 0.4534 \Rightarrow W_i = 0.4534 * 24.255 = 10.9972\ kg \quad (3\text{-}35)$$

$$\frac{W_c}{W_L} = 0.264\left(\frac{495}{200}\right)\tanh\left[3.16\left(\frac{200}{495}\right)\right] = 0.5591 \Rightarrow W_c = 0.5591 * 24.255 = 13.561\ kg$$

(3-36)

$$\frac{h_i}{H_L} = 0.375 \Rightarrow h_i = 0.375 * 200 = 75.0\ mm \quad (3\text{-}37)$$

$$\frac{h_c}{H_L} = 1 - \frac{\cosh\left[3.16\left(\frac{200}{495}\right)\right]-1}{3.16\left(\frac{200}{495}\right)\sinh\left[3.16\left(\frac{200}{495}\right)\right]} = 0.5584 \Rightarrow h_c = 0.5584 * 200 = 111.68\ mm \quad (3\text{-}38)$$

$$\lambda = \sqrt{3.16g\tanh[3.16\left(\frac{200}{495}\right)]} = 5.1501\sqrt{{}^{m}/_{s^2}} \quad (3\text{-}39)$$

$$\omega_c = \frac{\lambda}{\sqrt{L}} = \frac{5.1501}{\sqrt{0.495}} = 7.3201\ rad/s \quad (3\text{-}40)$$

$$T_c = \frac{2\pi}{\omega_c} = \left(\frac{2\pi}{\lambda}\right)\sqrt{L} = 0.8583\ s \quad (3\text{-}41)$$

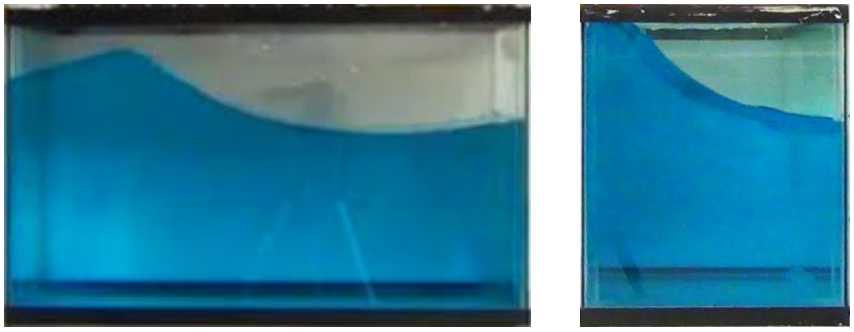

Figure 3- 11 Tank 2, depth 200 mm

Figure 3- 12 Displacement time history for harmonic excitations of tank 2, depth 200 mm

3.4. Observations

In this project, eighty tests were performed. Different base excitations were applied to two tanks partially filled with coloured water. The tanks were shaken by various types of base excitations, from resonant harmonic to actual earthquake. The following results were obtained:

3.4.1. Resonance frequency

In the previous studies (e.g. Jaiswal et. al., 2008, Moslemi et. al., 2011, Barakati, 2015) the Housner's simplified model was found accurate in predicting the natural frequency of the first mode in a liquid tank, whether it was circular-cylindrical or rectangular. In this study, the frequency obtained by this method was confirmed to be the frequency of the first mode, so it is the resonance frequency. In other words, for all tank-depth combinations, resonant frequency based on Housner's method caused the maximum displacement of the liquid surface and in this frequency range, there was a concordance between the movement of the liquid and the general movement of the system.

3.4.2. Effect of tank orientation

In this study, each reservoir was placed on the shaking table with four different orientations: 0º, 30º, 60º and 90º. The following results were observed during the tests:

Rotating the tank by 30º and 60º on the shaking table results in more sloshing near the sharp corners of the tank, regardless of liquid depth and excitation type. This can lead to more hydrodynamic pressure and uplift forces on the roof of the container near the corners. For 0º and 90º, waves are more linear and there is no significant difference between the water level in the middle of the wall and on the corners (Figure 3-13). In other words, the tank should be designed for higher hydrodynamic pressure in order to be able to resist bi-lateral excitations.

Another observation related to the tank orientation was the relationship between the excitation frequency and general motion of the liquid inside the tank when the tank was oriented either 30º or 60º. While exciting the reservoir with resonance frequency calculated based on its length causes longitudinal movement of the liquid, changing the frequency and making it closer to the resonance frequency based on its width, causes transverse waves. Effect of frequency on general motion of the liquid is presented in Figures 3-14 and 3-15.

a) 

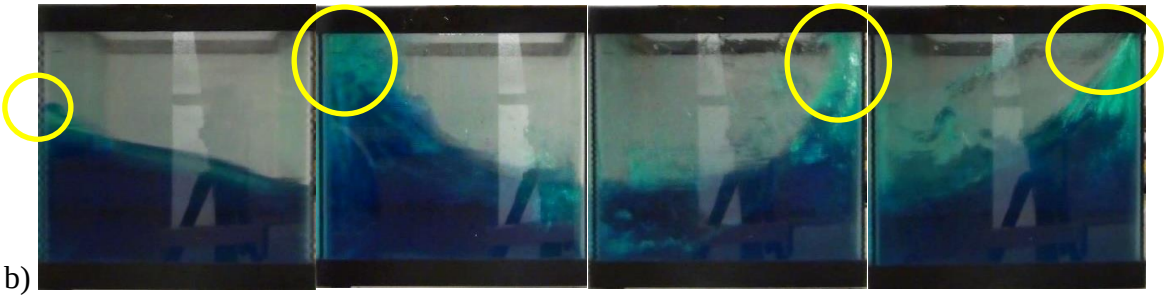

Figure 3- 13 Effect of tank orientation on sharp corners of 30º-oriented tank a) Harmonic excitation, b) Earthquake excitation

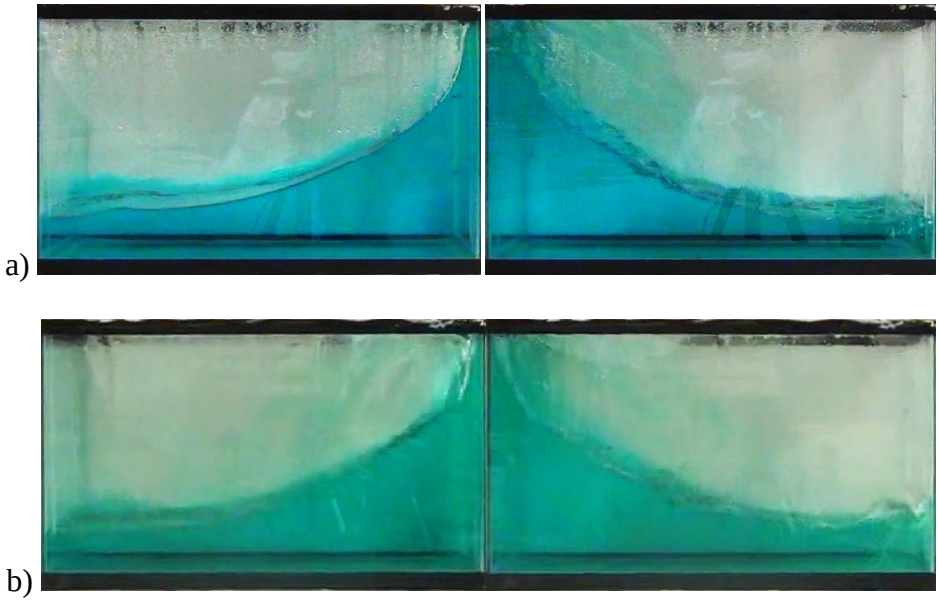

Figure 3- 14 Effect of excitation frequency on general motion of the liquid; a) 30º oriented and b) 60º oriented tank excited by resonance frequency calculated based on tank length create longitudinal waves

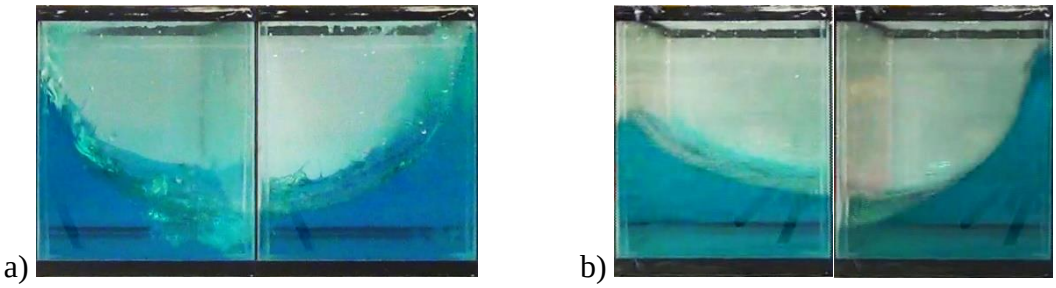

Figure 3- 15 Effect of excitation frequency on general motion of the liquid; a) 30º oriented and b) 60º oriented tank excited by resonance frequency calculated based on tank width create transverse waves

3.4.3. Effect of tank size

As mentioned previously in this section, two tank sizes were used in this series of experiments with the following dimensions:

- Tank 1: 755 × 305 × 300 mm^3
- Tank 2: 495 × 245 × 300 mm^3

The first difference between the two tanks is definitely their resonant frequency, which is a function of tank size and liquid depth. In addition, in the larger tank, impulsive and convective masses are distinguished from one another while in the smaller tank this was not observed. In other words, the liquid separated into two parts in the larger tank while it did not happen in the smaller one. Other than that, in all orientations more non-linear sloshing motions were observed in the smaller tank.

3.4.4. Effect of excitation type and frequency

Among the harmonic motions, the excitation with frequency lower than resonance causes the least movement in the liquid. In terms of liquid motion, the excitation with frequency higher than resonance comes next. The resonance frequency has of course the most violent motion. Figure 3-16 presents a schematic graph of motion against frequency.

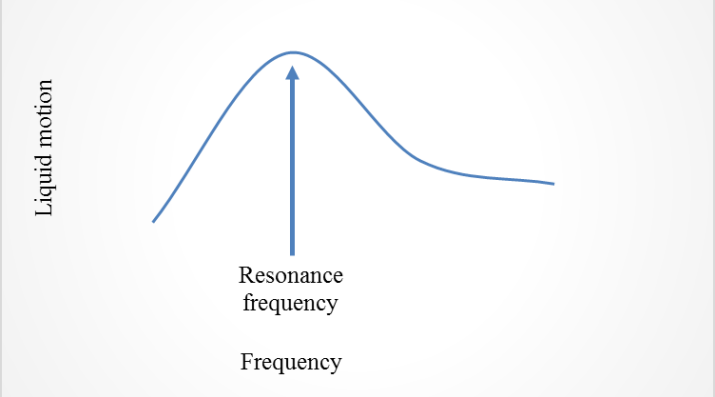

Figure 3- 16 Excitation frequency versus liquid motion

The two earthquake excitations (i.e. real and downscaled El-Centro ground motions) cause the same motion pattern in the liquid surface for each tank the only difference between the two motions is the amount of change in the liquid surface. In other words, the liquid surface moves at the same time with the same shape, but the amount of movement is less in the downscaled earthquake.

To compare the earthquake and harmonic excitations, it was observed that the harmonic ones created constant and steady (i.e. predictable) motion in the liquid while during the earthquakes, the motion was unpredictable.

3.5. Summary

In this experimental study, two different tanks were tested on a shaking table using different types of excitations. The tanks were placed on the table with different orientations in order to find out the effect of bi-lateral ground motion on the liquid. The process was filmed and then frames were extracted and investigated. The results showed that regardless of the excitation type or frequency, in the 30º and 60º oriented tanks the liquid approaches the roof of the tank faster in the corner regions while in the 0º and 90º orientations, there is no significant difference between the corners and middle regions. This shows the importance of special design for the sharp corners in liquid storage tanks.

It was also observed that the Housner's simplified model (Housner, 1963) has a very good accuracy in finding the resonance frequency of the tank.

Chapter 4

Numerical Study

4.1. Introduction

Following the experimental study as was described in Chapter 3, the next part of this study was to develop a numerical solution for the sloshing problem in liquid storage tanks. To do so, a numerical software with ability to solve computational fluid dynamic problems was needed. Among several commercial, educational and open source tools, the OpenFOAM model was chosen for the numerical simulations.

4.1.1. OpenFOAM vs. commercial programs

There are several factors in choosing the proper simulation tool such as:

- Source codes: OpenFOAM is open source, hence one is able to find source codes and make changes in them.
- Operating system: OpenFOAM is available for both Linux (UBUNTU) and Windows platforms. Based on our observations UBUNTU version is relatively faster than Windows version, hence more simulations in less time are possible.
- Working in parallel: In OpenFOAM, the user is able to perform as many simulations as needed at the same time, while most of commercial programs are set to do a limited number of jobs.
- Limitations: There is no limitation in number of nodes, elements, etc. in OpenFOAM, while educational version of commercial programs restrict the user to a limited number of them.

- Price: Unlike commercial programs, OpenFOAM is a free software without any type of restrictions.

4.2. OpenFOAM

Released by OpenCFD Ltd, OpenFOAM is an open source software, able to solve a large variety of numerical problems (e.g. fluid flow in channels, wind tunnel test, heat transfer, etc.), but mainly used in Computational Fluid Dynamics (CFD). In order to solve CFD problems, the software uses Finite Volume Method (FVM). The software is able to solve Navier-Stokes equations (eq. 4.1) that govern the fluid motion.

$$\rho\left(\frac{\partial u}{\partial t} + u.\nabla u\right) = -\nabla p + \nabla.\{\mu\left[\nabla u + (\nabla u)^T\right] - \frac{2}{3}\mu(\nabla.u)I\Big\} + F \qquad (4.1)$$

Where

ρ is density;

u is velocity;

p is pressure;

μ is dynamic viscosity.

OpenFOAM is a C++ library used to create applications. The applications are categorized as: a) solvers and b) utilities. The former is designed to solve a specific problem in continuum mechanics while the later is designed to do operations that involve data manipulation. Numerous solvers and utilities are used in OpenFOAM in order to solve a wide range of problems.

An important feature of OpenFOAM is the ability to accept new solvers and utilities by users with a little knowledge of methods and programming techniques.

Pre- and post-processing environments are other important features of OpenFOAM. The overall structure of OpenFOAM is shown in Figure 4-1.

As mentioned, OpenFOAM is equipped with ready-to-use applications but users are also free to make changes in them or create their own. Applications are divided into two types; Solvers and utilities. The former is designed to solve a problem while the later is used for pre- and post-processing purposes.

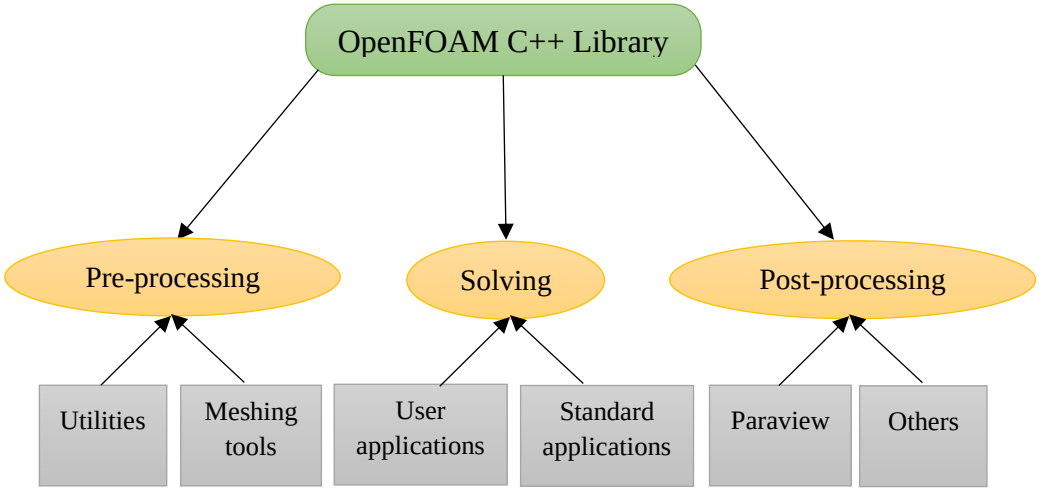

Figure 4- 1 OpenFOAM structure (OpenFOAM users' manual)

4.2.1. OpenFOAM solvers

OpenFOAM contains a variety of solvers for various types of problems. The solvers are designed to simulate a given problem. In order to simulate a problem, the user can either use built-in solvers available in the software package or design a specific solver when necessary. Table 4.1 categorizes some of the OpenFOAM standard solvers.

4.2.2. Generating a new solver

Since OpenFOAM is an open source software, users have access to the source files, hence can generate their own solver instead of using built-in solvers. This makes OpenFOAM a great option for those who want to solve problems with specific method.

Table 4- 1 Some of OpenFOAM standard solvers (OpenFOAM users' guide)

Category	Solver	Problem type to solve
Basic CFD codes	laplacianFoam	Simple Laplace Equation
	potentialFoam	Potential flow
	scalarTransportFoam	Transport equation
Incompressible flow	adjointShapeOptimizationFoam	Incompressible, turbulent flow of non-Newtonian fluids
	boundaryFoam	Incompressible, 1D turbulent flow
	icoFoam	Incompressible, laminar flow of Newtonian fluids
	nonNewtonianIcoFoam	Incompressible, laminar flow of non-Newtonian fluids
	pimpleFoam	Incompressible flow
	pisoFoam	Incompressible flow
	shallowWaterFoam	Inviscid shallow-water equations with rotation
	simpleFoam	Incompressible, turbulent flow
Compressible flow	rhoCentralDyMFoam	Density-based compressible flow with support for changes
	rhoCentralFoam	Density-based compressible flow
	rhoPimpleFoam	Laminar or turbulent flow of compressible fluids for HVAC
	rhoPorousSimpleFoam	Turbulent flow of compressible fluids
	rhoSimplecFoam	Laminar or turbulent RANS flow of compressible fluids
	sonicDyMFoam	Trans-sonic/supersonic, laminar or turbulent flow of a compressible gas with mesh motion
	sonicFoam	trans-sonic/supersonic, laminar or turbulent flow of a compressible gas
	sonicLiquidFoam	Trans-sonic/supersonic, laminar flow of a compressible liquid
Multiphase flow	cavitatingDyMFoam	Transient cavitation
	cavitatingFoam	Transient cavitation
	compressibleInterDyMFoam	Two compressible, non-isothermal immiscible fluids with optional mesh
	compressibleInterFoam	Two compressible, non-isothermal immiscible fluids
	compressibleMultiphaseInterFoam	n compressible, non-isothermal immiscible fluids
	driftFluxFoam	Two incompressible fluids using with the drift-flux approximation
	interFoam	Two incompressible, isothermal immiscible fluids
	interDyMFoam	Two incompressible, isothermal immiscible fluids with optional mesh
	interMixingFoam	Three incompressible fluids, two of which are miscible
	interPhaseChangeFoam	Two incompressible, isothermal immiscible fluids with phase-change
	interPhaseChangeDyMFoam	Two incompressible, isothermal immiscible fluids with phase-change and optional mesh
	multiphaseEulerFoam	System of many compressible fluid phases including heat-transfer
	multiphaseInterFoam	n incompressible fluids
	potentialFreeSurfaceFoam	Incompressible Navier-Stokes solver with inclusion of a wave height
	reactingEulerFoam	
	twoLiquidMixingFoam	Mixing two incompressible fluids
	twoPhaseEulerFoam	System of two compressible fluid phases with one phase dispersed

4.2.3. Running applications

The applications are planned to be run from a terminal window by reading and writing data from command lines. The applications can be executed in parallel. In addition, it is possible to get a log file while the compilation is in progress.

4.2.4. File and folder structure in an OpenFOAM project

Initially, in an OpenFOAM simulation project, there are three folders indicating initial conditions, boundary conditions, mesh generation, material properties, etc. Typical pre-simulation and post-simulation OpenFOAM project folders are shown in Figures 4- 2 and 4- 3 respectively.

4.2.4.1. “Constant”

In this folder physical properties of the case as well as the mesh type, etc. are described.

4.2.4.2. “System”

This folder contains files used to set parameters that are related to solution process. The following three files should be available in this folder: **a) controlDict;** including parameters such as start and end time, time steps, writing intervals, **b) fvSchemes;** used to choose discretization scheme, and **c) fvSolution;** equation solvers, tolerances and algorithms are controlled from this dictionary.

4.2.4.3. “0”

This folder represents initial conditions of the project. In this folder initial values and boundary conditions (for time t=0) are set by the user.

While the simulation is running, time folders are added by OpenFOAM, each containing data for that specific time step. Number of these folders can be controlled by a function that indicates

writing intervals from the controlDict file. Contents of folders ‘constant’, ‘system’ and ‘0’ are shown in Figure 4- 4.

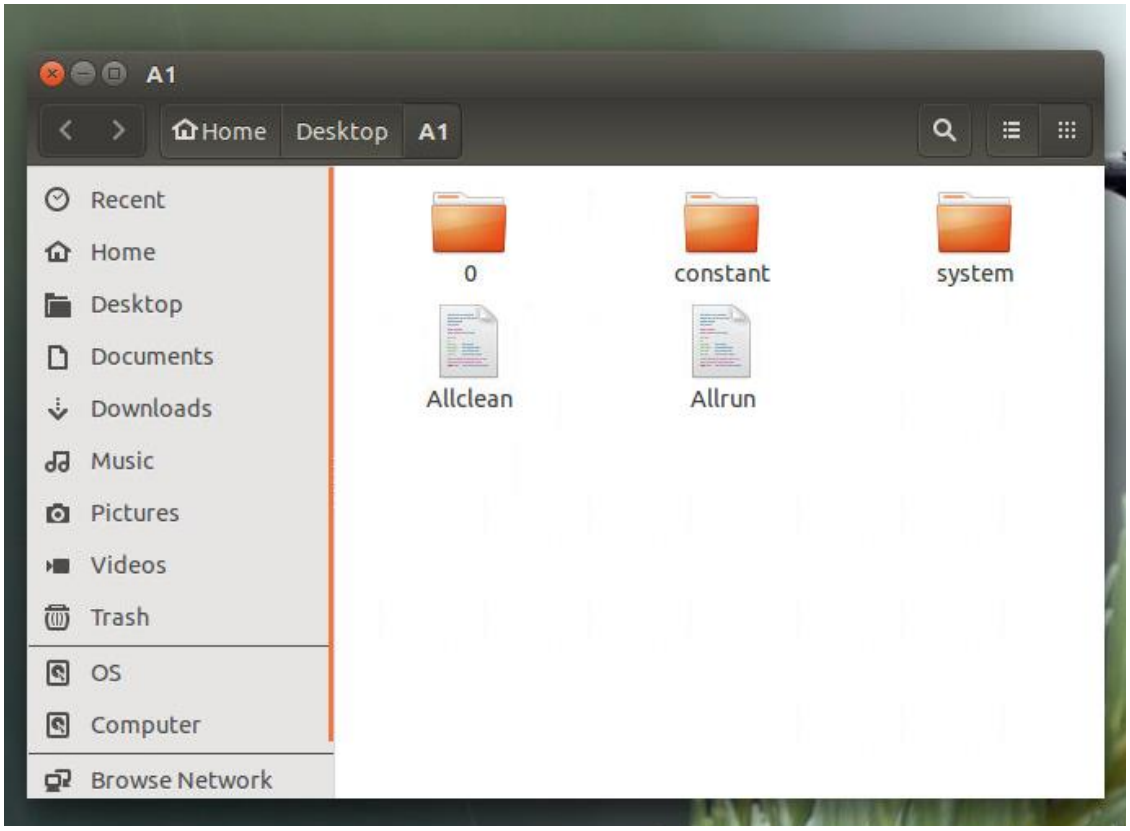

Figure 4- 2 OpenFOAM project folder before simulation

4.2.5. Mesh Generation

Mesh is a fundamental part of numerical methods. It should meet some specifications so that the solution can be acceptable. While running, the software validates the mesh and makes sure it fulfils the necessary characteristics. As a result, the user might be asked to ‘correct’ the mesh, especially when a mesh is generated by a third-party utility.

In OpenFOAM, the default mesh type is called polyMesh, with arbitrary polyhedral cells in 3-D, bounded by arbitrary polygonal faces. In this type of mesh, there is no limitation on number of

faces or edges and cell alignment. This gives the user a great freedom, especially when dealing with complicated geometry.

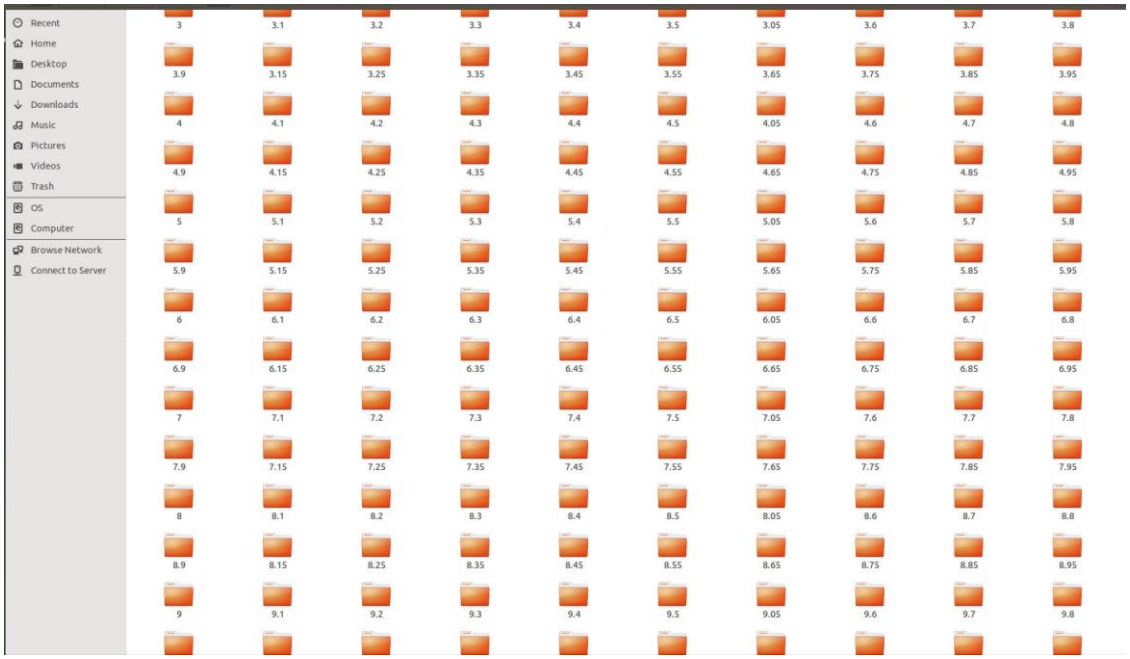

Figure 4- 3 OpenFOAM project folder after simulation

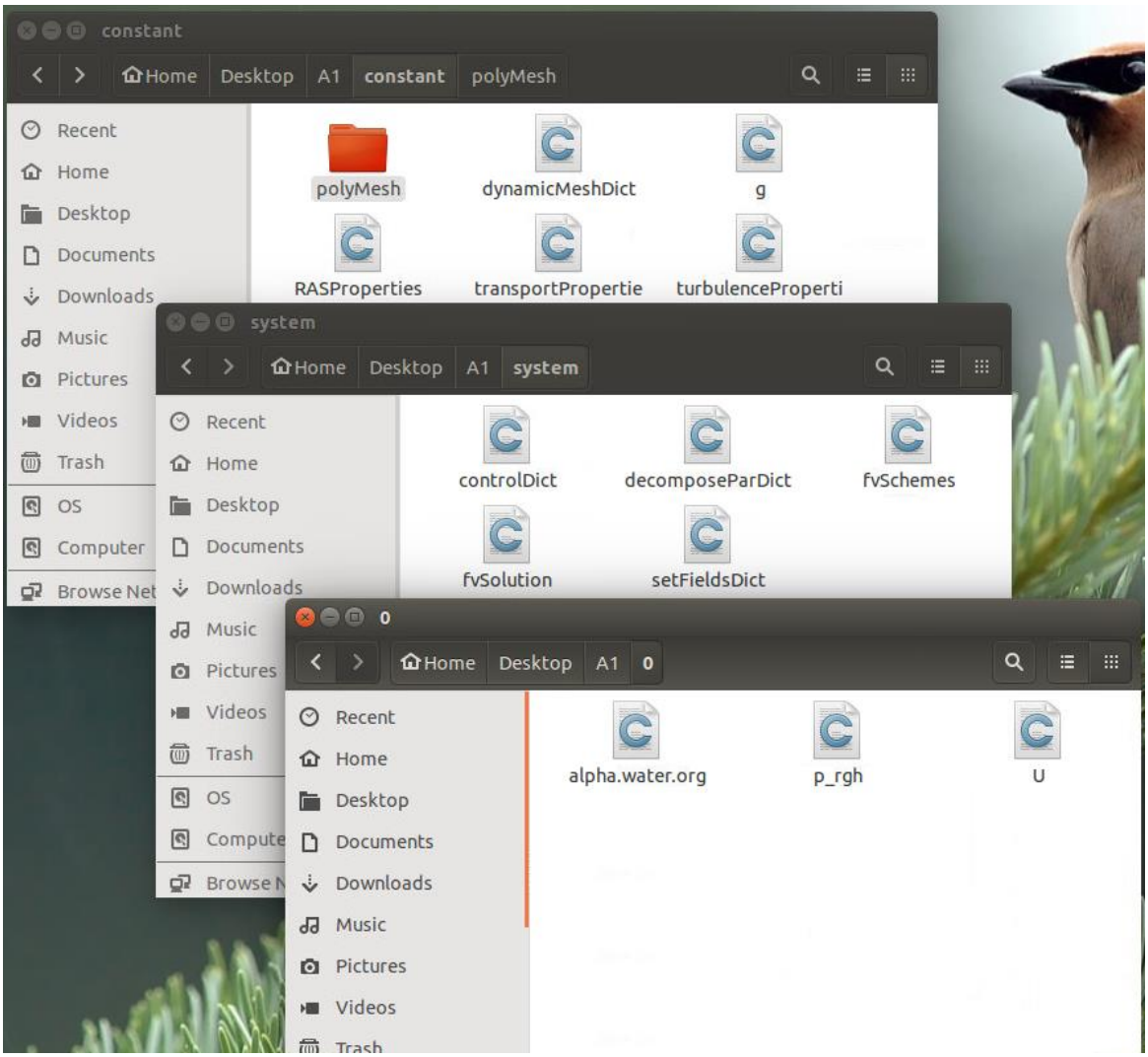

Figure 4- 4 Contents of folders 'constant', 'system' and '0'

4.2.6. Post-processing

For post-processing, commercial and free tools are available. OpenFOAM, is able to use either a third party software, or the pre-supplied tool named paraFoam. ParaFoam uses an open source visualization utility, ParaView (Figure 4- 5). This visualization tool is able to show different parameters such as liquid surface, pressure, velocity etc. in a simulation project.

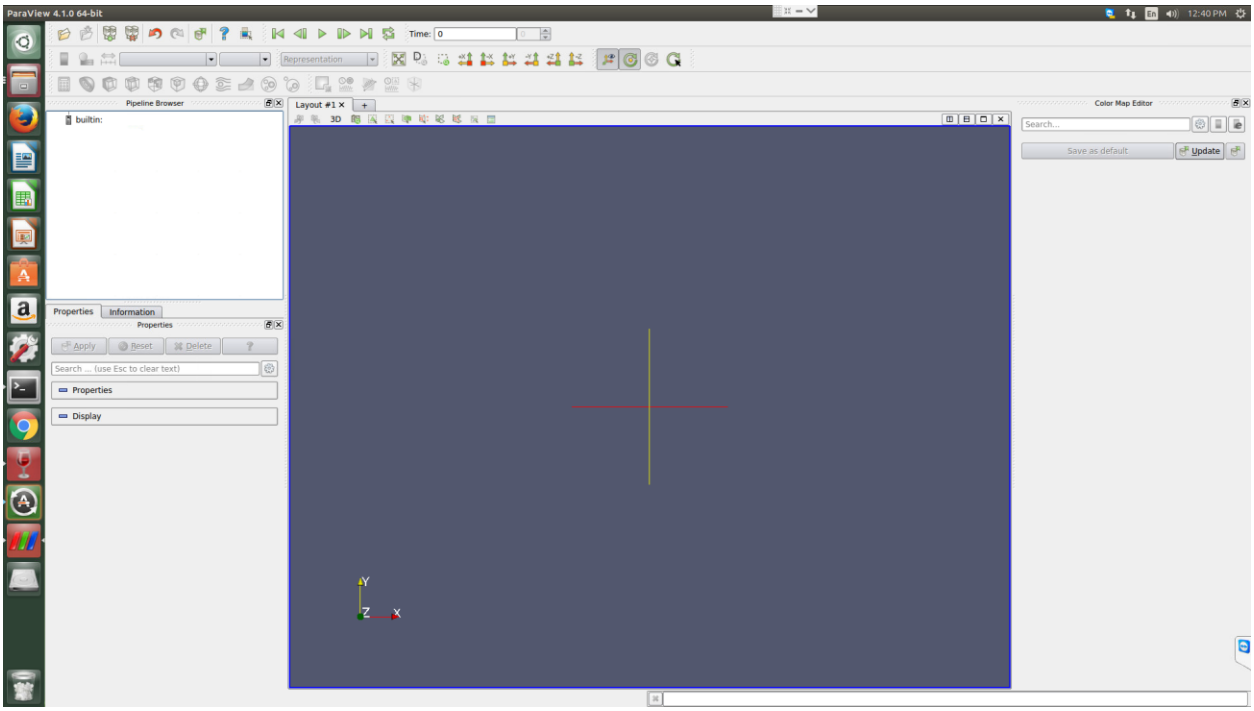

Figure 4- 5 ParaView

4.3. Current study; OpenFOAM simulations

In this part, the simulation procedure is presented. The steps are defining the geometry, mesh, time steps and characteristics of the tank movement and then running the code. After the cod was run and the simulation finished, post-processing analysis starts.

The numerical study was done with tanks with the same sizes as the experimental study so that the results can be compared.

4.3.1. Choosing the solver

In this study, a built-in solver - interDyMFoam - was used. The solver can simulate multiphase fluid (e.g. water and air). Finite volume method (FVM) is adopted by the solver to simulate the liquid part in conjugation with the volume of fluid (VOF) method to estimate the surface.

4.3.2. Defining the geometry

From the folder ‘constant’, sub-folder ‘polyMesh’, the file blockMeshDict (Figure 4- 6) defines the geometry and the mesh of the tank.

A block should be introduced with tank specifications e.g. dimensions and rotation angle. The block is defined by its points, edges, and faces. To apply the rotation angle, the angle should first be converted to radian, then rotation matrix should be applied to each node to ensure that the node’s position will change based on the angle.

For the code developed in this study, there are some parameters defined by the user i.e. tank size (length, width, height), water level, rotation angle, number of elements in each direction (which defines the mesh size). There are also parameters that are calculated based on user-defined parameters e.g. origin of the coordinate system and location of the points.

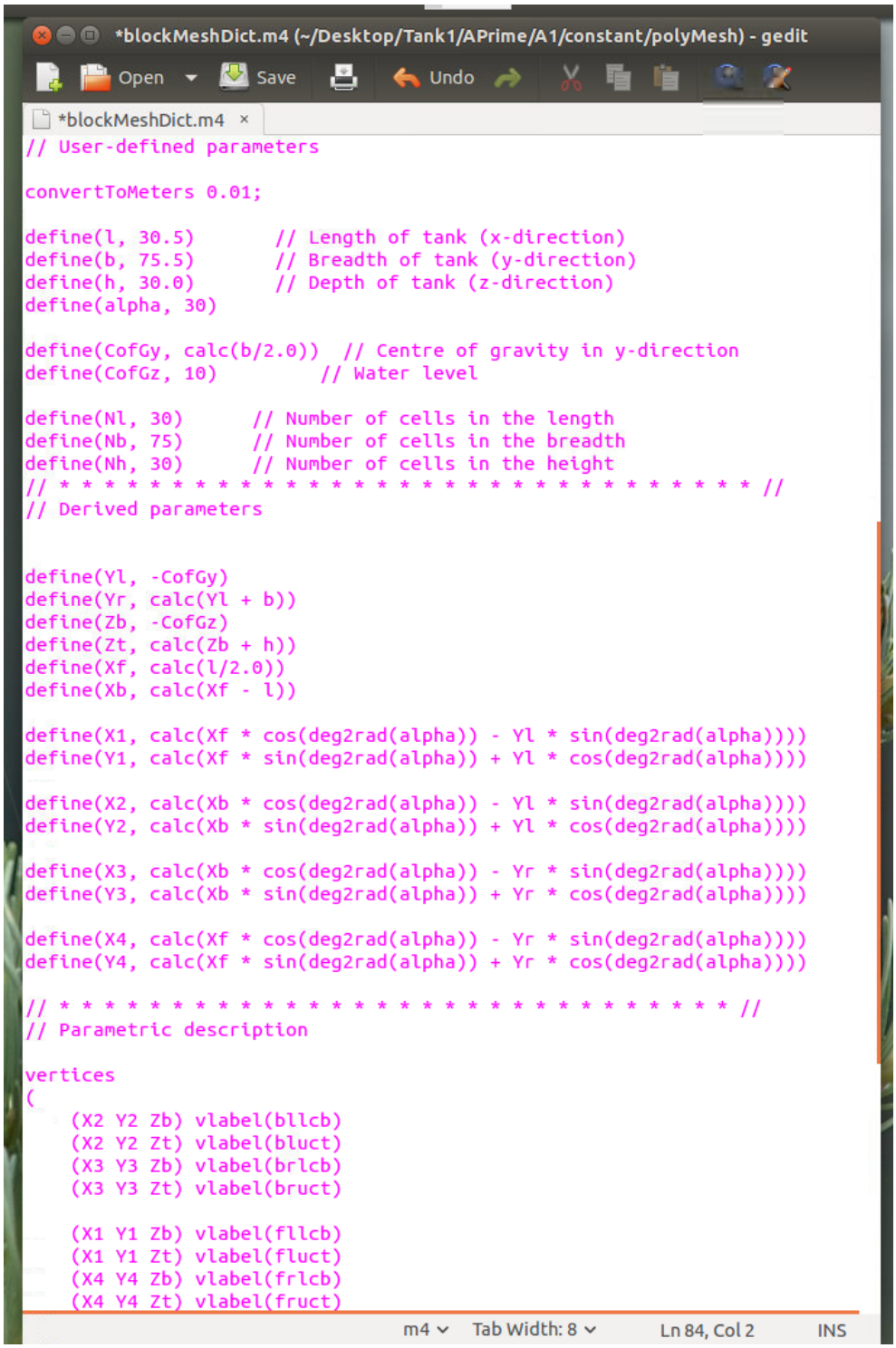

Figure 4- 6 blockMeshDict

4.3.3. Setting time and time controls

In the folder ‘system’ there is a dictionary to control the timing of the simulation, named controlDict (Figure 4- 7). From this dictionary, the user is able to set start/stop time, time steps and writing intervals.

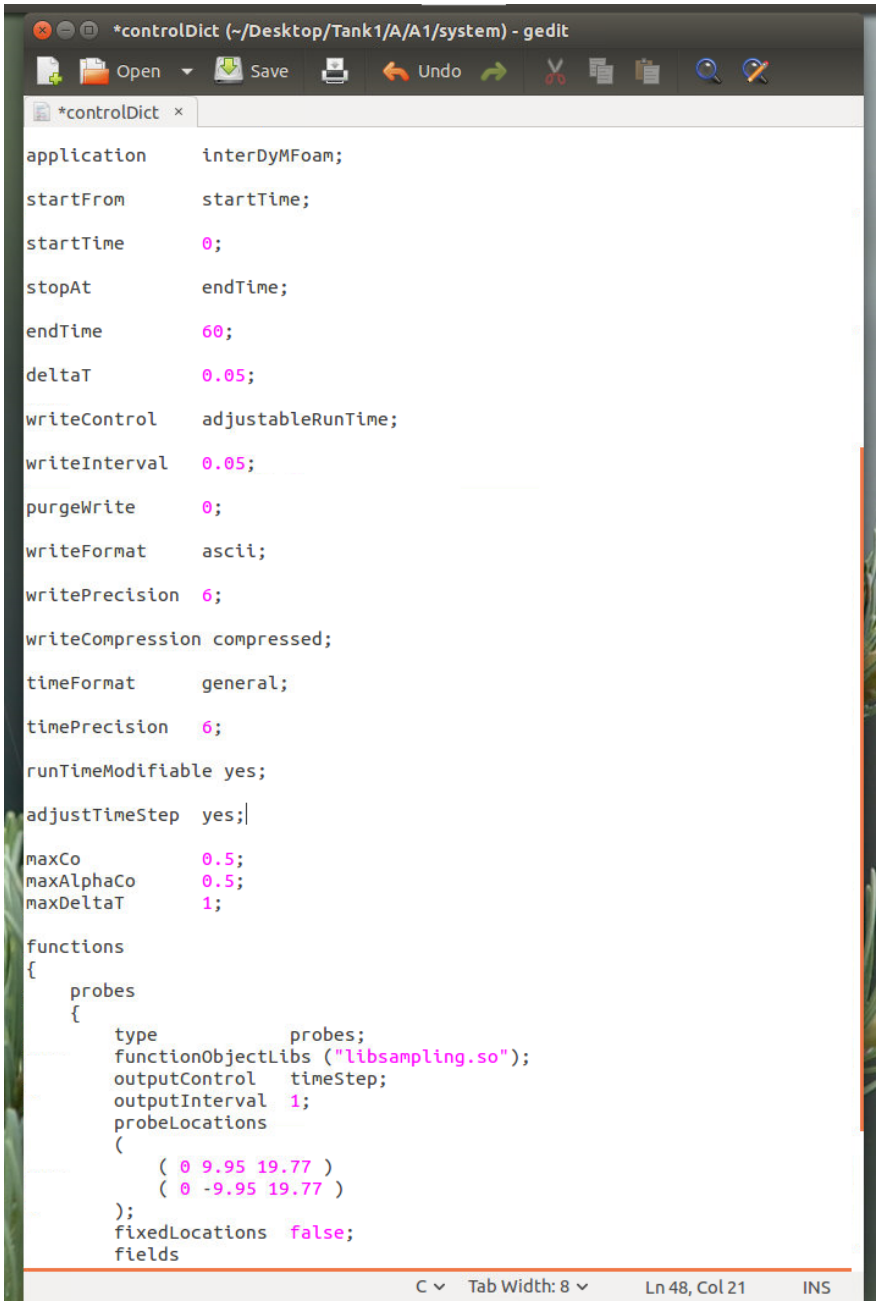

Figure 4- 7 controlDict

For this study, the time was set to start on 0 and end on 60, which gives a one-minute simulation. The time step and writing interval were chosen based on computation time and sensitivity of the simulation to time intervals.

4.3.4. Assigning the tank movement

To control the tank motion, a dictionary is available in the folder 'constant' called dynamicMeshDict (Figure 4-8). Through this dictionary, different types of movements can be applied to the tank, from harmonic translation (like what happens during an earthquake) to swinging movement (like what happens in a ship).

As indicated in Chapter 3, a harmonic motion follows the following equation:

$$u(t) = A \sin \omega t \qquad (4.2)$$

Where

u is the displacement;

A is the displacement amplitude;

ω is the excitation frequency;

t is the time.

To define the harmonic translation in the dictionary dynamicMeshDict, parameters amplitude (A) and omega (ω) should be determined.

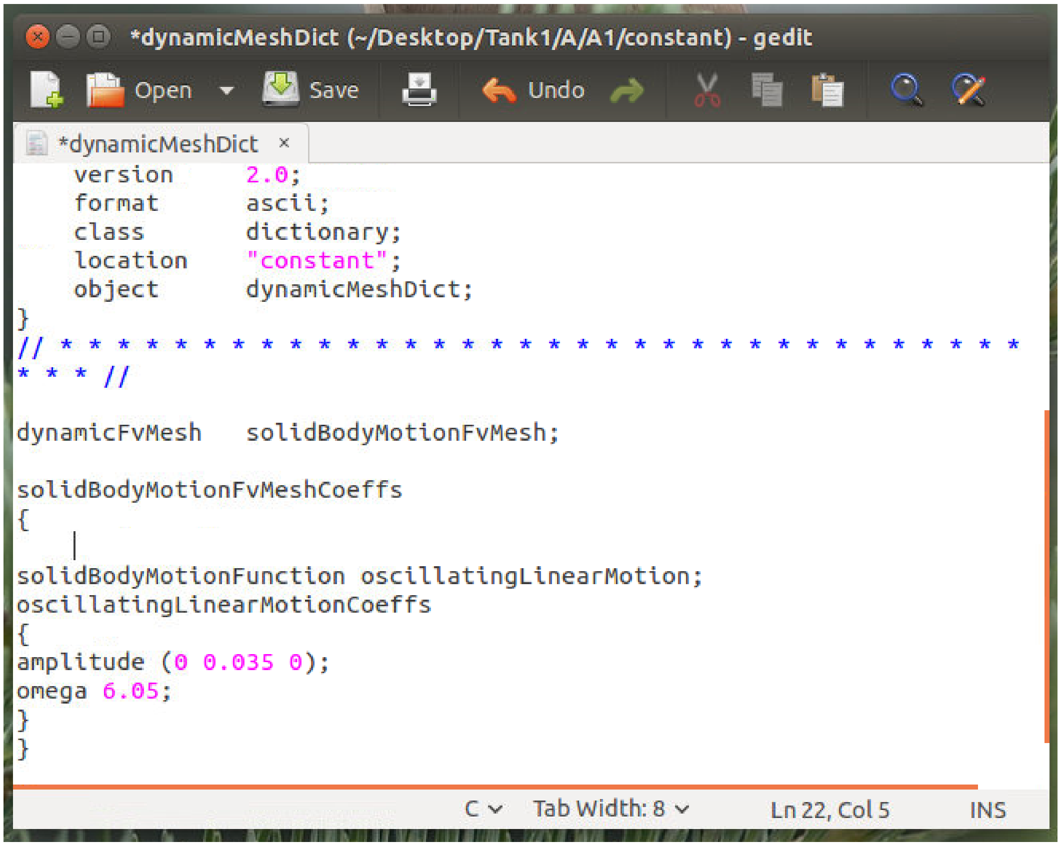

*dynamicMeshDict (~/Desktop/Tank1/A/A1/constant) - gedit

```
    version     2.0;
    format      ascii;
    class       dictionary;
    location    "constant";
    object      dynamicMeshDict;
}
// * * * * * * * * * * * * * * * * * * * * * * * * * * * * * * * * * * *
* * * //

dynamicFvMesh   solidBodyMotionFvMesh;

solidBodyMotionFvMeshCoeffs
{

solidBodyMotionFunction oscillatingLinearMotion;
oscillatingLinearMotionCoeffs
{
amplitude (0 0.035 0);
omega 6.05;
}
}
```

C Tab Width: 8 Ln 22, Col 5 INS

Figure 4- 8 Parameters in dynamicMeshDict

4.3.5. Turbulence model and transport properties

This section helps to assign turbulence model and transport properties of the liquid. From the folder constant, turbulence properties is assigned laminar and transport properties are set to Newtonian for both water and air. For liquids other than water (e.g. oil), one can change the density (ρ, rho) and viscosity (ν, nu) in the transport properties dictionary.

In the current study the gravity effect is higher than the turbulence effect, hence turbulence effects were ignored. Experimental study also approved this assumption.

4.3.6. Finite Volume Schemes

From the file fvSchemes, different finite volume characteristics (e.g. diversion scheme and interpolation scheme) can be defined. This can help the user find the best solution for their finite volume problem.

4.3.7. Running the simulation

After everything is set, the user can start running the application. This process starts with opening a terminal window. First the terminal should be directed to the project folder. Then the file blockMeshDict should be converted from m4 macro (application/x-m4) to C source code (text/x-crsc). This is done by the following order in the terminal:

"m4 constant/polyMesh/blockMeshDict.m4 > constant/polyMesh/blockMeshDict"

After that, the application is ready to create the block by this simple order: "blockMesh"

The next step that is similar in almost all OpenFOAM projects is to copy the file alpha.water.org to alpha.water in the folder '0'. This can be done manually by copying and pasting the file with the new name or by the following order: "cp 0/alpha.water.org 0/alpha.water". This order copies the file and pastes it with the new name in the same folder.

After the file is copied, the code "setFields" is the employed in the next step. This order prepares the boundary conditions, etc. for the project. Finally by typing the solver's name i.e. interDyMFoam, the project stars being executed.

4.3.8. Post-processing

The time needed for execution of the code depends on different factors e.g. mesh size, time steps, simulation duration, turbulence model, and computer's power. In this study, the amplitude and

frequency of the harmonic sinusoidal motions were also effective in simulation speed. On average, each simulation took around 50 hours with the available equipment.

After the simulation is done, one can start their post-processing analysis. To do so, the visualization tool - ParaView - can be used. ParaView is started by typing the code “paraFoam” in the terminal. This visualization tool was introduced briefly in the OpenFOAM section of this chapter.

The application has the ability to show different characteristics, e.g. liquid surface, hydrodynamic pressure on the walls, liquid velocity, etc. from different view angles. It also provides the user with a tool to create animations from the job with the desired frame rate and size.

In this study, the animation creation tool was used to make videos out of the simulations. Then frames were extracted from the videos so that they could be compared with the ones from the experimental part.

Since the time step in this project was 0.05 sec, the frame rate was chosen 20 fps so that the animations’ duration and timing did not change.

Animations were created from three different views, where two of them were XZ and YZ planes (i.e. the same view as cameras in the experimental part) and a 3D view to track the surface easier.

4.4. Observations

Numerical simulations resulted in some observations as follows:

- The experimental study (Chapter 3) showed that prediction of the resonance frequency is acceptable in Housner’s simplified model. The same frequency in the adopted numerical model resulted in resonance as well. In other words the model was accurate in finding the resonance frequency.

- In general, changing the tank orientation from 0º or 90º to 30º or 60º increases the liquid sloshing near sharp corners of the tank; i.e. if the tank is parallel or perpendicular to the direction of base excitation, it faces less pressure on the corners while in other directions the pressure in corner areas increases.
- The excitation frequency is more important than tank orientation in general motion of the liquid inside the tank. If the tank has a 0º, 30º or 60º orientation and is excited by a frequency close to resonance frequency calculated based on the tank length, the general motion of the liquid is longitudinal. But if the tank is oriented 30º, 60º or 90º the excitation frequency is close to resonance based on width of the tank, the general liquid motion becomes transverse

4.5. Comparison of the experimental and numerical studies

One of the goals of this study was to develop a numerical model to predict the liquid surface behavior in a tank subjected to seismic loading. In this section the two parts of the study i.e. experimental work and numerical simulations will be compared to examine the validity of the proposed model. In this comparison, these cases with respect to sloshing frequency were considered. These include frequencies higher, equal to and lower than the resonance frequency respectively.

4.5.1. Tank 1, water depth 100 mm, 0º orientation

For this case, a fairly acceptable agreement was observed between the two parts of study regarding the liquid surface as described below.

a) Frequency: higher than resonance

Extracted images from the videos of XZ plane, show a fairly acceptable agreement between the numerical and experimental studies for this frequency. The comparisons are presented in Figure 4-9.

a)

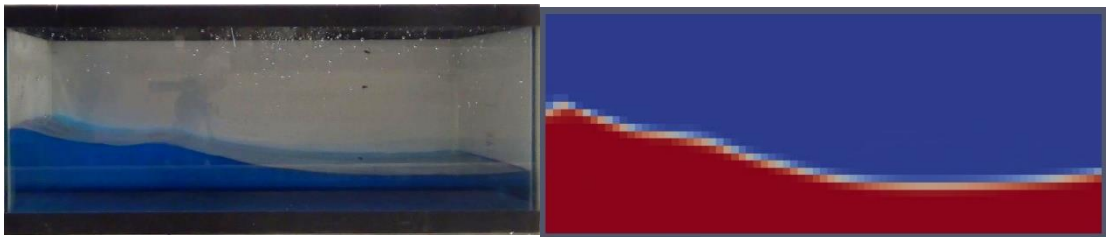

b)

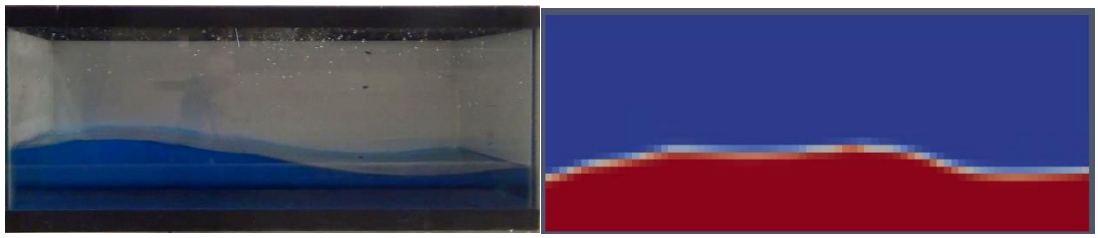

c)

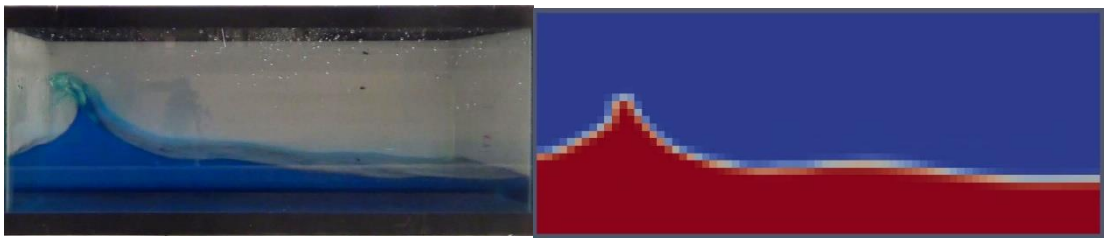

d)

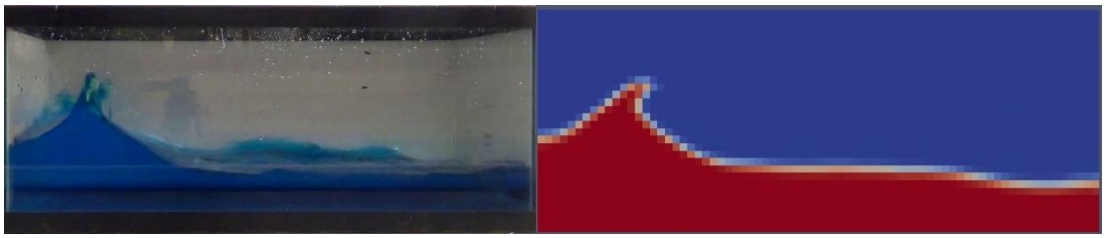

e)

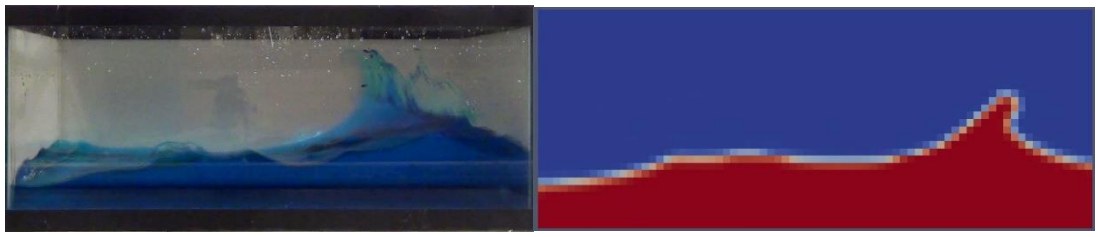

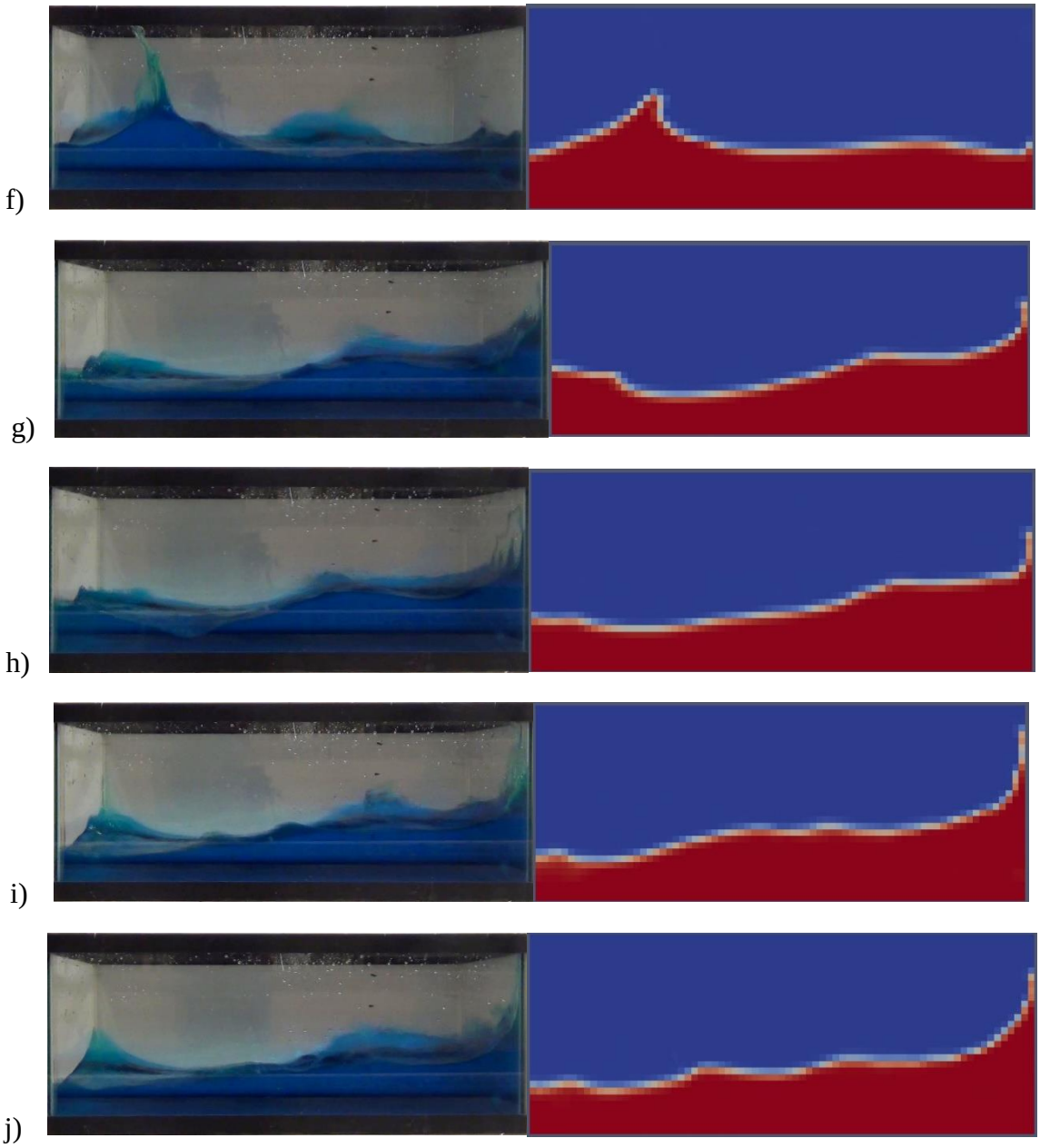

Figure 4- 9 Comparison of free surface in experimental (left) and numerical (right) studies in tank 1 with 100 mm of water, 0º orientation and frequency of higher than resonance

b) Frequency: Resonance

A very good agreement was observed in this frequency between the two parts of study. Both parts and the Housner's simplified method showed the same resonance frequency and the liquid surface well matched in experimental and numerical methods (Figure 4- 10).

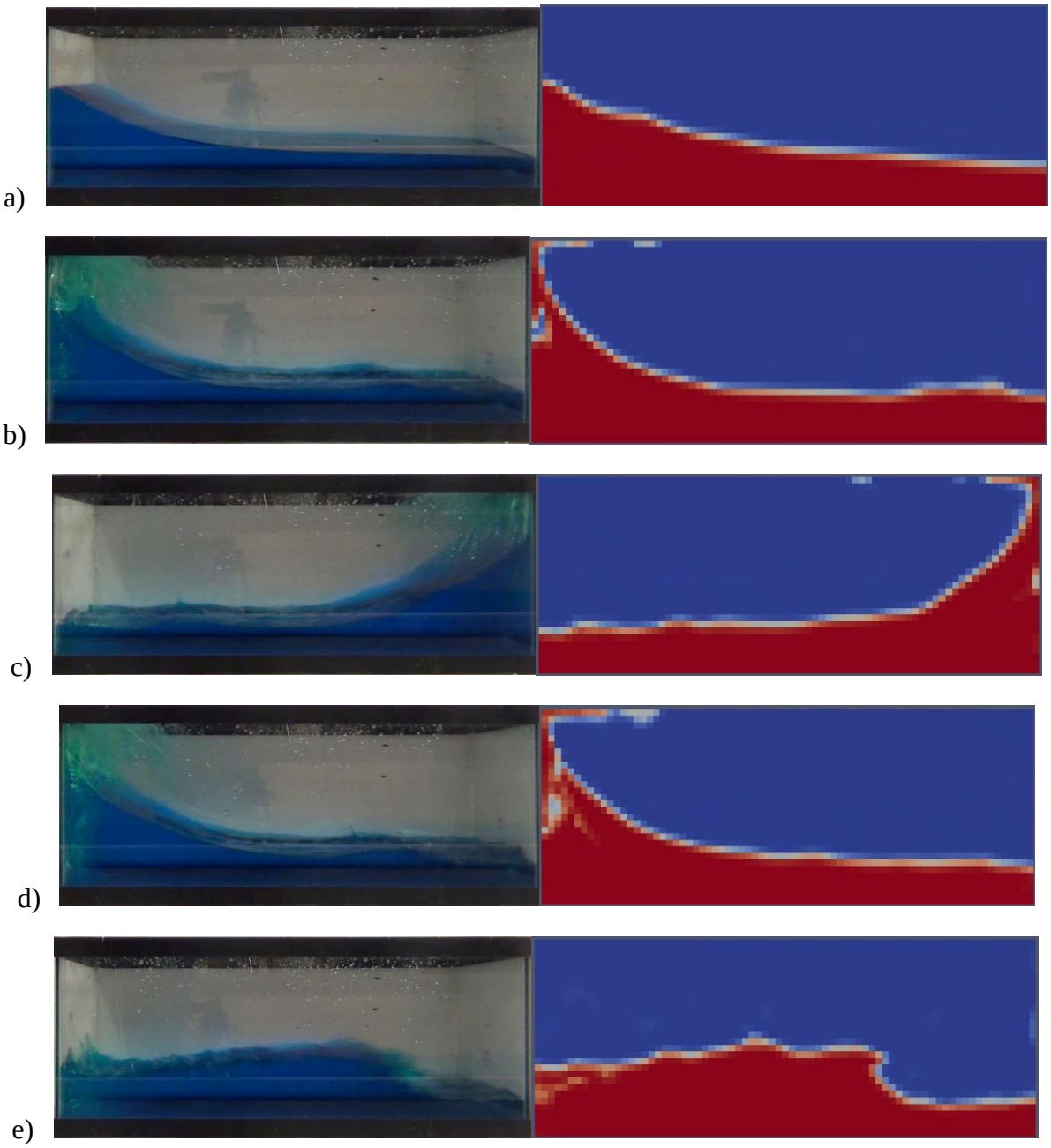

Figure 4- 10 Comparison of free surface experimental (left) and numerical (right) studies in tank 1 with 100 mm of water, 0^o orientation and resonance frequency

c) Frequency: Lower than resonance

Although in this frequency the liquid surface does not have significant motions in either case, the available small movements agree well. Figures 4- 11. a to 4- 11. e show these comparisons.

a)

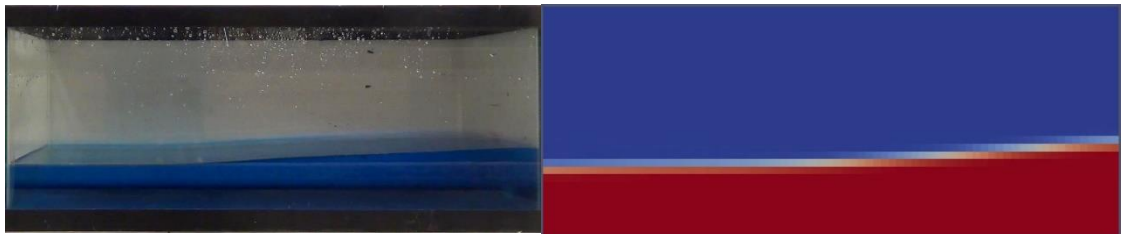

b)

c)

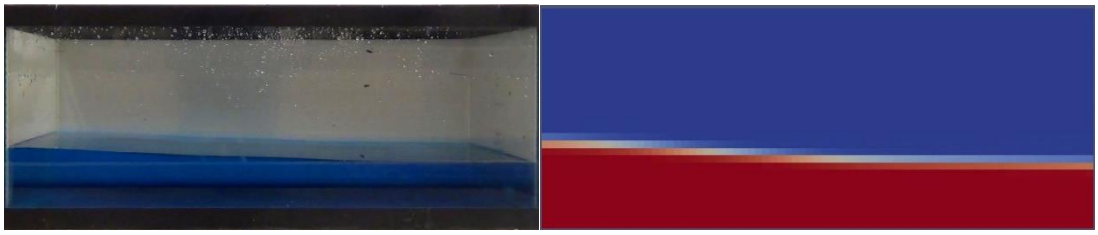

Figure 4- 11 Comparison of free surface in experimental (left) and numerical (right) studies in tank 1 with 100 mm of water, 0º orientation and frequency of lower than resonance

4.5.2. Tank 1, water depth 100 mm, 30º orientation

In this orientation the liquid surface should be investigated from both sides, in other words images extracted from both cameras (located on XZ and YZ plains) need to be reviewed and compared.

a) Frequency: higher than resonance

This frequency results in much motions but in different directions, hence damped by the liquid itself. Comparison of the surface in numerical and experimental studies in both directions (Figure 4- 12) show a good agreement but it can still be improved by improvement of the numerical model.

a)

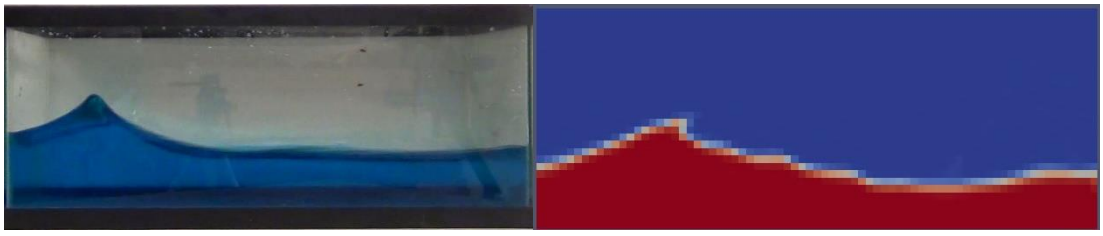

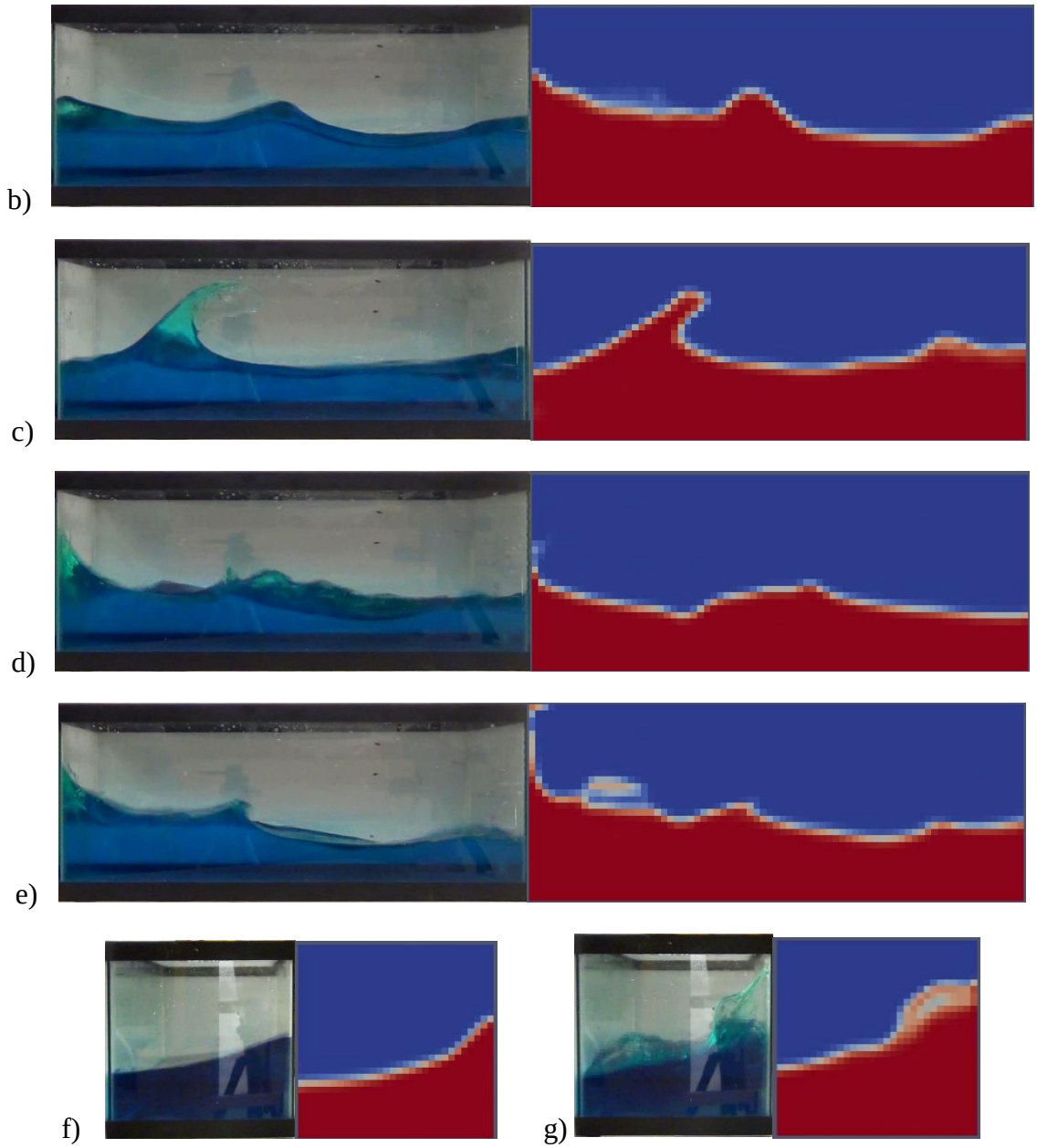

Figure 4- 12 Comparison of free surface in experimental (left) and numerical (right) studies in tank 1 with 100 mm of water, 30º orientation and frequency of higher than resonance

b) Frequency: Resonance

Resonance frequency images show an acceptable agreement between the numerical model and experimental test in this orientation (Figure 4- 13).

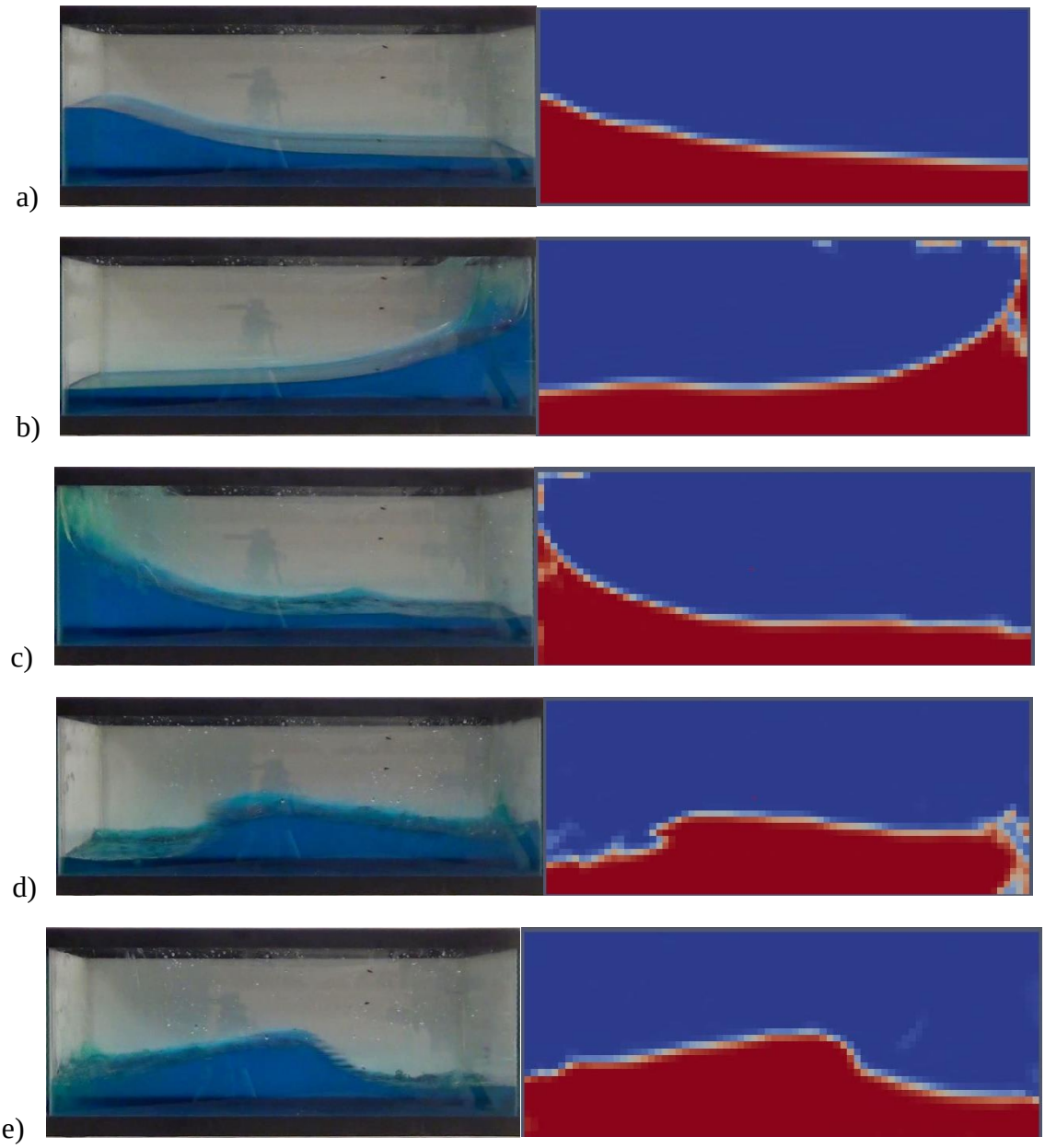

Figure 4- 13 Comparison of free surface in experimental (left) and numerical (right) studies in tank 1 with 100 mm of water, 30º orientation and resonance frequency

c) Frequency: Lower than resonance

As mentioned in the previous orientation, this frequency does not create strong motions (Figures 4- 14. a and 4- 14. b), but those available small motions are similar in both experimental and numerical parts.

a)

b)

Figure 4- 14 Comparison of free surface in experimental (left) and numerical (right) studies in tank 1 with 100 mm of water, 30º orientation and frequency of lower than resonance

4.5.3. Tank 1, water depth 100 mm, 60º orientation

In this orientation, general motion of the liquid depends on the excitation frequency. It can be either longitudinal or transverse. But regardless of the general motion, there is a higher water level in the corners of the tank.

a) Frequency: higher than resonance

Since this frequency is closer to resonance frequency based on the tank width, it causes transverse motions in the water surface. Images from the videos show an acceptable agreement between the numerical and experimental study, although the numerical model can be improved to make a better agreement (Figure 4- 15).

a)

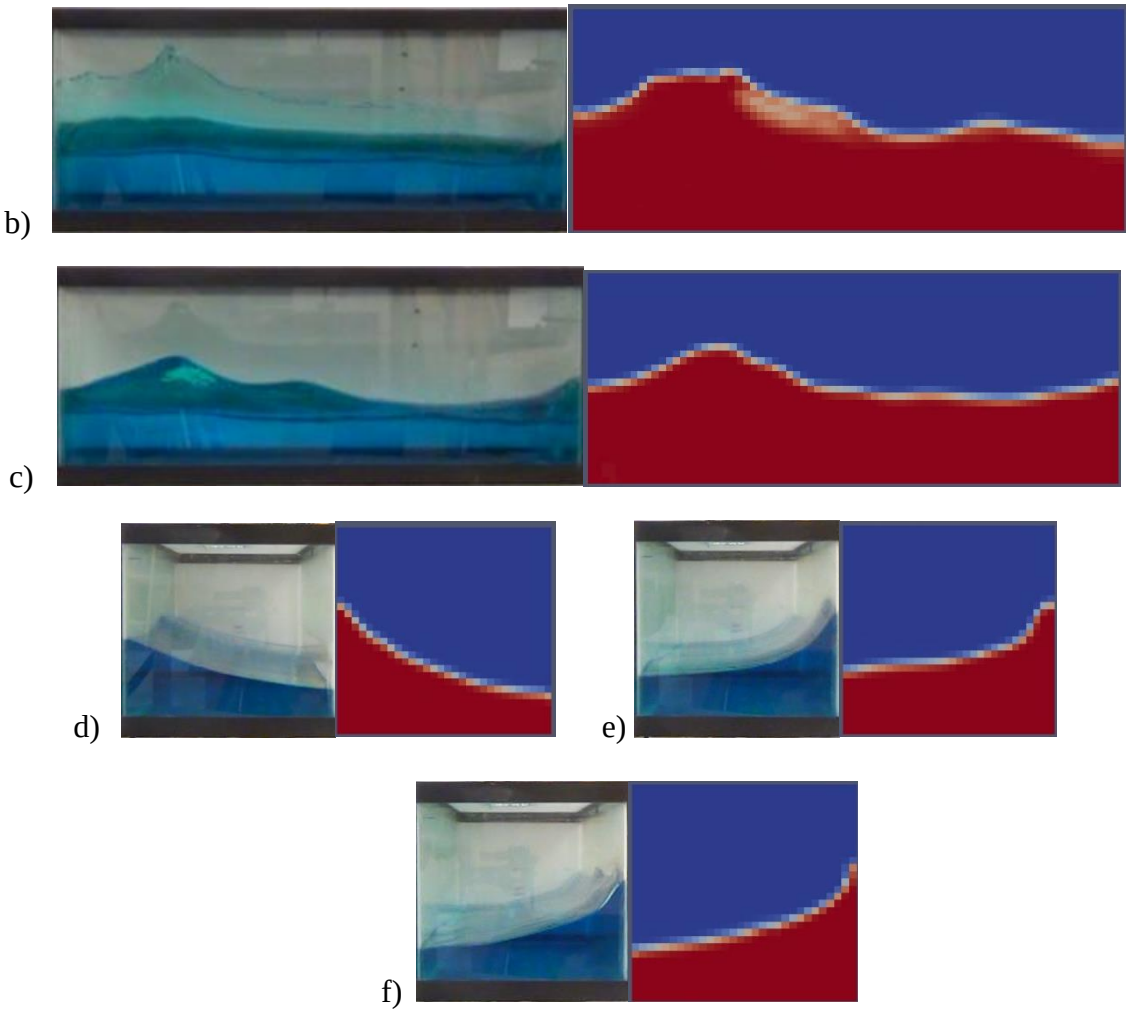

Figure 4- 15 Comparison of free surface in experimental (left) and numerical (right) studies in tank 1 with 100 mm of water, 60º orientation and frequency of higher than resonance

b) Frequency: Resonance

In this frequency, general motion of the liquid is longitudinal. The images show a really good agreement between the experiment and simulation (Figure 4- 16).

b)

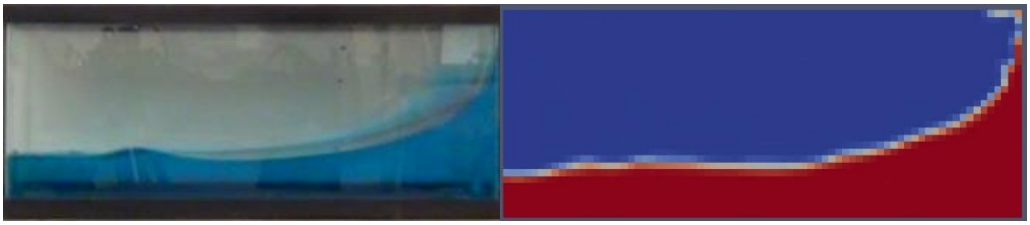

c)

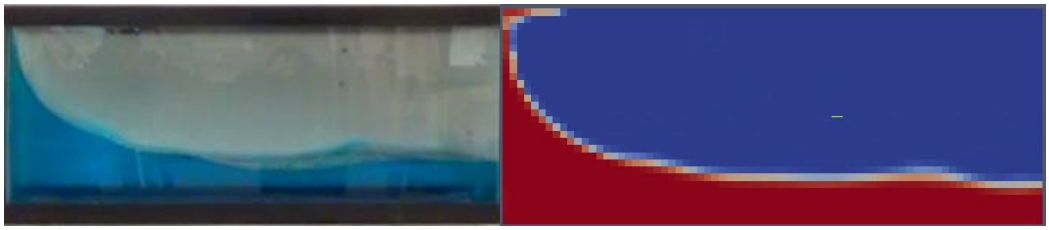

Figure 4- 16 Comparison of free surface in experimental (left) and numerical (right) studies in tank 1 with 100 mm of water, 60º orientation and resonance frequency

c) Frequency: Lower than resonance

Figure 4- 17 shows that the liquid does not move much, like previous orientations in this frequency, but the small movement agrees in both parts.

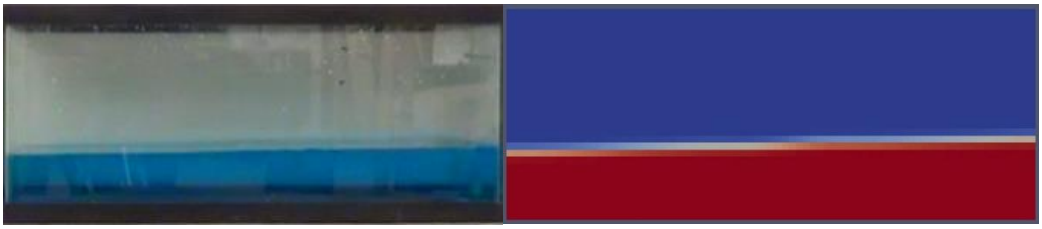

Figure 4- 17 Comparison of free surface in experimental (left) and numerical (right) studies in tank 1 with 100 mm of water, 60º orientation and frequency of lower than resonance

4.5.4. Tank 1, water depth 100 mm, 90º orientation

This final orientation of the tank was the least crucial among all orientations. Longitudinal resonance frequency does not cause resonance motion anymore and the liquid motion is damped quickly.

a) Frequency: higher than resonance

Extracted images show that in this frequency the model and experiment have a good agreement in YZ plain (Figures 4- 18. c to 4- 18. f) but the model needs improvement for XZ plain (Figures 4- 18. a and 4- 18. b)

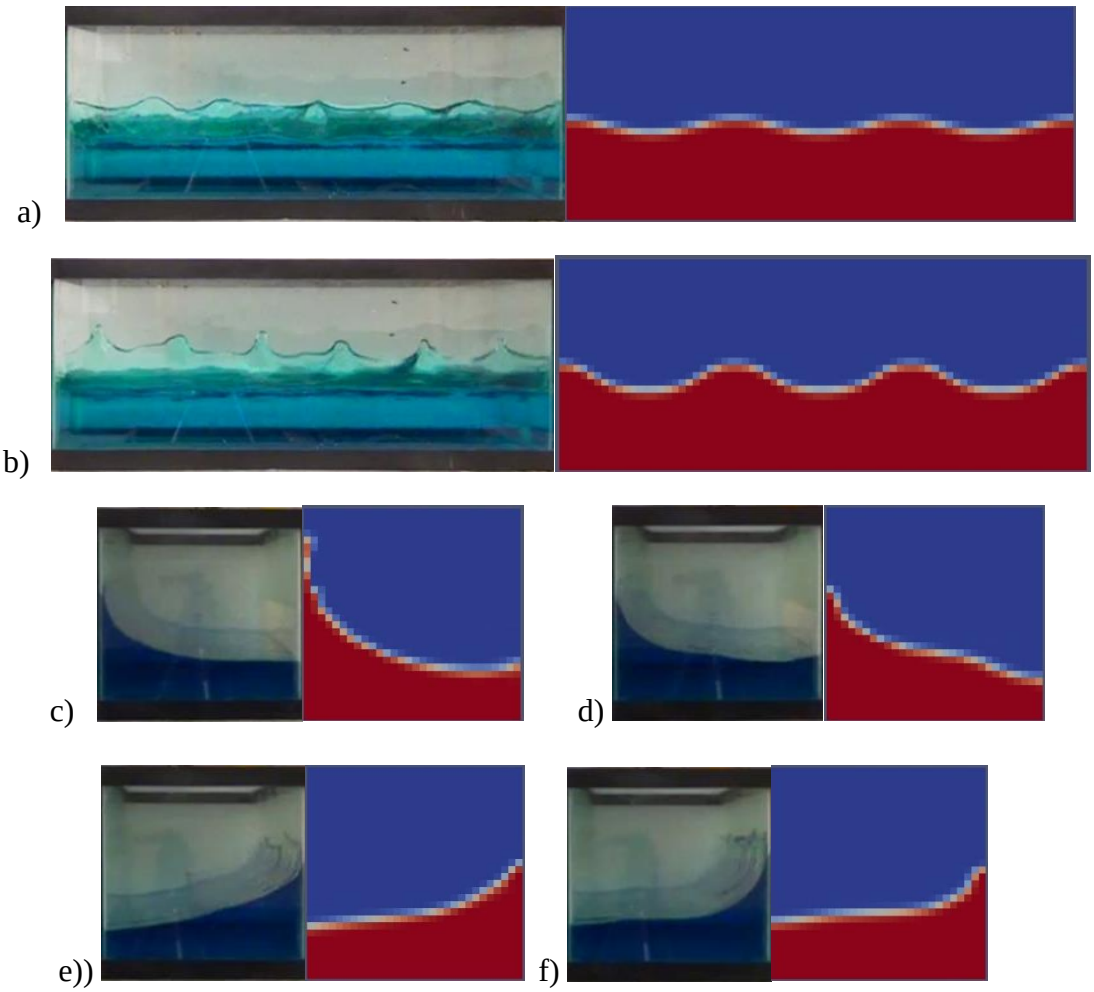

Figure 4- 18 Comparison of free surface in experimental (left) and numerical (right) studies in tank 1 with 100 mm of water, 90º orientation and frequency of higher than resonance

b) Frequency: Resonance

As mentioned above, this frequency does not create resonance motion in the liquid. Only a few waves are produced. Comparisons (Figures 4- 19. a and 4- 19. b) show a good agreement in this motion.

a)  b) 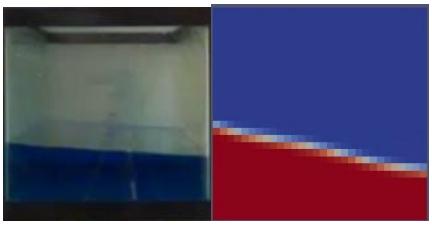

Figure 4- 19 Comparison of free surface in experimental (left) and numerical (right) studies in tank 1 with 100 mm of water, 90º orientation and resonance frequency

c) Frequency: Lower than resonance

Motions in this frequency are much less than other frequencies and again the experimental and numerical results agree well (Figure 4- 20).

a) 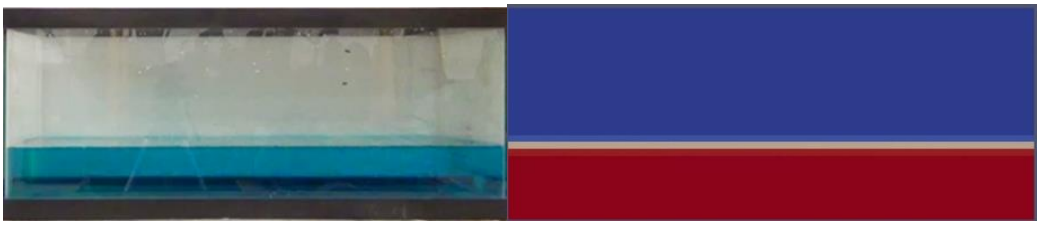

b) 

Figure 4- 20 Comparison of free surface in experimental (left) and numerical (right) studies in tank 1 with 100 mm of water, 90º orientation and frequency of lower than resonance

4.5.5. Tank 1, water depth 200 mm, 0º orientation

The added water changes the resonance frequency of the tank as it causes a change in convective and impulsive masses and heights. In this new depth, the accuracy of the numerical model decreases in most cases. This fact shows that the model needs to be improved in order that one can use it regardless of the liquid depth. Comparisons between numerical and experimental studies for this water depth (i.e. 200 mm) are presented in Figures 4- 21 to 4- 33.

a) Frequency: higher than resonance

a)

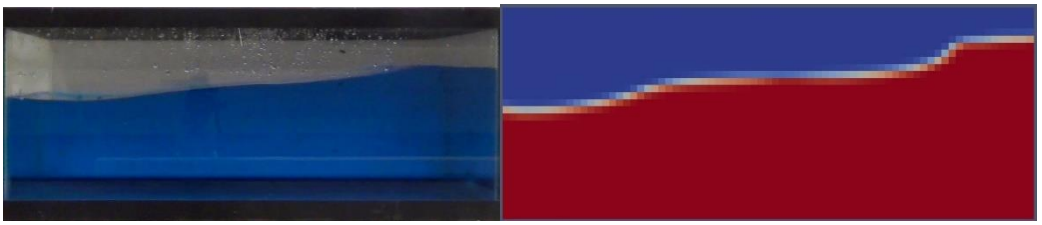

b)

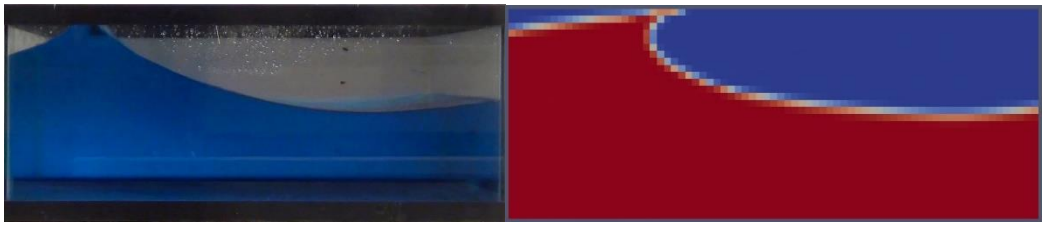

c)

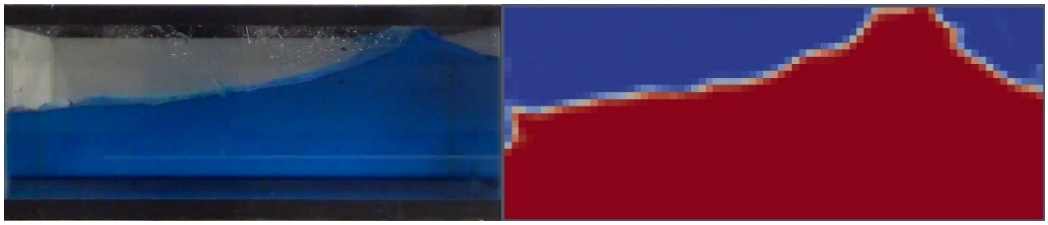

Figure 4- 21 Comparison of free surface in experimental (left) and numerical (right) studies in tank 1 with 200 mm of water, 0º orientation and frequency of higher than resonance

b) Frequency: Resonance

a)

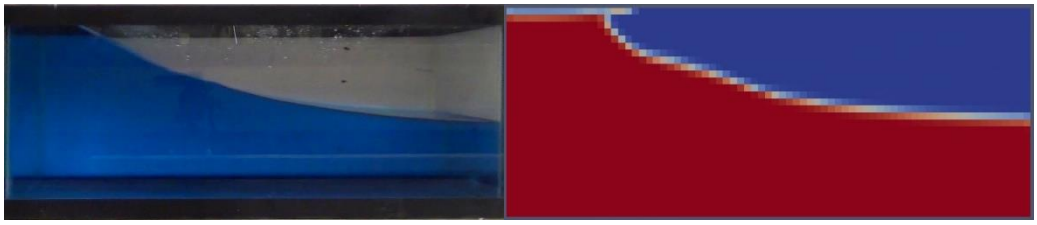

b)

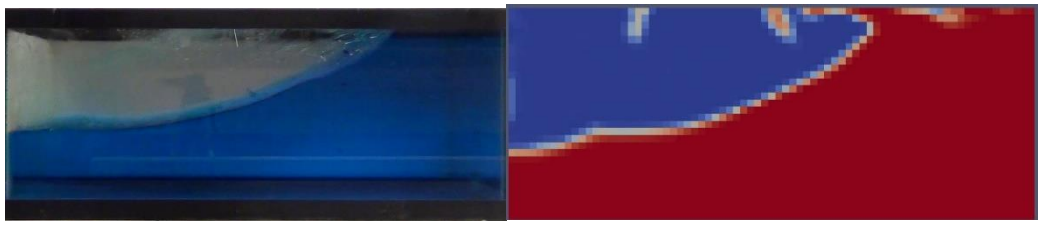

c) 

Figure 4- 22 Comparison of free surface in experimental (left) and numerical (right) studies in tank 1 with 200 mm of water, 0º orientation and resonance frequency

c) Frequency: Lower than resonance

a) 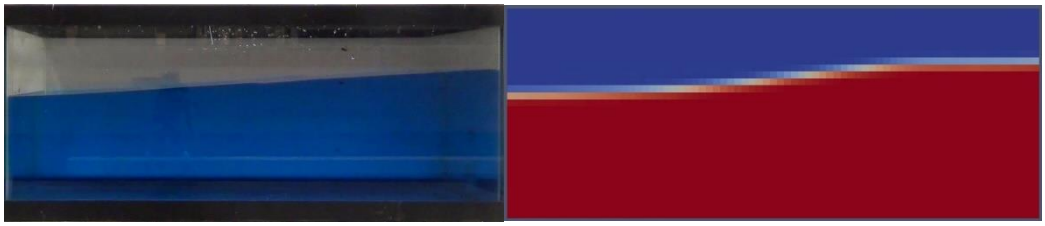

b) 

Figure 4- 23 Comparison of free surface in experimental (left) and numerical (right) studies in tank 1 with 200 mm of water, 0º orientation and frequency of lower than resonance

4.5.6. Tank 1, water depth 200 mm, 30º orientation

a) Frequency: higher than resonance

a) 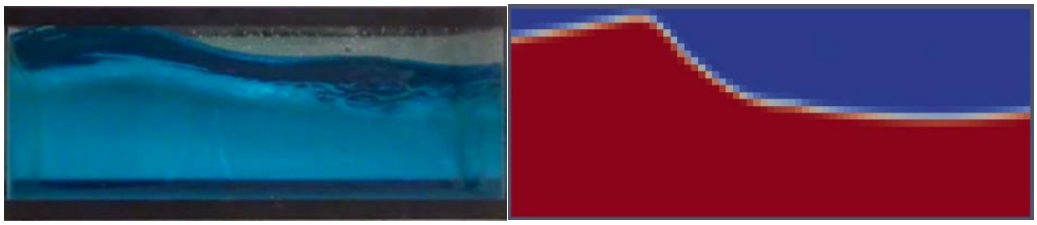

b) 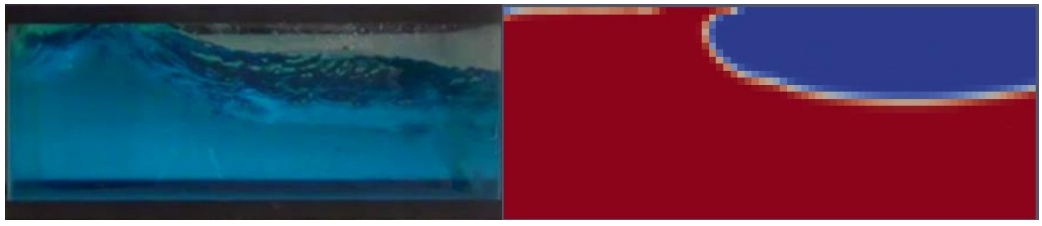

c)  d) 

Figure 4- 24 Comparison of free surface in experimental (left) and numerical (right) studies in tank 1 with 200 mm of water, 30º orientation and frequency of higher than resonance

b) Frequency: Resonance

a) 

b) 

Figure 4- 25 Comparison of free surface in experimental (left) and numerical (right) studies in tank 1 with 200 mm of water, 30º orientation and resonance frequency

c) Frequency: Lower than resonance

a) 

b) 

c) 

Figure 4- 26 Comparison of free surface in experimental (left) and numerical (right) studies in tank 1 with 200 mm of water, 30º orientation and frequency of lower than resonance

4.5.7. Tank 1, water depth 200 cm, 60º orientation

a) Frequency: higher than resonance

a) 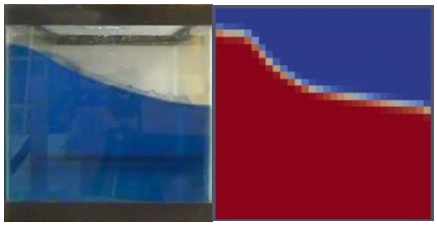 b) 

Figure 4- 27 Comparison of free surface in experimental (left) and numerical (right) studies in tank 1 with 200 mm of water, 60º orientation and frequency of higher than resonance

b) Frequency: Resonance

a) 

b) 

c) 

Figure 4- 28 Comparison of free surface in experimental (left) and numerical (right) studies in tank 1 with 200 mm of water, 60º orientation and resonance frequency

c) Frequency: Lower than resonance

a) 

b) 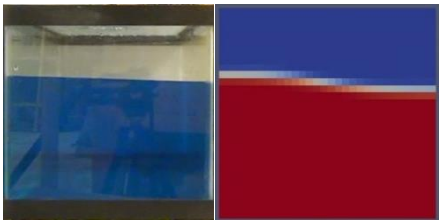

Figure 4- 29 Comparison of free surface in experimental (left) and numerical (right) studies in tank 1 with 200 mm of water, 60º orientation and frequency of lower than resonance

4.5.8. Tank 1, water depth 200 mm, 90º orientation

a) Frequency: higher than resonance

a) 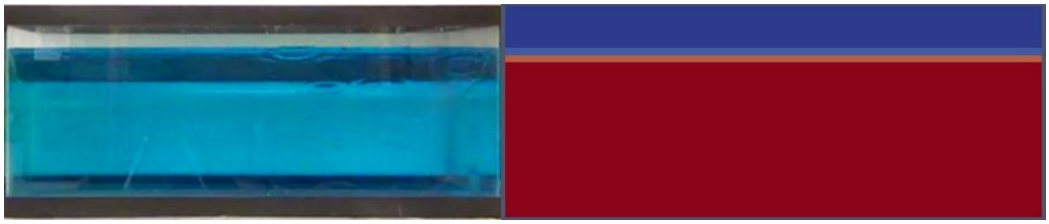

b) 

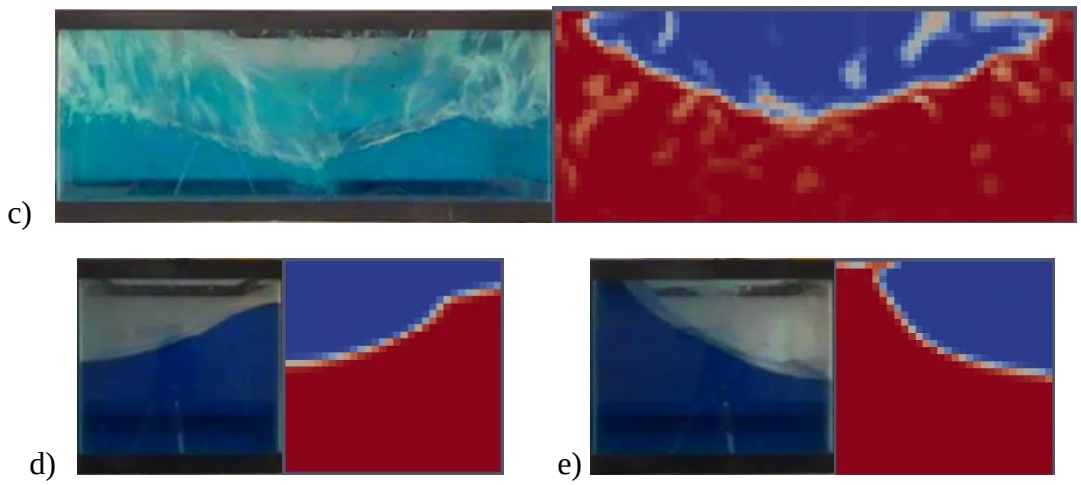

Figure 4- 30 Comparison of free surface in experimental (left) and numerical (right) studies in tank 1 with 200 mm of water, 90º orientation and frequency of higher than resonance

b) Frequency: Resonance

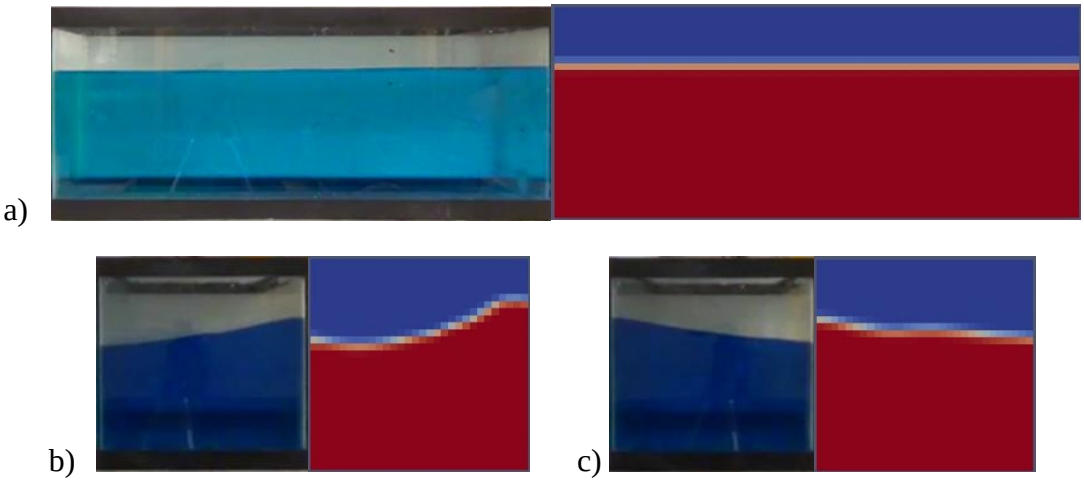

Figure 4- 31 Comparison of free surface in experimental (left) and numerical (right) studies in tank 1 with 200 mm of water, 90º orientation and resonance frequency

Note: In this frequency, the following surface shapes were not observed in the simulations, i.e. the model has to be improved for this type of base excitation (Figure 4- 32):

a)  b) 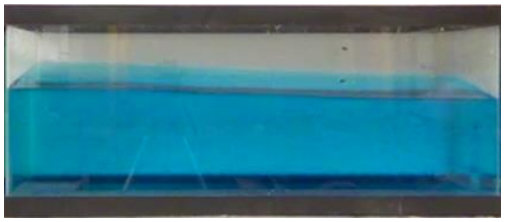

Figure 4- 32 Free Surfaces observed only in experimental study during resonance excitation of tank 1 with 200 mm water and 90º orientation

c) Frequency: Lower than resonance

a) 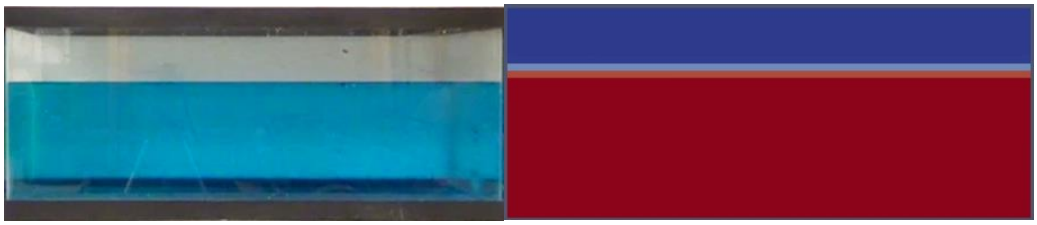

b) 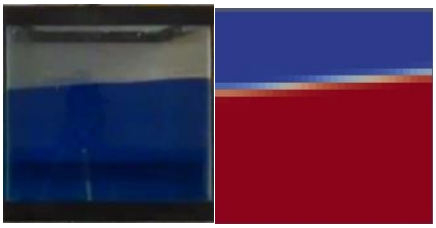

Figure 4- 33 Comparison of free surface in experimental (left) and numerical (right) studies in tank 1 with 200 mm of water, 90º orientation and frequency of lower than resonance

4.5.9. Tank 2, water depth 100 mm, 0º orientation

In this orientation for the second tank (i.e. smaller tank), the liquid surface moved only in one direction in all frequencies, hence the second camera view did not give any further information and is not presented in this section.

Like the previous tank, the numerical model for this tank also showed a very good accuracy for 100 mm water depth. Comparisons are shown in Figures 4- 34 through 4- 45.

a) Frequency: higher than resonance

a)

b)

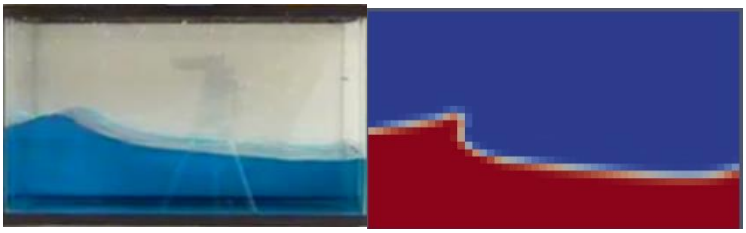

c)

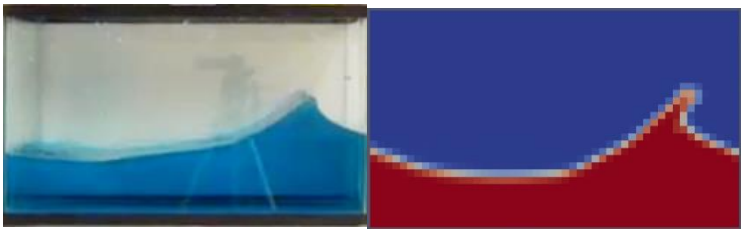

d)

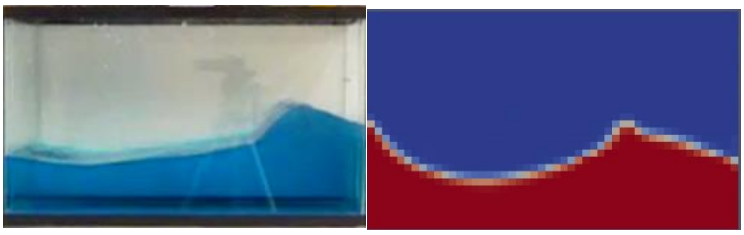

e)

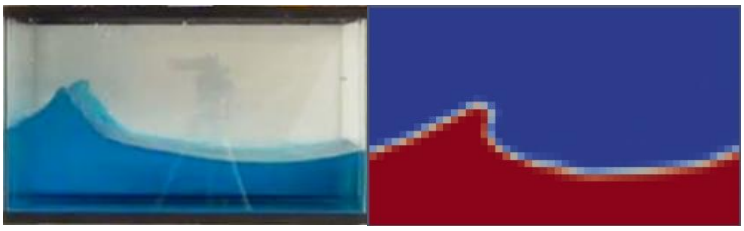

f)

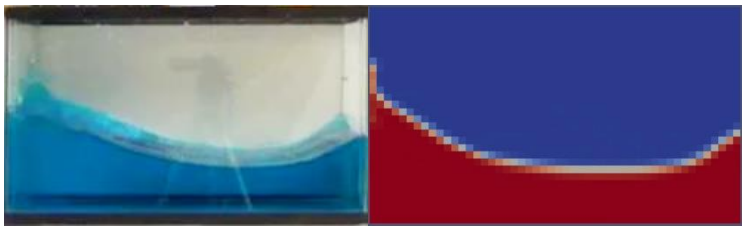

g) 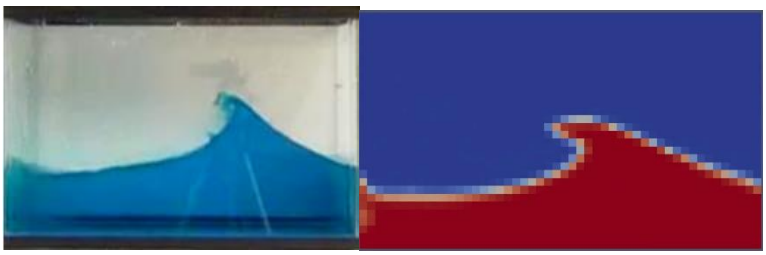

Figure 4- 34 Comparison of free surface in experimental (left) and numerical (right) studies in tank 2 with 100 mm of water, 0º orientation and frequency of higher than resonance

b) Frequency: Resonance

a) 

b) 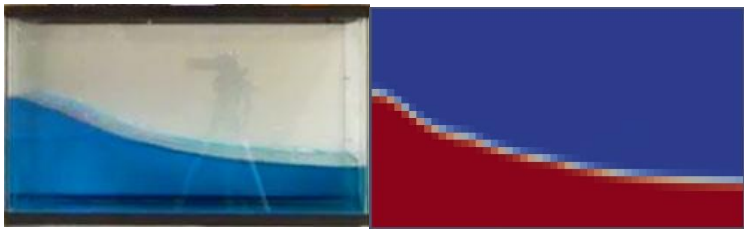

c) 

d) 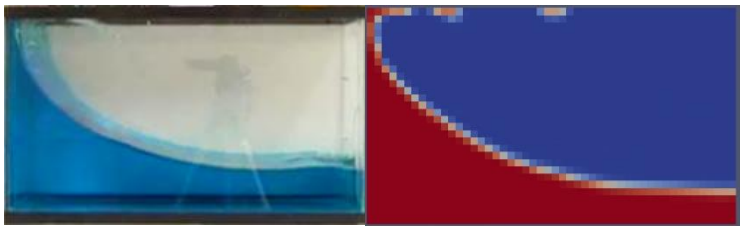

e) 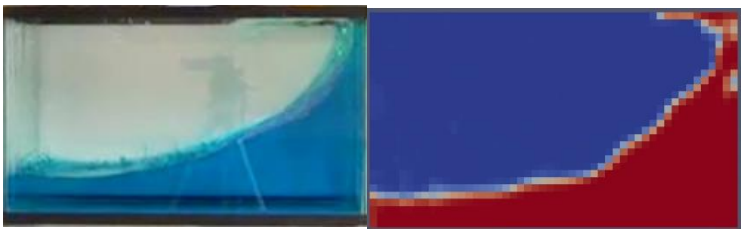

Figure 4- 35 Comparison of free surface in experimental (left) and numerical (right) studies in tank 2 with 100 mm of water, 0º orientation and resonance frequency

c) Frequency: Lower than resonance

a) 

b) 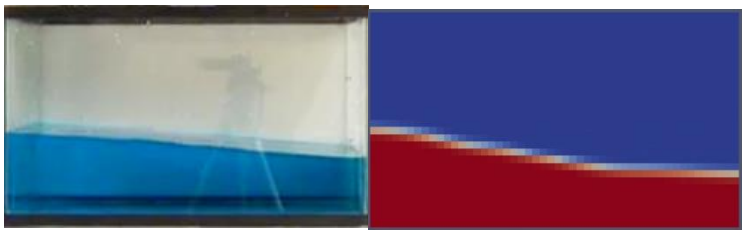

Figure 4- 36 Comparison of free surface in experimental (left) and numerical (right) studies in tank 2 with 100 mm of water, 0º orientation and frequency of lower than resonance

4.5.10. Tank 2, water depth 100 mm, 30º orientation

a) Frequency: higher than resonance

a) 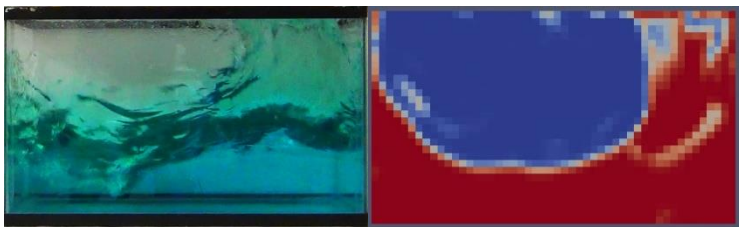

b) 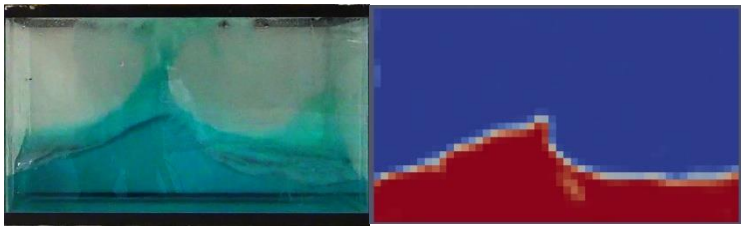

c)

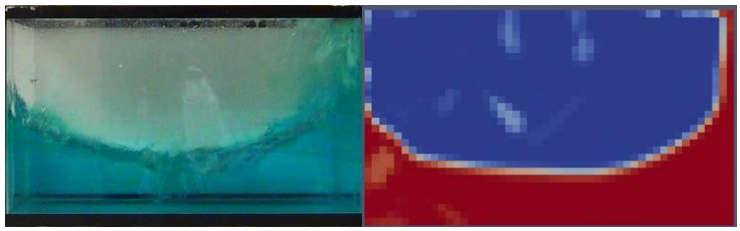

d)

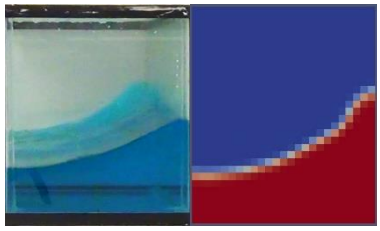

e)

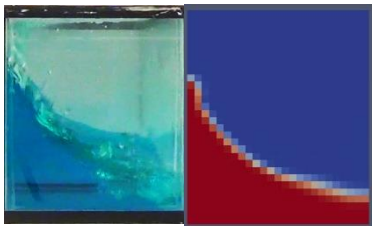

f)

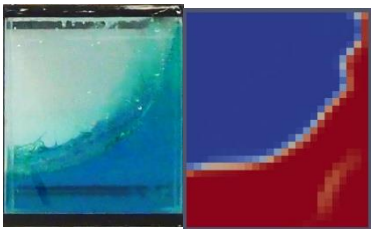

g)

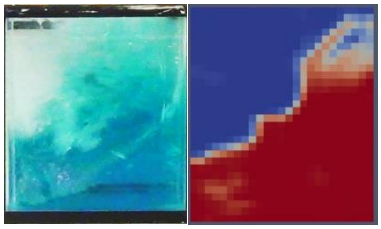

Figure 4- 37 Comparison of free surface in experimental (left) and numerical (right) studies in tank 2 with 100 mm of water, 30º orientation and frequency of higher than resonance

In this frequency, a rotation motion of the liquid was observed in both parts of the studies that can show the model works well in this case.

b) Frequency: Resonance

In this frequency, although the tank has a 30º rotation on the shaking table, the liquid has no perpendicular movement in the tank, hence the camera in the other direction does not show any specific type of motion.

a)

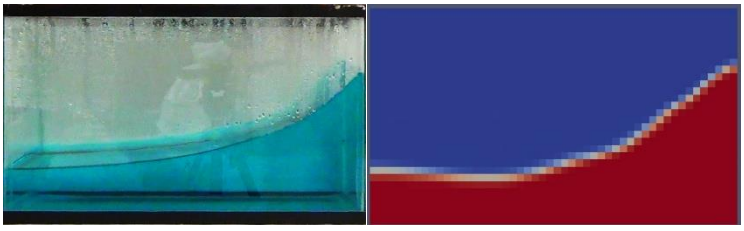

b)

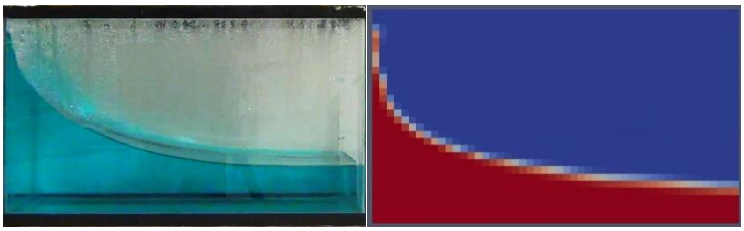

c)

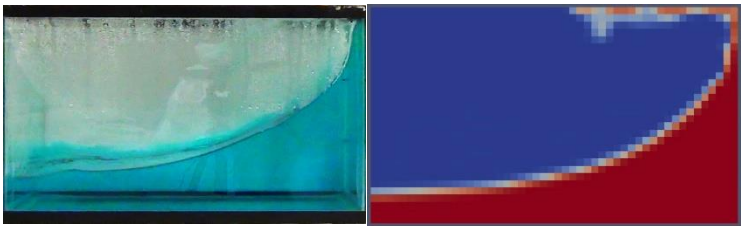

d)

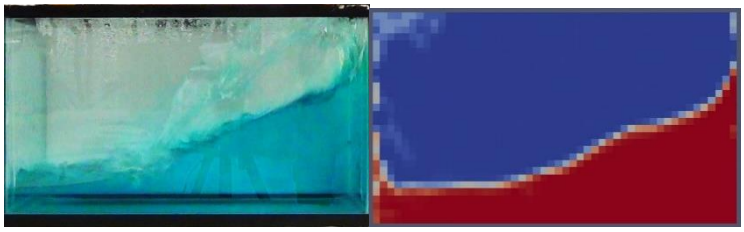

e)

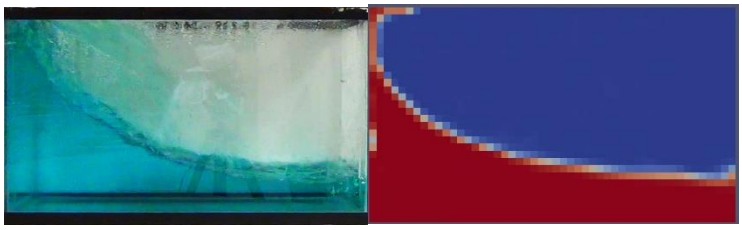

Figure 4- 38 Comparison of free surface in experimental (left) and numerical (right) studies in tank 2 with 100 mm of water, 30º orientation and resonance frequency

c) Frequency: Lower than resonance

a)

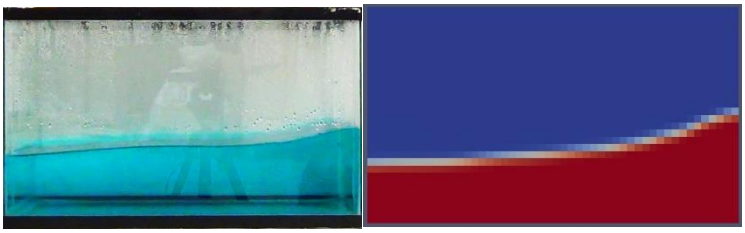

b)

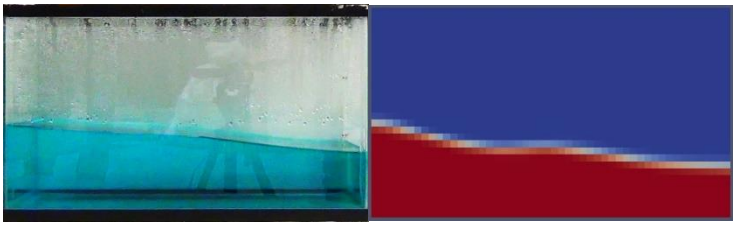

c) 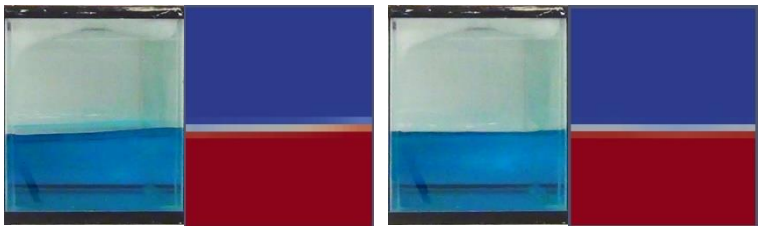

Figure 4- 39 Comparison of free surface in experimental (left) and numerical (right) studies in tank 2 with 100 mm of water, 30º orientation and frequency of lower than resonance

4.5.11. Tank 2, water depth 100 mm, 60º orientation

a) Frequency: higher than resonance

In this excitation frequency, a rotational movement of the liquid in both experimental and the numerical studies was observed. In addition, videos of numerical and experimental study show a good agreement in terms of the liquid surface (Figure 4- 40).

a) 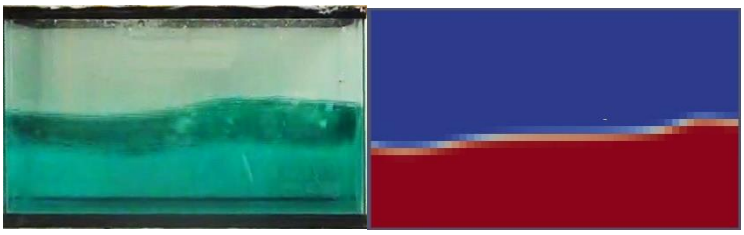

b) 

c) 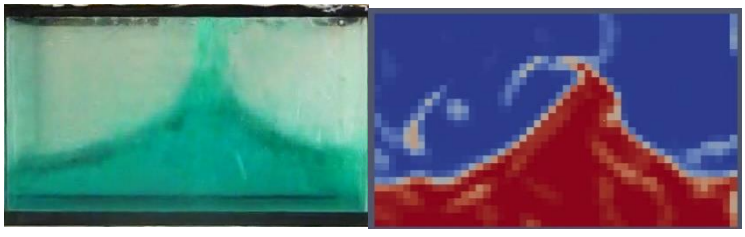

d) 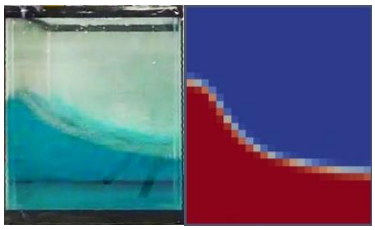 e) 

Figure 4- 40 Comparison of free surface in experimental (left) and numerical (right) studies in tank 2 with 100 mm of water, 60º orientation and frequency of higher than resonance

b) Frequency: Resonance

a) 

b) 

c) 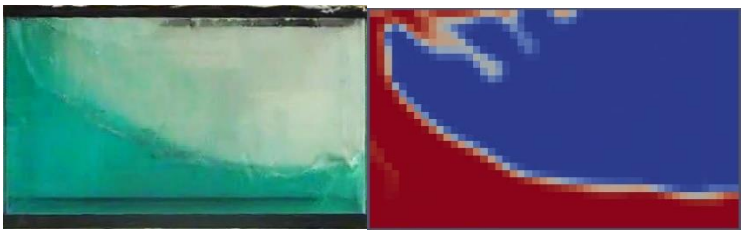

d) 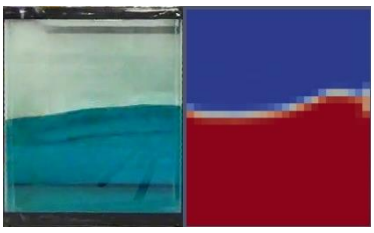 e) 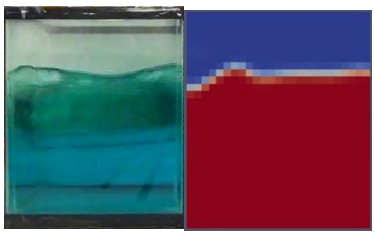

Figure 4- 41 Comparison of free surface in experimental (left) and numerical (right) studies in tank 2 with 100 mm of water, 60º orientation and resonance frequency

c) Frequency: Lower than resonance

a)

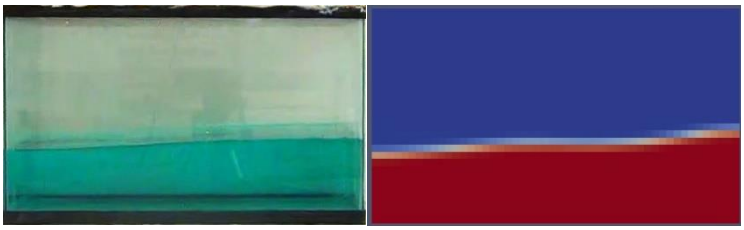

b)

c)

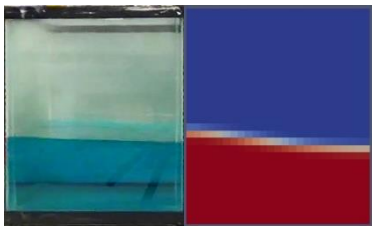

Figure 4- 42 Comparison of free surface in experimental (left) and numerical (right) studies in tank 2 with 100 mm of water, 60º orientation and frequency of lower than resonance

4.5.12. Tank 2, water depth 100 mm, 90º orientation

a) Frequency: higher than resonance

a)

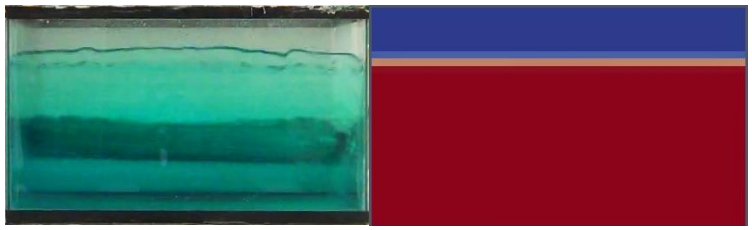

b)

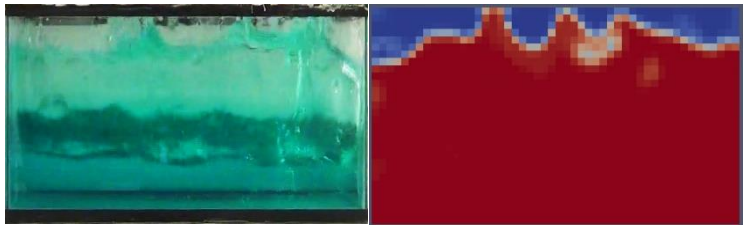

c)

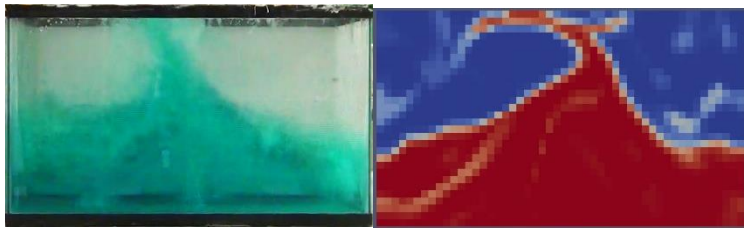

d) 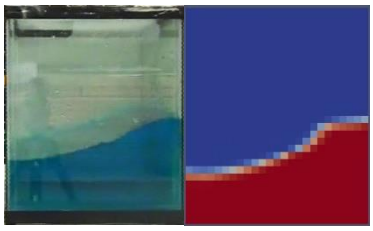 e) 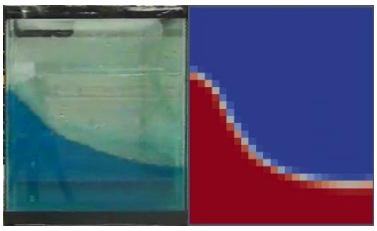

f) 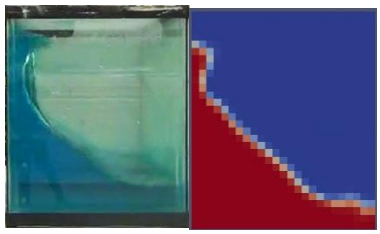

Figure 4- 43 Comparison of free surface in experimental (left) and numerical (right) studies in tank 2 with 100 mm of water, 90º orientation and frequency of higher than resonance

In this frequency, rotation movement of the liquid was observed in the experiment as well as the simulated model.

b) Frequency: Resonance

a) 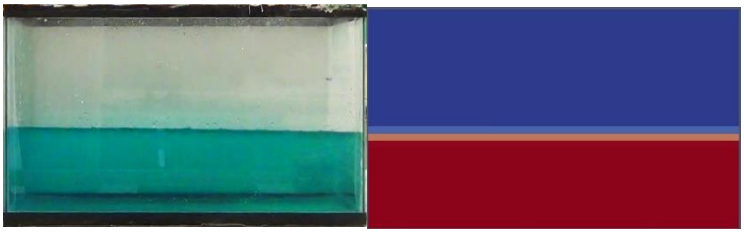

b)  c) 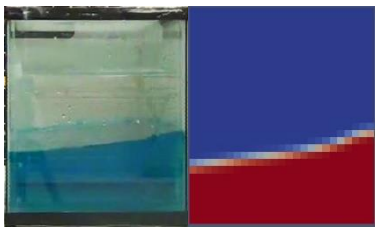

Figure 4- 44 Comparison of free surface in experimental (left) and numerical (right) studies in tank 2 with 100 mm of water, 90º orientation and resonance frequency

c) Frequency: Lower than resonance

a)

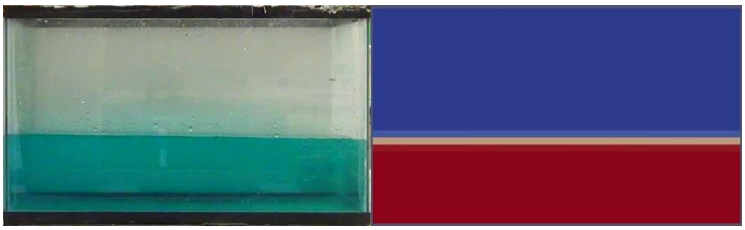

b)

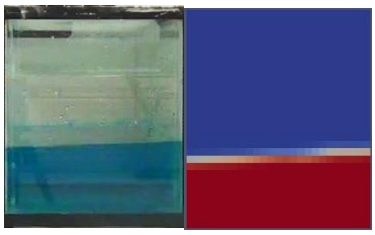

c)

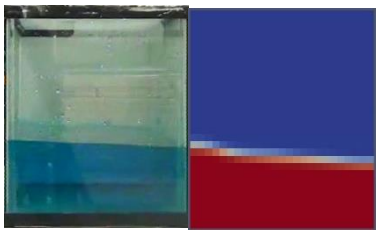

Figure 4- 45 Comparison of free surface in experimental (left) and numerical (right) studies in tank 2 with 100 mm of water, 90º orientation and frequency of lower than resonance

4.5.13. Tank 2, water depth 200 mm, 0º orientation

Water depth of 200 mm for previous tank size showed some inaccuracies for the numerical model compared to 100 mm depth. But for this tank (i.e. smaller) the model is accurate for this depth (Figures 4- 46 to 4- 57). This can show that the model may cause more inaccuracy as the tank size and water depth increase.

a) Frequency: higher than resonance

a)

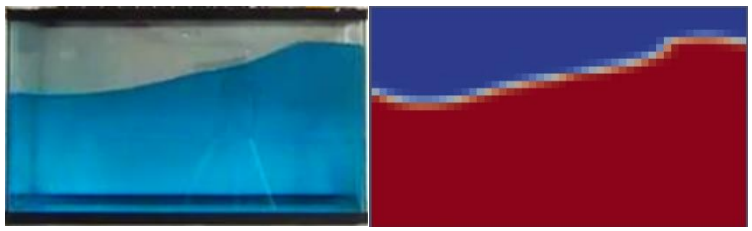

b)

c)

d)

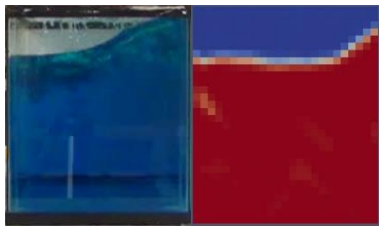

e)

Figure 4- 46 Comparison of free surface in experimental (left) and numerical (right) studies in tank 2 with 200 mm of water, 0º orientation and frequency of higher than resonance

b) Frequency: Resonance

a)

b)

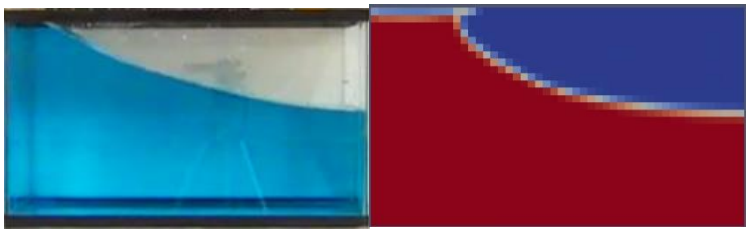

c)

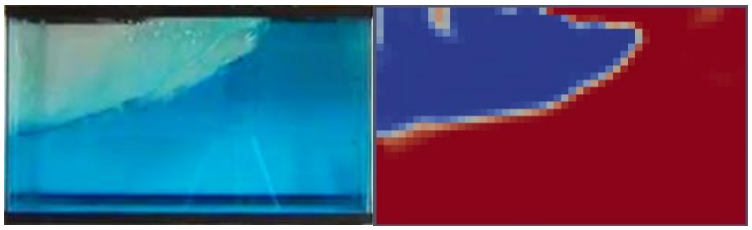

Figure 4- 47 Comparison of free surface in experimental (left) and numerical (right) studies in tank 2 with 200 mm of water, 0º orientation and resonance frequency

c) Frequency: Lower than resonance

a)

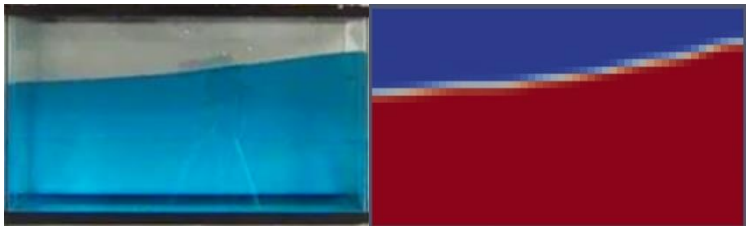

b)

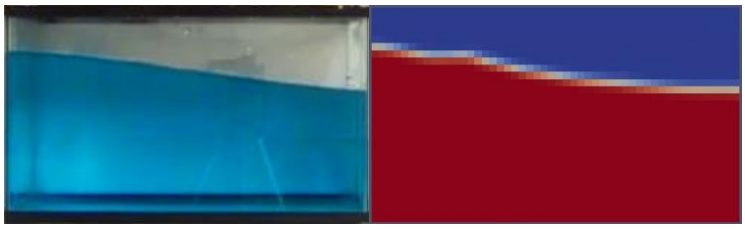

Figure 4- 48 Comparison of free surface in experimental (left) and numerical (right) studies in tank 2 with 200 mm of water, 0º orientation and frequency of lower than resonance

4.5.14. Tank 2, water depth 20 cm, 30º orientation

a) Frequency: higher than resonance

In this frequency, after three cycles the motion changed from longitudinal to latitudinal that was observed in both experimental and numerical parts of the study.

a)

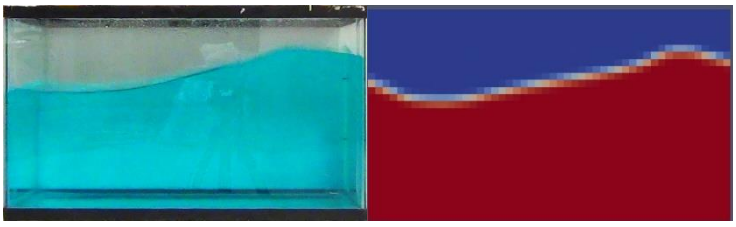

b)

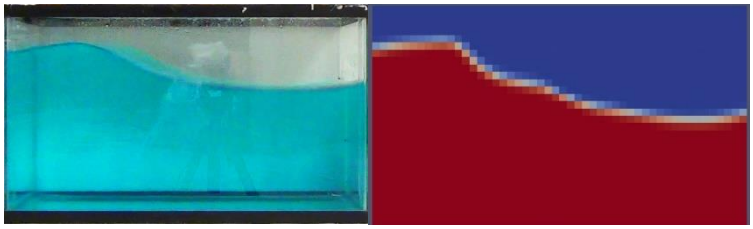

c) 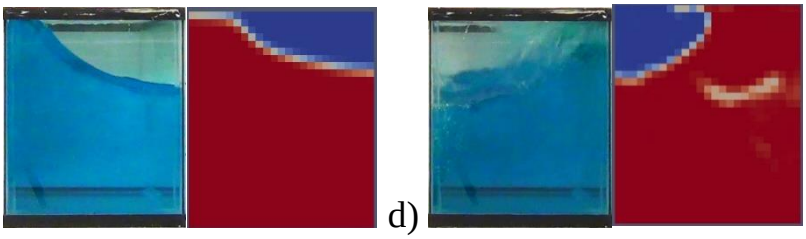 d)

Figure 4- 49 Comparison of free surface in experimental (left) and numerical (right) studies in tank 2 with 200 mm of water, 30º orientation and frequency of higher than resonance

b) Frequency: Resonance

This frequency creates only longitudinal motions in the liquid surface.

a) 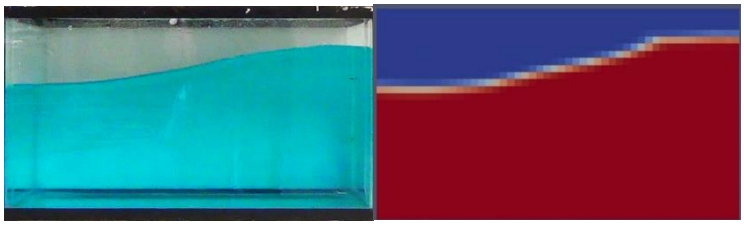

b) 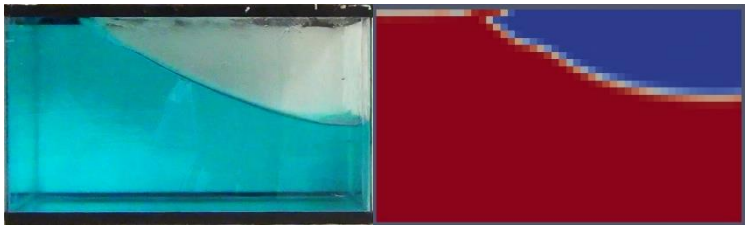

c) 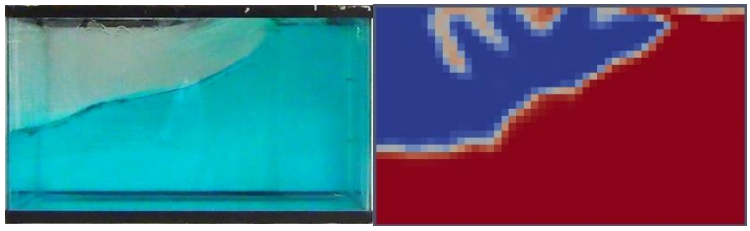

d) 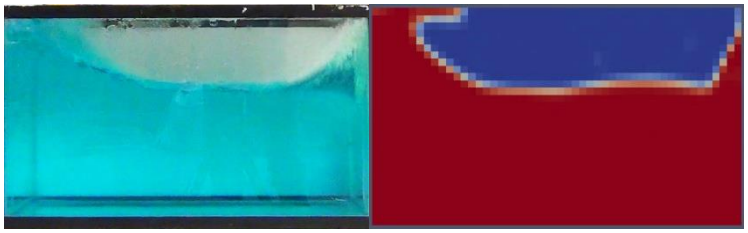

Figure 4- 50 Comparison of free surface in experimental (left) and numerical (right) studies in tank 2 with 200 mm of water, 30º orientation and resonance frequency

c) Frequency: Lower than resonance

a)

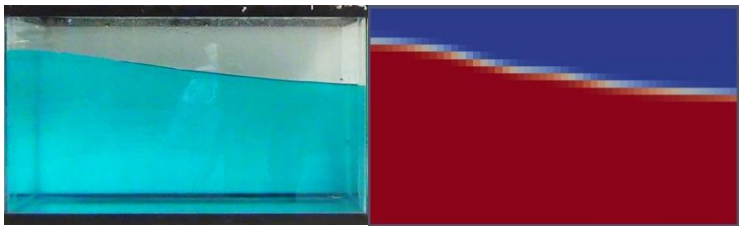

b)

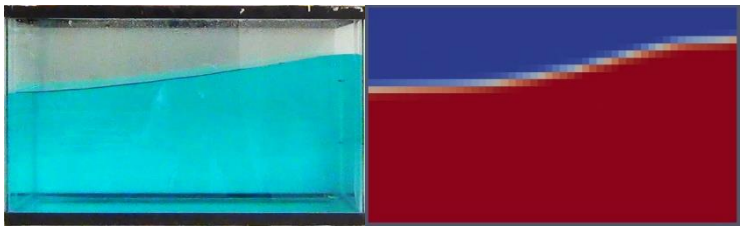

c)

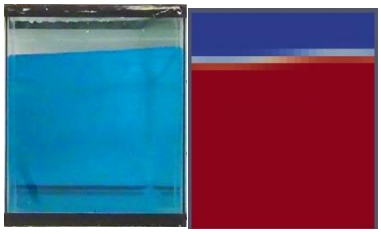

d)

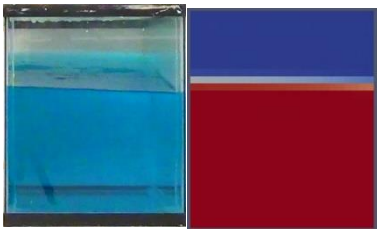

Figure 4- 51 Comparison of free surface in experimental (left) and numerical (right) studies in tank 2 with 200 mm of water, 30º orientation and frequency of lower than resonance

4.5.15. Tank 2, water depth 200 mm, 60º orientation

a) Frequency: higher than resonance

After a few cycles, the liquid starts a rotational movement in both numerical and experimental models.

a)

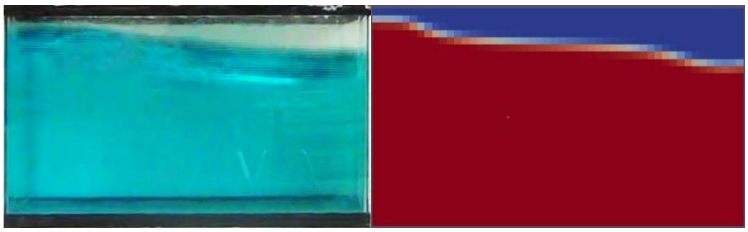

b) 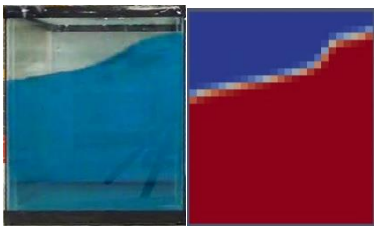 c) 

Figure 4- 52 Comparison of free surface in experimental (left) and numerical (right) studies in tank 2 with 200 mm of water, 60º orientation and frequency of higher than resonance

b) Frequency: Resonance

a) 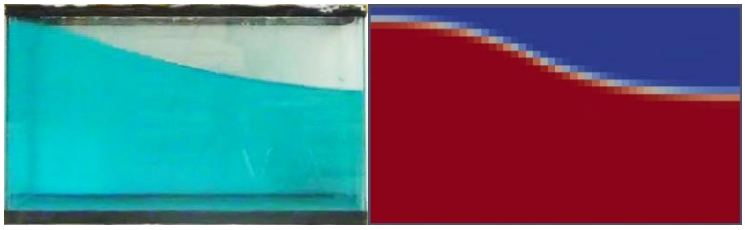

b) 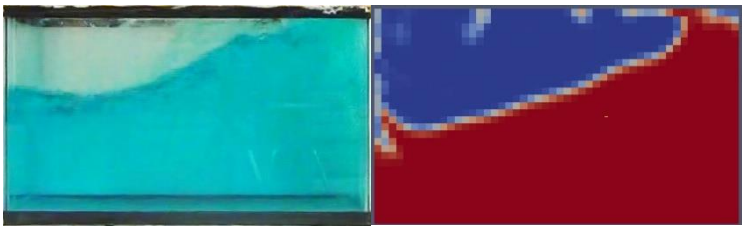

c) 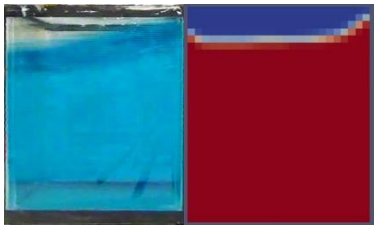

Figure 4- 53 Comparison of free surface in experimental (left) and numerical (right) studies in tank 2 with 200 mm of water, 60º orientation and resonance frequency

c) Frequency: Lower than resonance

a) 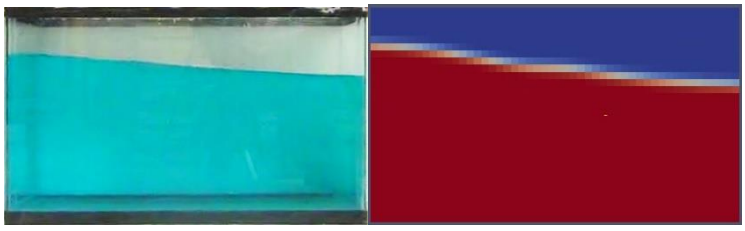

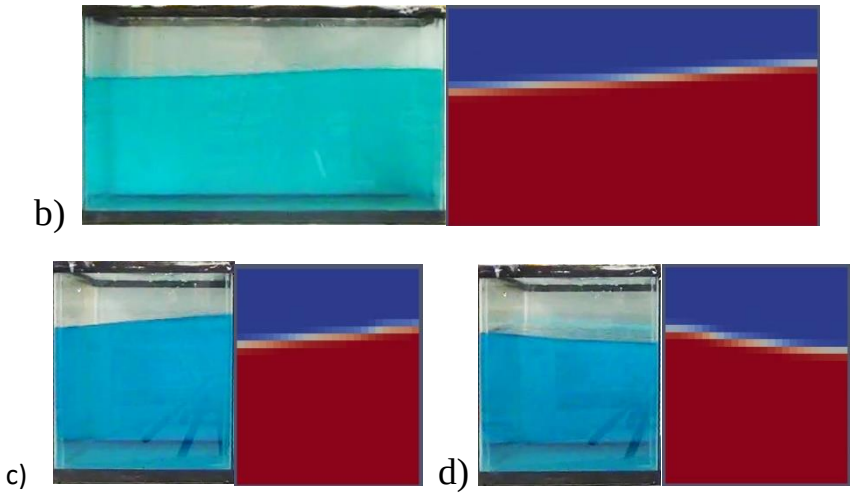

Figure 4- 54 Comparison of free surface in experimental (left) and numerical (right) studies in tank 2 with 200 mm of water, 60º orientation and frequency of lower than resonance

4.5.16. Tank 2, water depth 200 mm, 90º orientation

a) Frequency: higher than resonance

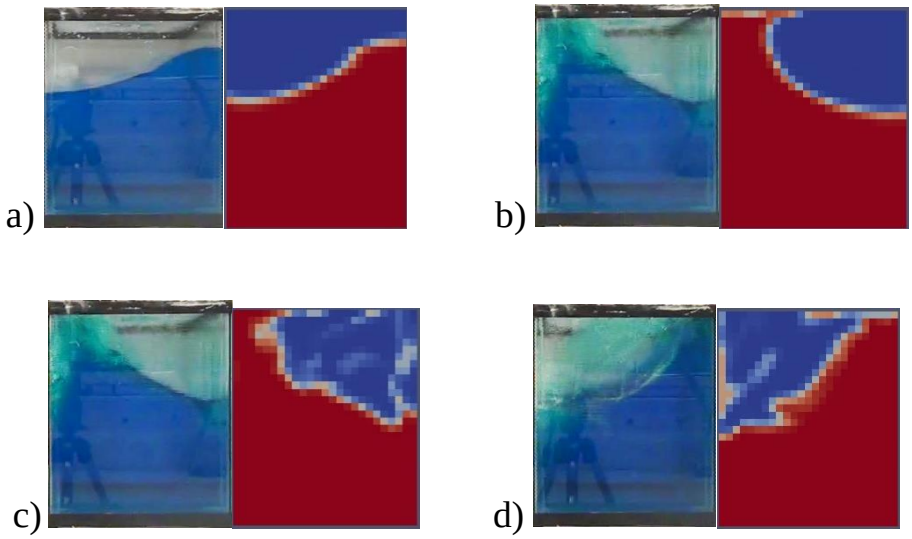

Figure 4- 55 Comparison of free surface in experimental (left) and numerical (right) studies in tank 2 with 200 mm of water, 90º orientation and frequency of higher than resonance

b) Frequency: Resonance

a)

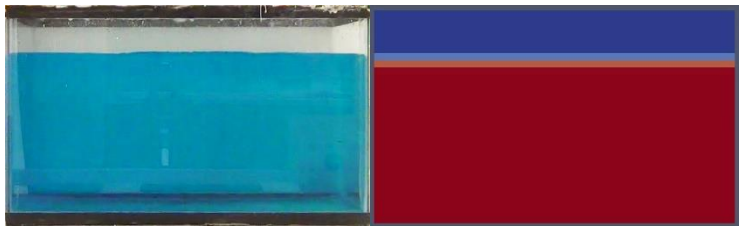

b)

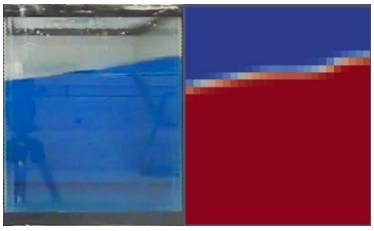

c)

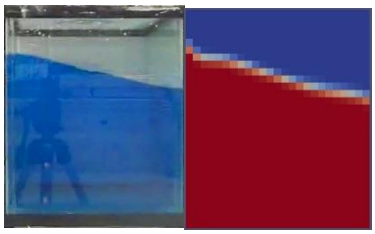

Figure 4- 56 Comparison of free surface in experimental (left) and numerical (right) studies in tank 2 with 200 mm of water, 90º orientation and resonance frequency

c) Frequency: Lower than resonance

a)

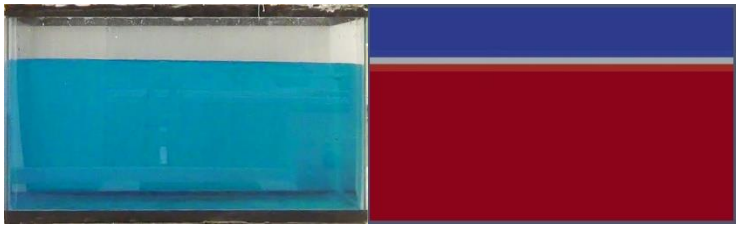

b)

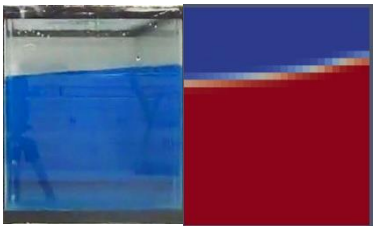

c)

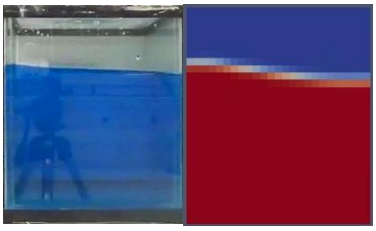

Figure 4- 57 Comparison of free surface in experimental (left) and numerical (right) studies in tank 2 with 200 mm of water, 90º orientation and frequency of lower than resonance

4.6. Discussion

A comparison of numerical simulations with the corresponding experimental tests, it was found that in the model was appropriate in predicting the general motion of the liquid (longitudinal or transverse) in any orientations and frequency.

The model performance was also acceptable for the liquid surface for 0º and 90º orientations, while it can be improved for other orientations (i.e. 30º and 60º).

In addition, the numerical model was found accurate in prediction of the resonance frequency.

Time consumption of the numerical simulations depend on tank orientation, frequency, tank size and liquid depth. With the same mesh size and time steps, resonance frequency in 30º and 60º orientations with 200 mm of water in the larger tank (tank 1) takes the longest time (40+ hours) for the simulation to be completed while the frequency lower than resonance in smaller rank (tank 2) on 0º orientation with 100 mm of water takes 20% of that time.

The numerical model had a high accuracy in more than 75% of the times and a reasonable accuracy in more than 21%. It also needs more improvement for about 4% of the tests. Basically, as the tank size and liquid depth increase, the model becomes less accurate. This shows that more research is needed on this model for real size tanks.

Chapter 5

Conclusion

5.1. Summary

A significant number of studies have been conducted by researchers on sloshing phenomena in liquid storage tanks, however the demand for more information on seismic behavior of these structures still exists. At present there is no Canadian standard for design of liquid tanks under seismic loading. Most of the previous studies have considered the effect of uni-directional earthquake on response of rectangular tanks. Since the direction of an earthquake is not predictable and also the effects of bi-lateral base excitation on rectangular liquid containing structures were neglected in previous studies, the study in this field was necessary to consider such effect.

On the other hand, poor seismic design of liquid storage tanks can lead to structural failures with enormous economic and environmental problems.

In this study the focus was on ground-supported rectangular liquid containing structures that are widely used in industry and municipality applications to store different types of liquid and liquefied gas (e.g. water, petroleum, toxic materials).

The research presented in this thesis consists of experimental tests and numerical studies. The goal was to investigate the effect of various types of base excitation on partially filled liquid storage tanks and develop a numerical model for predicting the liquid surface in them.

For the first part of the research, i.e. experimental investigation, two sizes of tanks with different plan dimensions but same height were used. The tanks were partially filled with water (i.e. 1/3 and

2/3 of the tank height) and excited on a shaking table with both harmonic (including resonance frequency) and actual earthquake (North-South component of 1940 El-Centro earthquake) loads. The excitations were applied to the tanks in different orientations (i.e. 0º, 30º, 60º and 90º) so that the bilateral effect could be observed.

For the numerical study, an open source application - OpenFOAM - was used to simulate the harmonic motion of the same tanks used in the experimental tests.

Finally, the results from experimental tests and numerical study were compared in order to validate the numerical model used in OpenFOAM.

5.2. Conclusion

Based on experimental and numerical studies as discussed in this thesis, the following conclusions can be drawn:

1- Canada as a country that is prone to earthquakes, needs reliable codes for design of liquid storage tanks under seismic loading. Currently there is no Canadian design code available for this purpose.
2- Available design codes in North America (i.e. ACI 350.3 and ASCE 7) need to be improved in terms of bi-lateral base excitations of liquid containing structures.
3- Prediction of the resonance period of the system is a fundamental part for design of liquid storage tanks. Keeping the system away from resonance conditions is one of the goals in the design process.

4- During resonance excitation, the motion of the liquid free surface changes to a non-linear, violent movement. This can cause inaccuracies in prediction of forces and pressures as well as sloshing heights using the design codes.

5- Housner's simplified model (Housner, 1963) that is adopted in North American codes (ACI 350.3 and ASCE 7) is accurate in predicting the resonance frequency of the first mode of the liquid motions inside the tanks.

6- Tank orientation on the shaking table has a significant effect on the motion of the liquid free surface regardless of liquid depth, excitation type or tank size. In other words, changing the direction of excitation can change the hydrodynamic forces on tank walls and roof near sharp corners of the tank.

7- A special design procedure for walls and roof of the tank near sharp corners is desirable.

8- Changing the tank orientation does not affect the resonance frequency significantly. If excited by this frequency in any direction, the liquid will have a longitudinal movement inside its container. In other words, the same frequency can be used as the resonance frequency when the tank is oriented in any direction.

9- During the experimental tests, it was observed that the lower part of the liquid moves with the tank while top part moves independently which agrees with the Housner's model (Housner, 1963). The former is called impulsive part and the latter is the convective component.

10- The numerical model needs to be improved as the tank size and liquid depth increase. The current model is very accurate for smaller size of tank and with less liquid inside.

5.3. Recommendations for future studies

For future studies on seismic loading of liquid storage tanks the following recommendations can be made:

1- In the current study the liquid inside the tank was water. Further studies could be carried out with liquid other than water having different densities.
2- The model used in this study needs improvements in order to lead to more accurate results. This improvement can be a start for newer studies.
3- In this study, the tank walls were assumed rigid, but actual tank behavior may be simulated better by assuming wall flexibility. In addition the tank base was fixed in this study which can be questioned in real tank foundations.
4- Investigating parameters other than liquid surface and resonance frequency such as hydrodynamic pressure by using pressure transducers in experimental studies and comparing them with numerical results based on OpenFOAM model is recommended.
5- In this study only two tank sizes were investigated. Further studies considering different tank sizes and various liquid depths to find a relationship between tank size, aspect ratio and resonance frequency could be made.
6- Monitoring the liquid depth in certain points and studying its spectrum and comparing the spectra of experimental and numerical studies is also recommended.
7- More investigation is necessary on real size liquid tanks in order for the numerical model to be acceptable as a reliable method.

References:

1- ACI 350 Committee, Seismic Design of Liquid-Containing Concrete Structures and Commentary (ACI 350.3-6), American Concrete Institute, 2006

2- Akyildiz, H., Ünal, E., Experimental investigation of pressure distribution on a rectangular tank due to the liquid sloshing, J Ocean Engineering 32 (2005) 1503–1516

3- Barakati, A., Numerical modelling of liquid containing structure under dynamic loading, University of Ottawa, 2015

4- Chen, Y.G., Djidjeli, K., Price, W.G. Numerical simulation of liquid sloshing phenomena in partially filled containers, J Computers & Fluids 38 (2009) 830–842

5- Cho, K.H., Cho, S.Y., Seismic Response of Cylindrical Steel Tanks Considering Fluid-Structure Interaction, J Steel Structures 7 (2007) 147-152

6- Chopra, A.K., Dynamics of structures: theory and applications to earthquake engineering, Prentice hall Inc. 1995

7- Gui, F., Jiang, S., Numerical simulation of liquid sloshing problem under resonant excitation, J Advances in mechanical engineering, (2014) Article ID 834657

8- Hirt, C.W., Nichols, B.D., Volume of Fluid (VOF) Method for the Dynamics of Free Boundaries, Journal Of Computational Physics 39 (1981) 201-225

9- Housner, W.G., The Dynamic Behavior Of Water Tanks, Bulletin of the Seismological Society of America, 53 (1963) 381-387

10- Ikeda, T., Harata, Y., Ibrahim, R.A., Nonlinear Responses of Sloshing in Square Tanks Subjected to Horizontal Random Ground Excitation, Matec web of conferences 1, 03006, 2012.

11- Isaacson, M., Earthquake-induced hydrodynamic forces on reservoir roofs, Can. J. Civ. Eng. 37: 1107–1115 (2010)

12- Jaiswal, O. R., Rai, D.C., Jain, S.K, Review of Seismic Codes on Liquid-Containing Tanks, Earthquake Spectra, Volume 23, No. 1, pages 239–260, February 2007

13- Jaiswal, O. R., Kulkarni, S., Pathak, P., A Study On Sloshing Frequencies Of Fluid-Tank System, The 14th World Conference on Earthquake Engineering

14- Kheirkhah Gildeh, H., Numerical Modeling of Thermal/Saline Discharges in Coastal Waters, University of Ottawa, 2013

15- Kolukula, S.S., Chellapandi, P., Nonlinear Finite Element Analysis of Sloshing, Advances in Numerical Analysis, Volume 2013, Article ID 571528

16- Koshizuka, S., Oka, Y., Moving-Particle Semi-Implicit Method for Fragmentation of Incompressible Fluid, Nuclear Science and Engineering, 123, (1996) 421-434

17- Lee, C.J.K., Noguchi, H., Koshizuka, S., Fluid–shell structure interaction analysis by coupled particle and finite element method, Computers and Structures 85 (2007) 688–697

18- Li, Y., Zhu, R., Miao, G., Fan, J., Simulation of tank sloshing based on OpenFOAM and coupling with ship motions in time domain, Journal of Hydrodynamics, 2012,24 (3): 450-457

19- Liu, D., Lin, P., A numerical study of three-dimensional liquid sloshing in tanks, Journal of Computational Physics 227 (2008) 3921–3939

20- Logan, D.L., A First Course in the Finite Element Method, Thomson-Engineering, 1986

21- Ming, P., Duan, W., Nemirical simulation of sloshing in rectangular tank with VOF based on unstructured grids, Journal of Hydrodynamics, 2010, 22 (6): 856-864

22- Mitra, S., Sinhamahapatra, K.P., Slosh dynamics of liquid-filled containers with submerged components using pressure-based finite element method, Journal of Sound and Vibration 304 (2007) 361–381

23- Moslemi, M., Kianoush, M.R., Parametric study on dynamic behavior of cylindrical ground-supported tanks, Engineering Structures 42 (2012) 214–230

24- Moslemi, M., Kianoush, M.R., Pogorzelski, W., Seismic response of liquid-filled elevated tanks, Engineering Structures 33 (2011) 2074–2084

25- Panigrahy, P.K., Saha, U.K., Maity, D., Experimental studies on sloshing behavior due to horizontal movement of liquids in baffled tanks, Ocean Engineering 36 (2009) 213–222

26- Rebouillat, S., Liksonov, D., Fluid–structure interaction in partially filled liquid containers: A comparative review of numerical approaches, Computers & Fluids 39 (2010) 739–746

27- Sadjadi, R., Kianoush, M.R., Response Modification Factors For Reinforced Concrete Liquid Containing Structures, The 14th World Conference on Earthquake Engineering

28- Sriram, V., Sannasiraj, S.A., Sundar, V., Numerical simulation of 2D sloshing waves due to horizontal and vertical random excitation, Applied Ocean Research 28 (2006) 19–32

29- VakilaadSarabi, A., Miyajima, M., Study of the Sloshing of Water Reservoirs and Tanks due to Long Period and Long Duration Seismic Motions, The 15th World Conference on Earthquake Engineering

30- Wu, C.H., Chen, B.F., Transient Response Of Sloshing Fluid In A Three Dimensional Tank, Journal of Marine Science and Technology, Vol. 20, No. 1, pp. 26-37 (2012)

31- Xiong, Y.P., Xing, J.T., Transient Dynamic Responses Of An Integrated Air-Liquid-Elastic Tank Interaction System Subject To Earthquake Excitations, 2008 ASME Pressure Vessels and Piping Division Conference

32- OpenFOAM users' guide